Winter 1999

Unbound pavement base courses: Parallel study of stiffness and drainage characteristics

Moussa Issa
Louisiana Tech University

UNBOUND PAVEMENT BASE COURSES PARALLEL STUDY OF STIFFNESS AND DRAINAGE CHARACTERISTICS

By

Moussa Issa, B.S., M.S.

A Dissertation Presented in Partial Fulfillment
of the Requirements for the Degree of
Doctor of Engineering

COLLEGE OF ENGINEERING AND SCIENCE
LOUISIANA TECH UNIVERSITY

March 1999

UMI Number: 9918274

LOUISIANA TECH UNIVERSITY

THE GRADUATE SCHOOL

February 19, 1999
Date

We hereby recommend that the dissertation prepared under our supervision

by **MOUSSA ISSA**

entitled **UNBOUND PAVEMENT BASE COURSES**

PARALLEL STUDY OF STIFFNESS AND DRAINAGE CHARACTERISTICS

be accepted in partial fulfillment of the requirements for the Degree of

Doctor of Engineering

Supervisor of Thesis Research (NDP)

Head of Department (BP)

Civil Engineering
Department

Recommendation concurred in:

(FLR)

(RFN)

(MM)

Advisory Committee

Approved:

Director of Graduate Studies (RG)

Dean of the College (LG)

Approved:

Director of the Graduate School (TM)

GS Form 13
2/97

ABSTRACT

The purpose of this project was to study the effects of fines (minus #4 sieve) on permeability and stiffness characteristics of unbound base materials and to propose an optimum gradation that will satisfy these two parameters. One type of highway base material-crushed limestone-was used in the study. A total of 75 laboratory tests were conducted and distributed--25 respectively on permeability, resilient modulus and unconfined compression. The permeability test data were collected using a low-head permeameter. The resilient modulus and unconfined compression test data were collected by the mean of the MTS (Machine Testing System) with a load cell capacity of 22-kips. The major steps of the research are summarized as follows:

A. Conduct intensive laboratory testing on open and dense-graded materials with respect to their drainage (permeability) and stiffness (resilient modulus and unconfined compressive strength) characteristics. The determination of permeability is necessary if an evaluation of drainage capability of an existing or new base layer is needed. The determination of the resilient modulus is necessary because it is an input data for pavement design using the AASHTO procedure.

B. Perform permeability and resilient modulus tests to study the effect of introducing fines (percent passing #4) to open-graded base layers on permeability and resilient modulus.

C. From the data collected from these tests on both drainage and strength characteristics, perform regression analysis to develop formulas that relate percent fines to permeability and to resilient modulus.

D. Combine the tests results from permeability and resilient modulus to provide a range of percent fines gradation band that will satisfy the two parameters as pavement design inputs.

E. Provide some tools and techniques used to prevent the base course from being contaminated by subgrade material and to check whether the proposed base course is able to drain water as quickly as possible.

The project produced some formulas that predict the coefficient of permeability for pavement base materials, unconfined compression strength, and resilient modulus. The study also provided an optimum gradation, permeable enough to withstand heavy traffic. A highway engineer can use these equations to estimate the coefficients of permeability and resilient modulus of aggregate bases for preliminary design or for evaluation of an existing unbound pavement layer.

TABLE OF CONTENTS

Page

ABSTRACT iii

LIST OF TABLES viii

LIST OF FIGURES xi

LIST OF ABBREVIATIONS xiii

ACKNOWLEDGMENTS xv

CHAPTER 1 INTRODUCTION 1

CHAPTER 2 REVIEW OF LITERATURE 3

2.1 Introduction 3

2.2 Sources of Water and Methods of Damage Minimization 4

2.3 Open-Graded Base Materials 7

2.3.1 Summary 11

2.4 Permeability 11

2.4.1 Field Measurement 11

2.4.2 Laboratory Testing 12

2.4.3 Empirical Estimation 14

2.4.4 Summary 17

2.5 Resilient Modulus 18

2.5.1 Introduction 18

Page

2.5.2 The Concept of Resilient Modulus 18

2.5.3 Parameters Affecting Resilient Modulus 20

2.5.4 Summary 23

CHAPTER 3 PLAN OF STUDY 25

3.1 Research Approach 25

3.2 Proposed Design Parameters 25

3.3 Design of Experiment 25

3.4 Tasks...31

CHAPTER 4 TEST PROCEDURE 32

4.1 The Barber and Sawyer Permeameter 32

4.1.1 Apparatus Description 32

4.2 Preliminary Tests 34

4.3 Permeability Tests 34

4.3.1 Using the Barber and Sawyer Permeameter 34

4.4 Resilient Modulus Test Equipment 36

4.4.1 Specimen Preparation for Resilient Modulus Tests 38

4.4.2 Test Procedure 41

CHAPTER 5 TEST RESULTS 43

5.1 Permeability Test Results 43

5.2 Resilient Modulus Test Results 50

5.3 Unconfined Compression Test Results 52

CHAPTER 6 ANALYSIS OF RESULTS 63

Page

6.1 Permeability 63

6.2 Resilient Modulus and Unconfined Compression Tests 67

6.3 Permeability and Resilient Modulus 69

6.4 Geotextiles 71

6.5 Pavement Infiltration 74

6.6 Summary of Analysis 82

6.7 Summary of the Results 83

CHAPTER 7 CONCLUSIONS AND RECOMMENDATIONS 86

7.1 Conclusions 86

7.2 Recommendations 87

APPENDIX A GRAIN SIZE DISTRIBUTION BEFORE AND AFTER PERMEABILITY TESTING AND PERMEABILITY 88

APPENDIX B PROGRAMS USED FOR DATA ACQUISITION 97

APPENDIX C RESULTS FOR RESILIENT MODULUS TESTS AND UNCONFINED COMPRESSION TESTS 100

APPENDIX D SUBGRADE SOIL MATERIAL 108

REFERENCES 111

VITA 116

LIST OF TABLES

Page

Table 2.1 Some Currently Used Unstabilized Permeable Base Gradations 8

Table 3.1 Testing Program 29

Table 3.2 Results of the Stress Analysis Using Elsym5 30

Table 4.1 Test Stress of States and Repetitions 42

Table 5.1 Permeability Test Results Using B/S Permeameter: AASHTO 67 44

Table 5.2 Permeability Test Results Using B/S Permeameter: A84_S15 45

Table 5.3 Permeability Test Results Using B/S Permeameter: A75_S25 46

Table 5.4 Permeability Test Results Using B/S Permeameter: A65_S35 47

Table 5.5 Permeability Test Results Using B/S Permeameter: Louisiana Base 48

Table 5.6 Summaries of Values of k_1, k_2 and R^2 as Function of Fines 52

Table 5.7 Unconfined Compression Test Results 52

Table 6.1 Compromise Gradation 71

Table 6.2 Physical Requirements[1,2] for Drainage Textiles 75

Table 6.3 Summary of Design Criteria for Selecting Geotextiles 76

Page

Table 6.4 AASHTO Drainage Recommendation for Time to Drain Based on 50% Saturation 77

Table 6.5 Pavement Rehabilitation Manual Guidance for Time to Drain Based on 85% Saturation 77

Table 6.6 Compromise Gradation 85

Table A.1 Grain Size Distribution: AASHTO 67 89

Table A.2 Grain Size Distribution: A85_S15 89

Table A.3 Grain Size Distribution: A75_S25 90

Table A.4 Grain Size Distribution: A65_S35 90

Table A.5 Grain Size Distribution: Louisiana Base 91

Table A.6 Permeability Test Results Using B/S Permeameter: AASHTO 67 92

Table A.7 Permeability Test Results Using B/S Permeameter: A85_S15 93

Table A.8 Permeability Test Results Using B/S Permeameter: A75_S25 94

Table A.9 Permeability Test Results Using B/S Permeameter: A65_S35 95

Table A.10 Permeability Test Results Using B/S Permeameter: Louisiana Base 96

Table C.1 Test Data of Specimen A67_1 101

Table C.2 Test Data of Specimen A67_2 101

Table C.3 Test Data of Specimen A67_3 101

Table C.4 Test Data of Specimen A67_4 101

Table C.5 Test Data of Specimen A67_5 102

Table C.6 Test Data of Specimen A85_S15_1 102

Page

Table C.7 Test Data of Specimen A85_S15_2 102

Table C.8 Test Data of Specimen A85_S15_3 102

Table C.9 Test Data of Specimen A85_S15_4 103

Table C.10 Test Data of Specimen A85_S15_5 103

Table C.11 Test Data of Specimen A75_S25_1 103

Table C.12 Test Data of Specimen A75_S25_2 103

Table C.13 Test Data of Specimen A75_S25_3 104

Table C.14 Test Data of Specimen A75_S25_4 104

Table C.15 Test Data of Specimen A75_S25_5 104

Table C.16 Test Data of Specimen A65_S35_1 104

Table C.17 Test Data of Specimen A65_S25_2 105

Table C.18 Test Data of Specimen A65_S35_3 105

Table C.19 Test Data of Specimen A65_S35_4 105

Table C.20 Test Data of Specimen A65_S35_5 105

Table C.21 Test Data of Specimen Louisiana Base_1 106

Table C.22 Test Data of Specimen Louisiana Base_2 106

Table C.23 Test Data of Specimen Louisiana Base_3 106

Table C.24 Test Data of Specimen Louisiana Base_4 106

Table C.25 Test Data of Specimen Louisiana Base_5 107

Table C.26 Unconfined Compression Test Results 107

LIST OF FIGURES

Page

Figure 2.1 Sources of Water........5

Figure 2.2 Some SHAs Open-Graded Permeable Bases........9

Figure 2.3 Estimation of Coefficient of Permeability of Granular Drainage and Filter Materials........16

Figure 2.4 Typical Gradation and Coefficient of Permeability of Open-Graded Bases and Filter Materials........17

Figure 2.5 Test Setup for Determining Resilient Modulus from Repeated Load Test........20

Figure 2.6 Definition of Resilient Modulus in a Repeated Loading Test........21

Figure 2.7 Relationship between Stability and Permeability........24

Figure 3.1 Gradation Curves for AASHTO #67, Louisiana Base and Screenings (mid-range specifications)........28

Figure 3.2 Cross-sections Used in Analysis........29

Figure 3.3 Load Configuration Used in Analysis........30

Figure 4.1 Sketch of a Barber and Sawyer Permeameter........33

Figure 4.2 F vs. hS/Q........37

Figure 4.3 Testing System........38

Figure 4.4 Haversine Load Pulse........39

Figure 4.5 Triaxial Chamber with External Mounted LVDTs and Load Cell........40

Page

Figure 4.6 Apparatus for Vibratory Compaction of Unbound Materials....41

Figure 5.1 Coefficient of Permeability vs. % passing #4....49

Figure 5.2 Resilient Modulus vs. Bulk Stress: AASHTO 67....53

Figure 5.3 Resilient Modulus vs.Bulk Stress: A85_S15....54

Figure 5.4 Resilient Modulus vs. Bulk Stress: A75_S25....55

Figure 5.5 Resilient Modulus vs. Bulk Stress: A65_S35....56

Figure 5.6 Resilient Modulus vs. Bulk Stress: LA Typical Base....57

Figure 5.7 Resilient Modulus vs. Bulk Stress: All Gradations....58

Figure 5.8 Resilient Modulus vs. % Fines: θ= 10.5, 20, 30, 40, 58.5 psi....59

Figure 5.9 Resilient Modulus and Permeability vs. Percent Fines....60

Figure 5.10 Load and Deformation Time History: A65_S35_1 Sequence #5....61

Figure 5.11 Unconfined Compression vs. % Fines....62

Figure 6.1 Compromise Gradation....72

Figure 6.2 Filter Formation....74

Figure 6.3 Time Factor T....80

Figure 6.4 Time Factor for 50 Percent Drainage....82

LIST OF ABBREVIATIONS

A65_S35	A blend of 65% AASHTO 67 and 35% Screenings
A67	AASHTO 67 stone
A75_S25	A blend of 75% AASHTO 67 and 25% Screenings
A85_S15	A blend of 85% AASHTO 67 and 15% Screenings
AASHTO	American Association of State Highway and Transportations Officials
B/S	Barber and Sawyer
CBR	California Bearing Ratio
Dx	Grain size corresponding to x% cumulative passing
ELSYM5	Elastic Layered System version 5
FHWA	Federal HighWay Agency
Fpd	Feet per day
i	Hydraulic gradient
IA	Iowa
K	Coefficient of Permeability
LA	Louisiana
LVDT	Linear Variable Differencial Trancuder
MN	Mennisota
MTS	Material Testing System

NJ	New Jersey
P_{200}	Percent passing sieve #200
PA	Pennsylvania
SC	Screenings
SHA	State Hyway Agency
U.C.	Unconfined Compression
US	United States
Vs.	Versus

ACKNOWLEDGMENTS

The author would like to express his sincere appreciation to his dissertation committee chairman Dr. Norm Pumphrey for his valuable guidance throughout the research. Sincere appreciation is given to his dissertation committee members, Dr. Freddy Roberts, Dr. Raja Nassar, Dr. Maureen McCurdy, for their valuable comments and suggestions while reviewing the manuscript.

Sincere appreciation is addressed to the Civil Engineering Program of Louisiana Tech for its financial support through assistantship. A special thanks goes to TL James and Company for the use of their materials and Louisiana Department of Transportation and Development for their collaboration through data collection. Special thanks go to David Hodnett, District Material Engineer in Monroe.

To all of the staff of Civil Engineering Program at Louisiana Tech University, the author would like to thank them for their help.

Finally, the author addresses his appreciation to his family. Special thanks for his wife Azaratou and his wonderful kids (Melissa, Samira, and Malick-Almoustapha) for their love and encouragement and to God through whom all things are possible.

CHAPTER 1

INTRODUCTION

The two most important characteristics of an unbound pavement base material are drainage and structural capacity. Inadequate drainage of the pavement structure has been identified as one of the primary contributing factors to the development of pavement distress [1, 2]. Excess water reduces the shear strength of the structural section and foundation materials by creating buoyancy within these materials [3]. Excess pore water pressure can be created within subgrade and pavement structural elements by wheel impacts, thus reducing structural capacity [4].

These situations can produce excessive deflection, cracking, rutting, reduction in load-carrying capacity, subgrade instability, pumping and loss of support [1, 3]. Drainable base course materials not only give the pavement strength just above the subgrade, but also provide a fairly rapid drainage path for water to flow through and out of the pavement before it can significantly weaken a vulnerable subgrade material.

To produce a free-draining layer, a major design consideration is the gradation of the aggregate. The gradation must also provides a reasonable balance between drainability and strength because higher permeability generally produces lower structural capacity i.e., these two factors work in opposition to one another [5]. Water always has been an enemy of highway and airport pavements. When a pavement subgrade, or the foundation soil, becomes saturated, it is weakened; the support for the pavement structure is reduced. Under the same traffic loading, a pavement structure with a weakened subgrade tends to deflect more, making the formation of cracks more likely and resulting in general weakening of the pavement. Unfortunately, when finer materials are removed from a dense-graded base course to make it more drainable, the strength of that base course generally is reduced so that the strength of the base course becomes more dependent on the confinement of the base than were the case before the fines were removed.

At what point does the base become drainable enough to be effective in protecting the subgrade from being saturated but continue to have sufficient structural integrity to withstand the applied traffic loads? Is there an "optimum" gradation that allows both effective drainage and provides adequate base strength? The main goal of this study is to develop a relationship between base drainability and base strength by conducting an extensive laboratory testing program on unbound base materials in which both drainability and strength are measured.

CHAPTER 2

REVIEW OF LITERATURE

2.1 Introduction

In the past, the primary function of a dense-graded base was to provide uniform support for pavements. As traffic loads increased however, erosion of fine gradation portion of the underlying material resulted and led to premature failure of the pavement section. To solve this problem a number of States Highway Agencies (SHAs) have began to use a more open-graded material to drain infiltrated water rapidly from the pavement structure [11]. This type of base is called a permeable base. A permeable base must serve three very important functions [11]:

1. The base material must be permeable enough so that the base course drains within the design time period.
2. The base course must have enough strength to support the pavement construction operation.
3. The base course must have enough strength to provide the necessary support for the pavement structure during service.

From the start SHAs recognized that permeable base design is a careful tradeoff between permeability and strength of the base material [12]. Efforts to produce this balance have followed two basic approaches toward producing the desired base material. First, some SHAs used their dense-graded aggregate base gradation and removed some of the fines to produce the necessary permeability. Second, other SHAs used the highest permeability that could be obtained with readily available material. These efforts resulted in two types of permeable bases:

1. Unstabilized material with no binder.
2. Stabilized material using asphalt cement, portland cement, or other some binder.

Unstabilized (i.e., unbound) bases consist of aggregate gradations that contain some finer-sized aggregates (passing the #4 sieve). The base develops its strength by good mechanical interlock of the aggregate, aided by the finer-sized material that fills some of the voids between the larger-sized particles [11]. Stabilized bases are more open-graded and thus much more permeable than unstabilized bases. Strength is produced by the cementing action of the stabilizer or binder material at the points of aggregate contact.

This study will focus on the unstablized permeable base. The permeable base must have enough strength to prevent rutting or displacement during the paving operation. Generally, if a permeable base has sufficient strength to perform adequately during construction, the base should have sufficient strength to support the design loads [12].

2.2 Sources of Water and Methods of Damage Minimization

The study of pavement drainage must begin by identifying the sources of water entering the pavement section. In the past, many sincere efforts to reduce the effect of moisture have been hampered by failure to recognize and provide relief for all water sources [14]. It is imperative that the engineer has a good understanding of the sources of water that may enter the pavement section. Figure 2.1 shows the various sources of water in pavements that have been identified, followed by a discussion of each.

1. Seepage from high ground. -This source may be significant in cut sections where ditches are shallow and in areas where poorly drained ditches hold water.

2. Ground water table rising into the pavement. -Seasonal fluctuations of the water

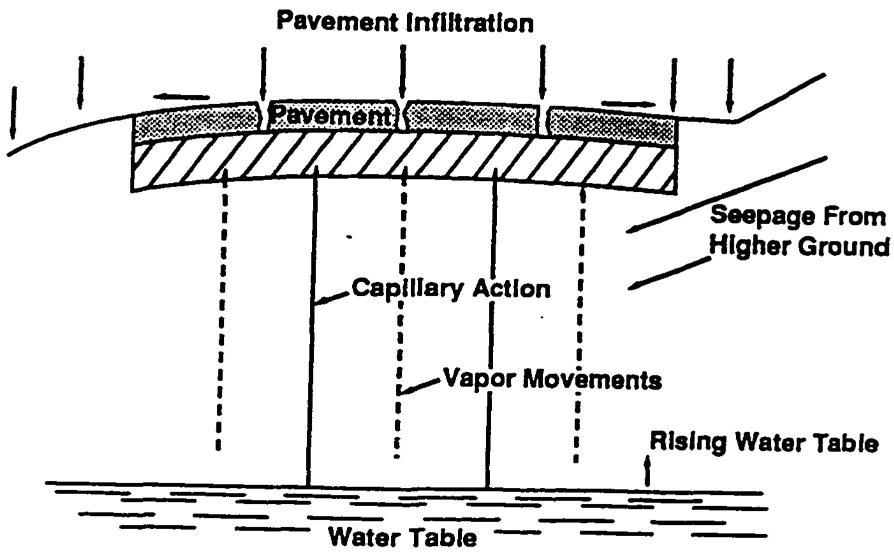

Figure 2.1 Sources of Water [11]

table (most commonly in the spring and winter) can be a significant source of water.

3. Surface infiltration of water. -Water enters through joints and cracks, making a very significant portion of the water in a pavement. Cedergren [15] found that during a normal rainfall, 33 to 67 percent of the precipitation could infiltrated into the pavement system trough surface cracks and joints. The actual amount entering the

pavement is limited by the ability of the pavement to store and remove water.

4. Capillary movement of water from the water table. -Like water being absorbed in a paper towel, surface tension and capillary action can transport water well above the water table, saturating the subgrade and adding water to pavement layers.

5. Water vapor movement. -Temperature gradient can cause the water vapor present in air filled voids to migrate and condense. Vapor water is involved in some forms of pavement distress (e.g., asphalt stripping).

Two methods are used to minimize moisture-induced damage to pavement systems [16]. The first method prevents moisture from entering the pavement system by sealing the joints and using impervious surface layers. As pavements age and cracks multiply, this method becomes increasingly impractical and expensive. The second method involves draining excess moisture from the system as quickly as possible. The presence of free water within a pavement structure can lead to the premature deterioration of a roadway [23]. To prevent this problem, a layer of permeable granular material can be placed within the pavement structure to enhance internal drainage. These drainage layers have proved to be highly effective in the efficient and rapid dissipation of water from a pavement structure and are used by many state and provincial agencies [6,7,8].

Due to their proximity to the pavement surface, however these permeable granular bases should also have adequate strength to resist traffic-induced shearing stress [9]. These shearing stresses may be amplified in the vicinity of pavement cracks (or joints in the case of reinforced concrete pavements) that can result in over-stressing the drainage layer [9]. The necessity of providing both adequate drainage and adequate strength are conflicting requirements [9,10]. If consideration had to be given only to the drainage aspect, round particles of a single size would appear to be the best suited, but there would be little strength in such material [10]. Conversely, a very dense and strong material, like a dense-graded base, would have poor or very poor drainage characteristics.

2.3 Open-Graded Base Materials

Some standard gradations have been developed by some SHAs to represent a careful trade-off between constructability/strength and permeability. Table 2.1 provides gradations of unstabilized permeable bases being used by some SHAs and their respective coefficient of permeability. Several of these gradations are plotted in Figure 2.2.

In 1988 the Federal Highway Administration (FHWA) conducted a survey [17] to identify the number of highway agencies using permeable bases found that number to be ten. A more recent FHWA survey [11] conducted in 1992 indicated that approximately twenty highway agencies have started using permeable bases in the construction of new pavements.

According to Baumgardner [12], a permeable base must provide both permeability and strength. Aggregate materials for permeable bases must be hard, durable, angular materials with good aggregate interlock. He suggests a minimum coefficient of 300 m/day (1000 fpd) for adequate drainage.

According to Ashraf and Lindly [16] a minimum permeability specification is necessary to take into account the variability between laboratory measured permeability and field permeability. The coefficient of permeability produced from laboratory test is in a fully saturated condition, rarely reached in the field. The laboratory measured permeability is higher than that experienced in the field.

Table 2.1 Some Currently Used Unstabilized Permeable Base Gradations [11]

Sieve Size	IA	MN	NJ	PA	AASHTO 67	LA Base
2"				100		
1-1/2"			100			100
1"	100	100	95-100		100	
3/4"		65-100		52-100	90-100	50-100
1/2"			60-80			
3/8"		35-70		33-65	20-55	
#4		20-45	40-55	8-40	0-10	35-65
#8	10-35		5-25		0-5	
#10		8-25				
#16			0-8	0-12		
#40		2-10				10-32
#50	0-15		0-5			
#200	0-6	0-3		0-5		3-15
K, fpd	500	200	2,000	1,000	18,000	N/A

Various researchers have made attempts to measure the coefficient of permeability of both open-graded material and stabilized open-graded materials. Zhou, et al. [18], measured the permeability of asphalt treated open-graded material and found it to vary from500 to 4,130 fpd. In a study conducted at the U. S. Army Engineers Experiment Station [19], a permeable base was built to achieve coefficients of permeability ranging from 1,000 fpd to 5,000 fpd. Tests performed in the laboratory on cored base specimens yielded coefficients of permeability of 40,000 fpd. A recent study conducted by Randolph, et al.

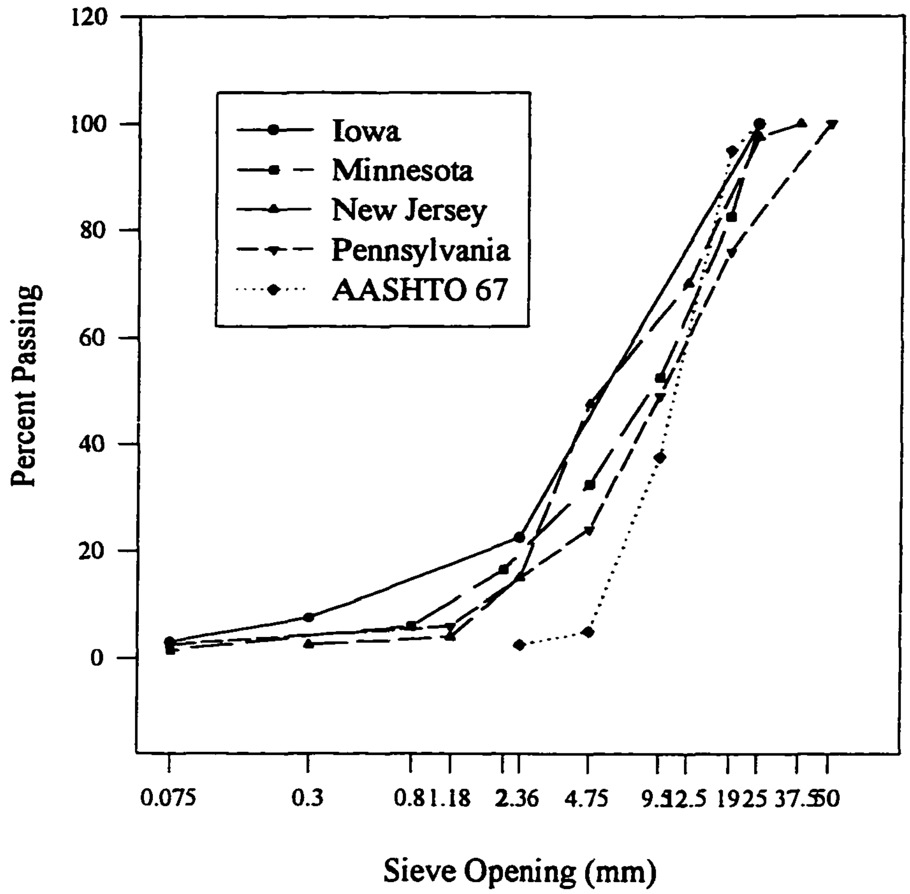

Figure 2.2 Some SHAs Open-Graded Permeable Bases [11]

[20], showed variations in coefficients of permeability from 5,000 to 8,000 fpd. Another study conducted by Jones and Jones [21] suggested that the currently available laboratory permeability tests are not precise to obtain repeatable coefficients of permeability.

To increase the permeability of aggregate base materials, researchers have suggested using the AASHTO No. 57 or 67 gradations. Both gradations have small amounts (0 to 5%) of material passing No. 8 sieve (see Table 2.1). According to Tandom and Picornell [22], base layers with these gradations have lower strength and stiffness because of poor mechanical interlock due to a lack of finer aggregates. In fact, a study conducted by Wisconsin Department of Transportation [23] established that if an open-graded material is used in a base layer, it is necessary to build haul roads for use during construction to prevent the permeable base layer from being damaged by the construction traffic.

Several researchers have studied strength and permeability of stabilized materials. Hall [23] has performed strength tests on cement stabilized open-graded material. These included compressive and bending tests on laboratory-cured specimens, compressive and split tensile tests on field-cured specimens, and split tensile tests core from the roadway. However, these tests were performed using static loads, not repeated dynamic loads. Zhou, et al. [18], measured resilient modulus and permeability of asphalt treated open-graded material in a project with the objective of proposing a new gradation for the state of Oregon. In 1997 Tandom and Picornell [22] presented results from a study in which they attempted to incorporate stiffness and strength together with drainability characteristics in the evaluation of materials for base layers. Their main goal was to select materials with an optimal compromise between high drainability while maintaining stiffness and strength at acceptable levels.

Recently, the FHWA has proposed new guidelines [11] for designing and constructing permeable bases. However, the design guidelines do not specify test methods or procedures for measuring strength and stiffness of the base material.

2.3.1 Summary

It can be concluded from the above discussion that:

1. Most of the research has been focused towards achieving higher permeability and little effort has been focused towards measuring stiffness or strength in the laboratory.
2. Unstabilized permeable base materials currently used have a coefficient of permeability on the order of 1000-3000fpd.
3. Little research has been performed that considers both permeability and structural stiffness and strength together study and attempts to identify an "optimal" relationship between the two opposing requirements.

For this reason a more detailed literature search follows which emphasizes the two important characteristics of an unbound pavement base; permeability and resilient modulus, which is the selected surrogate measure for strength.

2.4 Permeability

The coefficient of permeability can be used, for a given set of conditions, to determine the quantity of water that flows through the material. The quantity of flow increases as the coefficient of permeability increases (saturated hydraulic conductivity is used frequently in the literature instead of permeability). The coefficient of permeability of material can be estimated by field measurement, laboratory testing, or using empirically developed relationship.

2.4.1 Field Measurement

The best estimate for coefficient of permeability is determined from in-situ measurements [24]. A variety of reliable techniques have been developed for performing field permeability tests [25]. Moulton and Seals [26, 27] describe the development of an in-situ test device for determining the permeability of pavement aggregate base and subbase courses. This device has undergone an extensive program of laboratory and field testing [24].

2.4.2 Laboratory Testing

The nest best estimate for permeability is laboratory testing [28]. For laminar flow through soil, Darcy's law for one-dimensional flow can be used. This law states that the quantity of flow (Q) moving through a mass of soil or aggregate is equal to

$$Q = KiA \tag{2.1}$$

where Q is the quantity of flow (ft^3/sec),

K = coefficient of permeability (ft/sec),

i = hydraulic gradient (ft/ft)

A = cross-sectional area through which the flow occurs (ft^2).

The hydraulic gradient (i) is equal to the pressure head lost as water flows through the soil or aggregate divided by the actual length of the flow path over which the head is lost.

The flow in open-graded drainage material is often non-laminar (i.e., turbulent) even at low hydraulic gradients. As a result, Darcy's law, upon which most standard laboratory test methods are based, is invalidated [28]. According to Barksdale [24], two procedures can be used to correct for reduced efficiency caused by turbulent flow. The first procedure estimates the hydraulic gradient experienced in the field and the laboratory tests are performed at that estimated hydraulic gradient. Barksdale's second approach involves calculation of the Darcy permeability from laboratory tests performed under small hydraulic gradients that ensure laminar flow. Yemington [29] suggested using the time lag-permeameter to measure permeability under turbulent flow conditions. These tests results are then modified using a correction factor to account for the reduced efficiency caused by turbulence at the actual hydraulic gradients experienced in the field [28]. As mentioned earlier, transitional flow occurs at high velocities that can be characterized by the following equation for hydraulic gradient [22]

$$i = aq + bq^2 \tag{2.2}$$

where a and b are constants,

i = hydraulic gradient and q is the discharge velocity.

It has been shown that [21] Darcy's law is valid for base materials with hydraulic gradients smaller than about 0.05. To assess the laminar flow region [22], the measurements of "i" and "q" are fitted by regression to estimate parameters "a" and "b". The inverse of constant "a" is used to as estimate of the coefficient of permeability.

As reported by many researchers in testing open-graded unbound materials for permeability, a problem of soil migration occurs. According to Webb [45], soil particle migration occurs because of the large hydraulic gradient required to initialize flow through the specimen. He suggested that the hydraulic gradient be less than five. Highlands and Hoffman [46] reported that particles with a diameter of 2.0 mm (number 10 sieve) or smaller migrated within the material matrix during tests they performed. They also reported that the migration of 5% of materials tended to clog the water channels with the result that the coefficient of permeability decreased with testing time.

The problems created by particle migration demonstrated a need for a new permeameter. In 1952, Barber and Sawyer [47] introduced a falling-head permeameter designed to prevent turbulence, minimize particle migration, and maintain laminar flow conditions during testing.

2.4.3 Empirical Estimation

In practice, pavement designer often estimates the coefficient of permeability empirically without performing tests. Empirical equations are based on correlation between the coefficient of permeability and aggregate physical properties such as grain size characteristics, specific surface, dry density, and porosity or void ratio [16, 30, 31]. The nomograph given in Figure 2.3 can be used to estimate the coefficient of permeability of aggregate drainage material [32]. This nomograph was developed for material with a specific gravity value of 2.7. The most significant physical properties relating to permeability were effective grain size, D_{10}, porosity, n, and percent passing the No. 200 sieve, P_{200}. Figure 2.3 solves graphically the equation

$$K = \frac{6.24 \times 10^5 D_{10}^{1.478} n^{6.654}}{P_{200}^{0.597}} \tag{2.3}$$

According to Barksdale [24], these three parameters explain over 91% of the observed variation in the coefficient of permeability.

Cedergren [33] developed a formula to estimate the permeability of clean filter sand:

$$K\,(cm/sec) = CD_{10} \tag{2.4}$$

where D_{10} is the effective grain size in centimeters,

C is a regression coefficient that varies from 90 to 120, with a value of 100 often used.

One disadvantage of using this formula is that it ignores for the degree of packing or the porosity [16]. Cedergren [33] also developed a chart, reproduced in Figure 2.4 that can be used to estimate the coefficient of permeability for open-graded bases and filter material. Each curve in the chart has a specific gradation with an associated coefficient of permeability.

In 1979, Freeze and Cherry [38] presented the following formula to estimate the permeability of porous media:

$$K = \frac{C_1 d^2 \rho g}{\mu} \tag{2.5}$$

where C_1 = a constant that depends on the properties of the porous medium,

d = grain size of the uniform porous medium,

g = gravitational acceleration,

ρ = fluid density,

μ = fluid viscosity.

This formula was developed for use in groundwater hydrology, but its validity for estimating the permeability of highway drainage layers has not been validated.

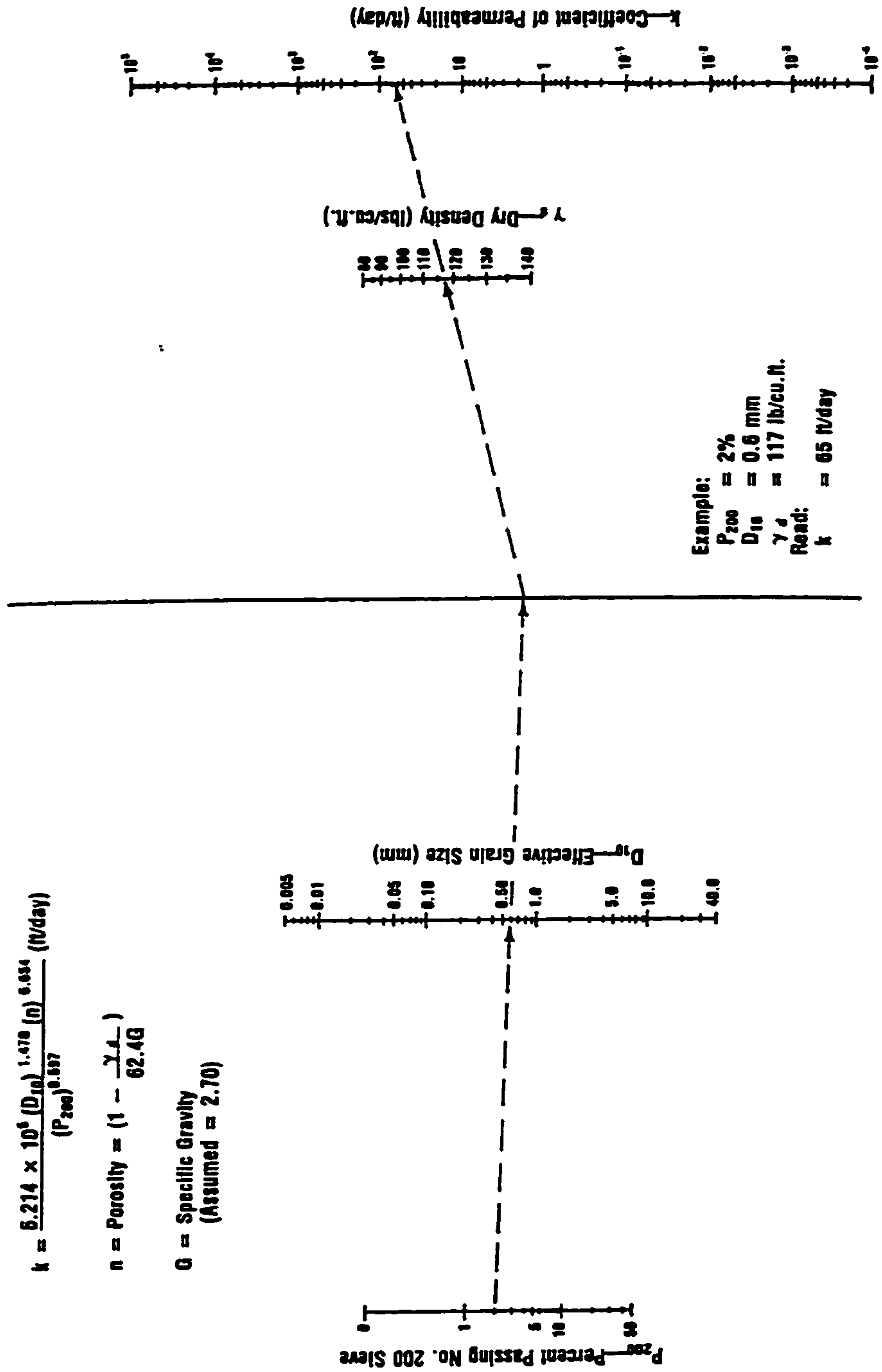

Figure 2.3 Estimation of Coefficient of Permeability of Granular Drainage and Filter Materials [32]

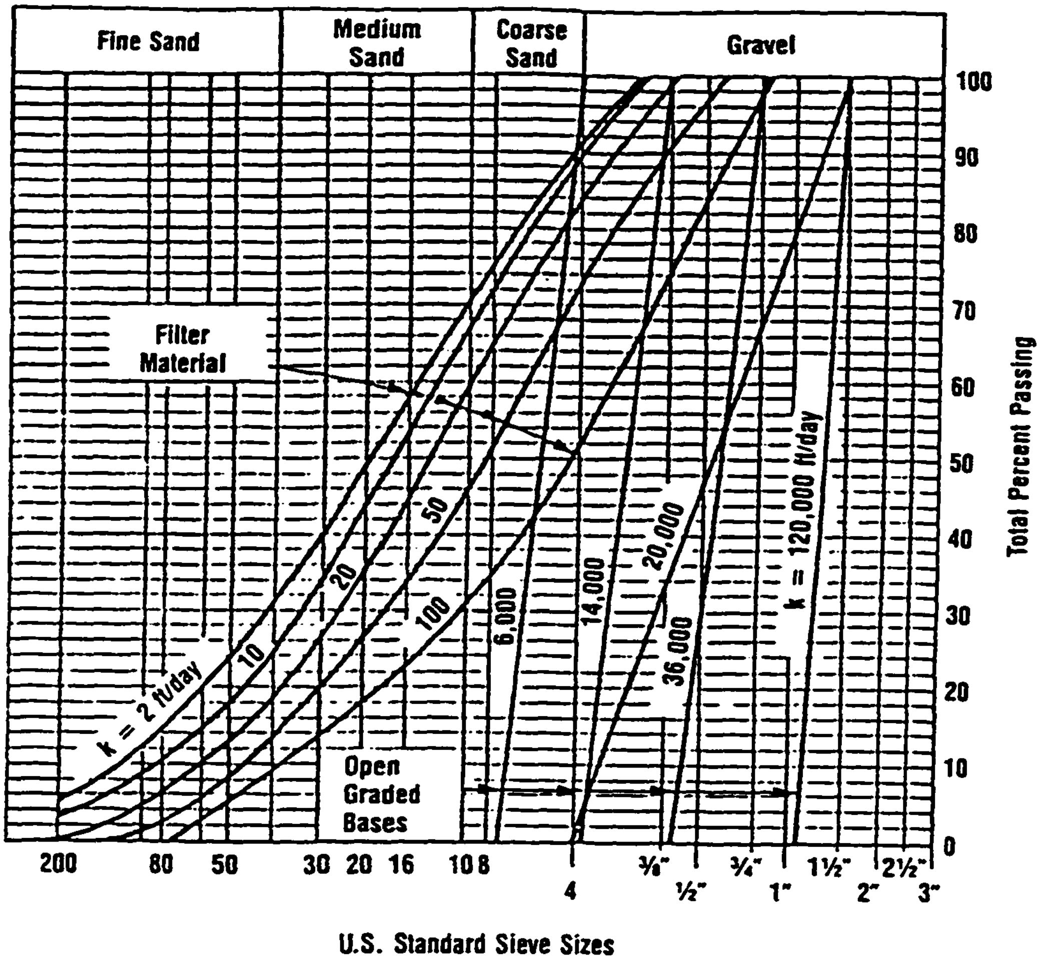

Figure 2.4 Typical Gradation and Coefficients of Permeability of Open-Graded Bases and Filter Materials [33]

2.4.4 Summary

The findings of the literature review on permeability can be summarized as follows:

1. To design drainage layers, Darcy's law is the basic formula, although some consideration must be given to the turbulent flow present in many open-graded materials.

2. Soil migration problems often occur when untreated, open-graded materials are tested for permeability using standard permeameter. Use of the low-head permeameter

introduced by Barber and Sayer appears to solve this problem for open-graded base materials.

2.5 Resilient Modulus

2.5.1 Introduction

Due to the amount of time and expense involved in building roads and highways, a considerable amount of laboratory work has been conducted to determine the engineering properties of base materials. A better understanding of these engineering properties should lead to higher quality roads that will last longer and need less repair. One of the most important properties of roadway base material is its load carrying capacity, i.e., its ability to withstand load without extensive deformation. In recent year a transition was made in laboratory of testing these materials from the static load triaxial to the repeated load triaxial test [39] in order to determine this property called the resilient modulus (M_r).

2.5.2 The Concept of Resilient Modulus

The resilient modulus is a measure of the load carrying capacity of a roadway material under repeated loading. M_r, similar to Young's modulus, is defined by the following equation:

$$M_r = \frac{\sigma_d}{\varepsilon_r} \qquad (2.6)$$

where σ_d = repeated axial deviator stress applied to the specimen,

(ε_r) = the recoverable strain

Figures 2.5 and 2.6 are graphs that show the test set-up for a M_r test and the load and deformation plots that can be obtained [40]. When a traffic load is applied to a pavement, the pavement layers deflect. Much of the deflection is recovered when the load is removed, but some remains and is called permanent deformation. Thus the results of the repeated loading test on a material tends to be more representative of reality than the result of a static test where virtually all deformation is permanent although both can provide insight into the performance of the material [40].

The shape and duration of the loading pulse applied to the specimen should simulate field loading conditions. The magnitude of stresses varies with the magnitude of the vehicle axle load, and the distance of the load from a point, the maximum stress occurs when the wheel load is directly over that point. The magnitude will generally reduce to zero as the wheel load moves away from the point under consideration. This situation implies that the pavement materials are subjected to two phases of loading [35]. The first phase consists of a pulse type loading with peak load of a certain magnitude. The loading phase will be followed by a relaxation phase in which no load is applied. Several different pulse shapes have been used by investigators [35] to simulate the loading on a pavement haversine, a triangular or a square function pulses. Vertical stress pulses measured at the American Association of State Highway Official (AASHO) Road Test were similar to a haversine pulse.

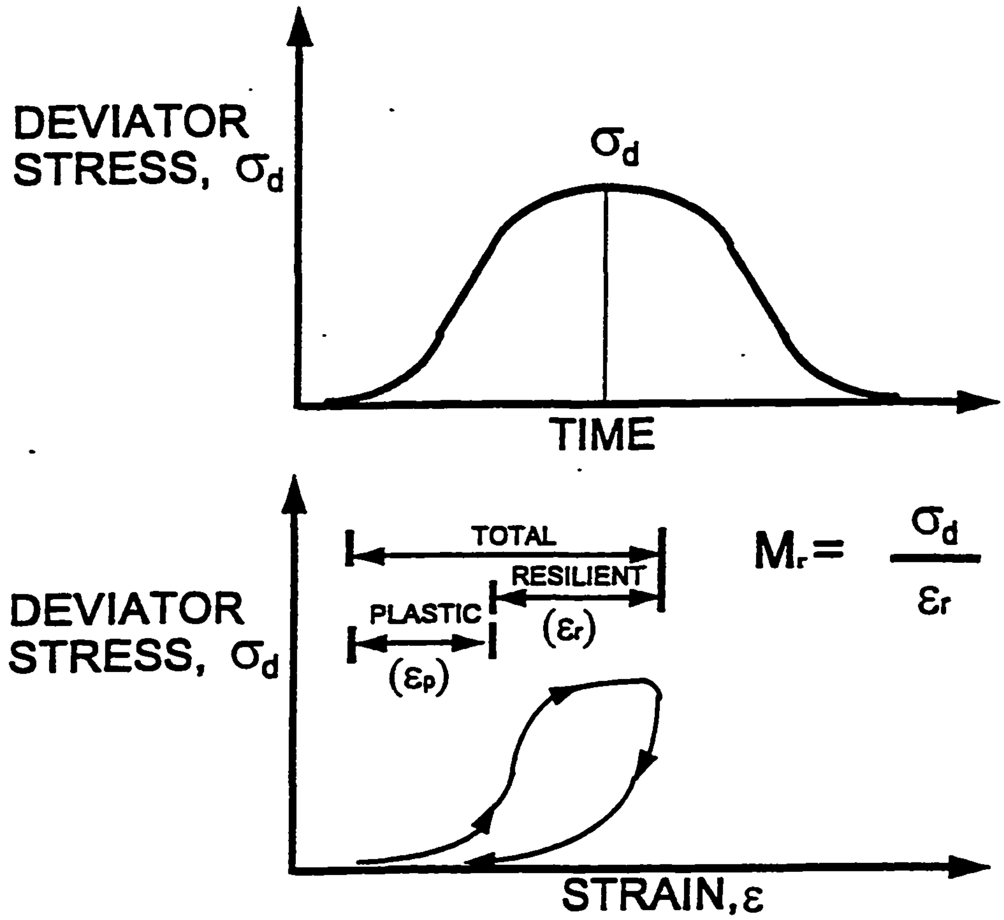

Figure 2.5 Test Setup for Determining Resilient Modulus from Repeated Load Test [35]

2.5.3 Parameters Affecting Resilient Modulus

The resilient modulus of base materials is dependent, on a number of factors including test factors (stress level, load duration, stress history) and sample factors (degree of saturation, density, fine content, aggregate type, aggregate size) [36].

The confining stress level has been determined to have the greatest effect on the resilient modulus [36, 37]. It has been shown that in the case of coarse-grained material, the resilient modulus increases considerably with increases in confining pressure and to a lesser degree with increases in the deviator stress, i.e., as confining pressure increases, the sample becomes stiffer. As long as shear failure does not occur the modulus can be approximately

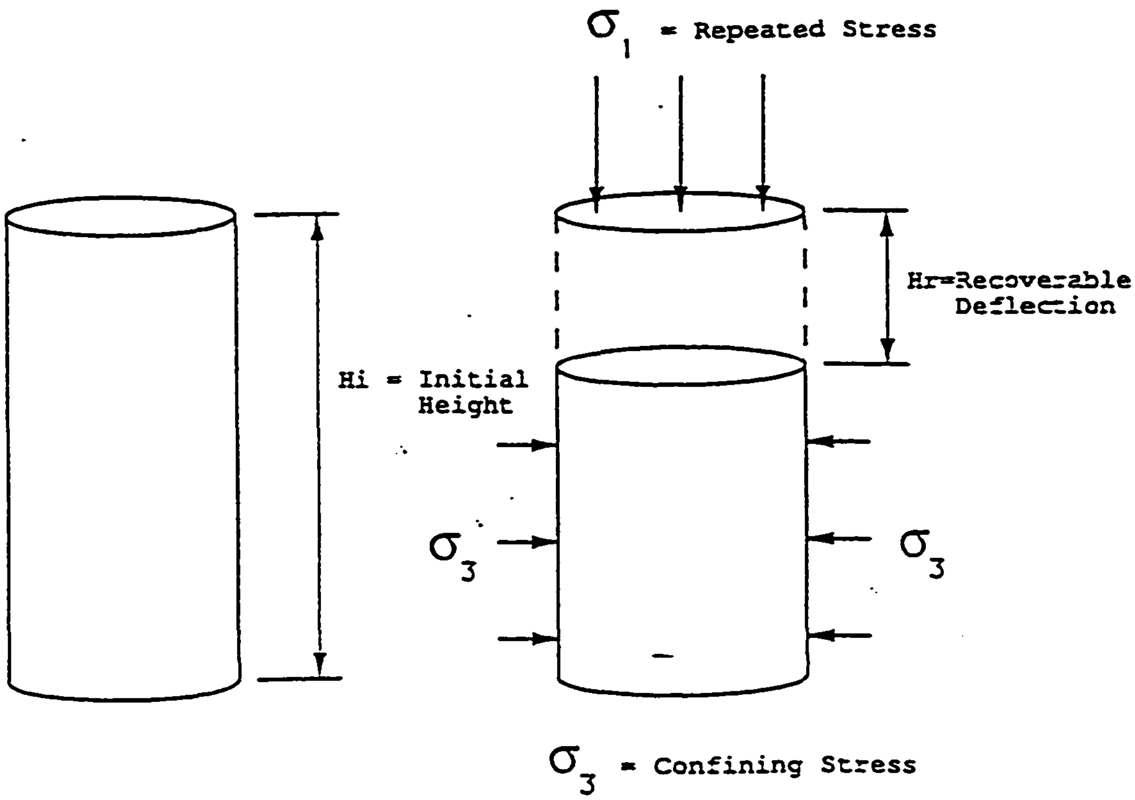

$$\sigma d = \sigma_1 - \sigma_3$$ = Repeated Deviator Stress

$$\frac{Hr}{Hi} = \varepsilon_r$$ = Recoverable Strain

$$M_r = \frac{\sigma d}{\varepsilon_r}$$ = Resilient Modulus

Figure 2.6 Definition of Resilient Modulus in a Repeated Loading Test [35] related to the confining pressure or the sum of the principal stresses. These relationship can be shown in the K-θ model by the following equation:

$$M_r = k_1 \theta^{k_2} \tag{2.7}$$

where k_1, and k_2 are material constants, and

θ is the bulk stress (first invariant).

Several researchers have examined the effect of load duration. Most repeated load triaxial tests with aggregate base materials are performed with a load duration of 0.1 to 0.2 seconds because most field loading conditions are in that range. Other research concludes that there is a minimal effect on resilient modulus when load duration is varied from 0.04 to 1.0 seconds [40].

The influence of stress sequence and number of repetition has been investigated on dry and partially saturated granular specimens by Hicks and Monismith [36]. They found that the resilient response determined after 50 to 100 axial stress repetitions could be used to properly characterize the behavior of granular materials. For a saturated granular material, they recommend that the samples be conditioned in a drained state with 100 to 200 axial stress repetitions before testing. The response after 50 to 100 axial stress repetitions provides a reasonable indication of resilient modulus (if the principal stress ratio does not exceed 6 to 7) for a material subjected to a complex stress history [36]. The effect of stress sequence has been found by others to be small if the test specimens were conditioned by stress applications prior to beginning to recording data.

The degree of saturation for a given aggregate plays a major role in the resilient response. Generally, the resilient modulus decreases as the degree of saturation increases.

According to Rada and Witczak [37], there is a critical degree of saturation near 80-85% above which granular material becomes unstable and deteriorates rapidly under repeated loading. Thompson [41] stated that for a given degree of saturation, soils compacted to the maximum dry density yield higher resilient moduli. Furthermore, resilient modulus obtained are higher on the dry side of optimum moisture content than on the wet side [42].

The other primary specimen preparation factor, which influences the resilient response, is the method of compaction employed to densify the specimen. It is reported that specimens prepared under static compaction yield higher resilient modulus than do those prepared under kneading compaction [43]. Also, the modulus measured on specimens prepared with static compaction is less repeatable when compared with that from specimens compacted using kneading compaction [44]. The resilient modulus of specimen compacted using the proctor method lies between the modulus obtained from specimens prepared with the static and kneading compaction methods [44].

Hicks and Monismith [36] stated that the resilient modulus of partially crushed aggregate decreases as the fine content increases (minus #200 sieve), while the modulus of crushed aggregate increases as the fines content increases. Thompson [42] agrees that for a given gradation the resilient modulus is higher for crushed material, than for partially or uncrushed material.

2.5.4 Summary

Because this research project focuses on the relationship between permeability and resilient modulus, the literature review reveals that the amount of fines has significant effect on both characteristics. From the above discussion, it can be concluded that:

1. Permeability decreases as the fines content increases.

2. Good drainability is provided by much more open-graded aggregate containing few if any fines.

3. As the fines content increases so does the strength (as measured by the CBR test) until an optimum level is reached; increases the fines above that level produces a decrease in strength (Figure 2.7).

A practical compromise between permeability and resilient modulus is most readily produced by blending a standard coarse aggregate size such as No. 67 stone (see Table 1), with a smaller-sized coarse aggregate or washed stone screenings [24]. According to Barksdale [24] an aggregate blend of two coarse crushed materials, should meet both strength and permeability requirements.

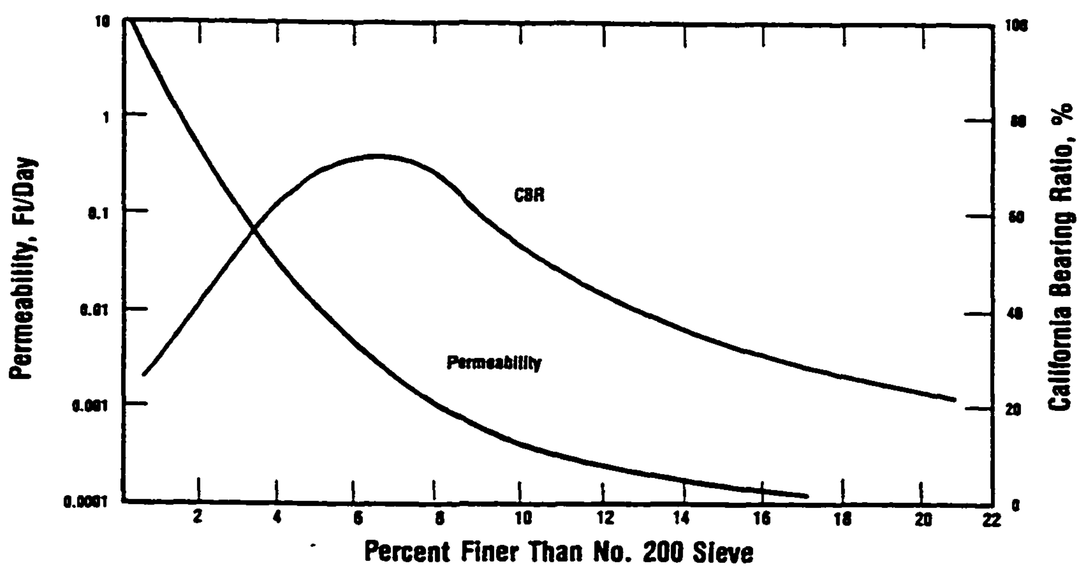

Figure 2.7 Relationship between Stability and Permeability [24]

CHAPTER 3

PLAN OF STUDY

3.1 Research Approach

One typical crushed base material widely used throughout Louisiana in a flexible pavement will be identified and sample several. This base material will first be characterized and then tested to evaluate the relationship between the coefficient of permeability and strength, and stiffness characteristics.

3.2 Proposed Design Parameters

Stiffness and strength characteristics of the base material will be assessed using the resilient modulus and /or compressive strength tests. The principal concern in evaluating the base drainability is how quickly the pore water accumulated in the base drains out of the matrix under forces of gravity. The saturated coefficient of permeability will be determined from a low-head permeameter test on six inches diameter specimens of the granular material of different gradations with a maximum one inch aggregate size.

3.3 Design of Experiment

The literature showed that State Highway Agencies (SHAs) which have experience with open-graded layers specify a coefficient of permeability for those layers in the wide range of 200 to 20,000 fpd, with most states specifying values from 1,000 to 3,000 fpd. This study will include three different gradations to cover the first range of coefficients of permeability while maintaining an acceptable level of strength and resilient modulus.

Before discussing the permeability and resilient modulus testing procedure, it is important to describe how the five gradation levels were selected. The grain size distribution tables and curves for all soils used in this study are listed in Appendix A. The first gradation (level 1) is a typical gradation for dense graded base layers used in highway construction by the Louisiana Department of Transportation and Development. This level was selected as a control gradation to represent a base with a large amount of fines. Level 5 consists of an AASHTO 67 base, which is considered as a very open gradation. Three other gradations for highly permeable bases were developed with low, medium and high levels of permeability. Level 2 (low) was developed to have a permeability around 2,000 fpd. This low permeability level was achieved by starting with an AASHTO 67 gradation, which has a nominal coefficient of permeability of 18,000 fpd (Table 2.1), and practically no fines. To achieve the 2,000 fpd, the AASHTO 67 gradation was altered by blending 65% AASHTO 67 gradation with 35% screenings (A65_S35 blend, Figure 3.1). This mixture was then used to manufacture the specimens representing both the low level of permeability and the resilient modulus test series. Levels 3 and 4 were produced to have coefficients of permeability of 4,000 and 12,000 fpd, respectively, by manufacturing a 75% AASHTO 67 with 25% screenings (A75_S25) blend and a 85% AASHTO 67 with 15% (A85_S15) screenings blend. Figure 3.1 shows the gradation curves of the AASHTO #67 and Louisiana base materials. At each level, 5 replicates of permeability, resilient modulus and compressive tests were conducted. Table 3.1 contains a matrix showing the various cells of the test program mentioned above.

Before starting the permeability and resilient modulus tests, some basic tests (specific gravity, and compaction) were conducted on each gradation to determine the sample density required during testing. Once the aggregate gradations were selected for the permeability testing, specimens from those same gradations were prepared and tested to measure M_r at different deviator and confining stresses.

The deviator stresses are mainly induced by vehicle loads and are estimated using elastic layer analysis (ELSYM5). In other words, after selecting a typical thin and a typical thick flexible pavement cross-sections with unbound granular material as base, and for different subgrade modulus values (Figure 3.2), three level of stress were calculated at the top, middle, and bottom of the base layer for a typical load combination (Figure 3.3). These loading and stress levels represent conditions to be encountered on the existing roadway pavement structure. The thin pavement represents a typical low-volume road, while the thicker section represents a primary or arterial facility. The range between the maximum and the minimum vertical stresses, induced by the load configuration considered is then divided approximately in five equal ranges, each representing a stress sequence. The confining stresses were estimated by taking the product of vertical stress on the base layer and earth pressure coefficient at rest that is assumed to be 0.4.

Tables 3.1 and 3.2 represent respectively the testing program and the results of the stress analysis using ELSYM5, a linear elastic pavement analysis program. Upon completion of the resilient modulus test, the confining pressure was reduced to zero, and a load at a rate of 0.5 mm per minute, was applied to drive the specimen to failure. During this test the applied axial strength was recorded to calculate the unconfined compressive strength.

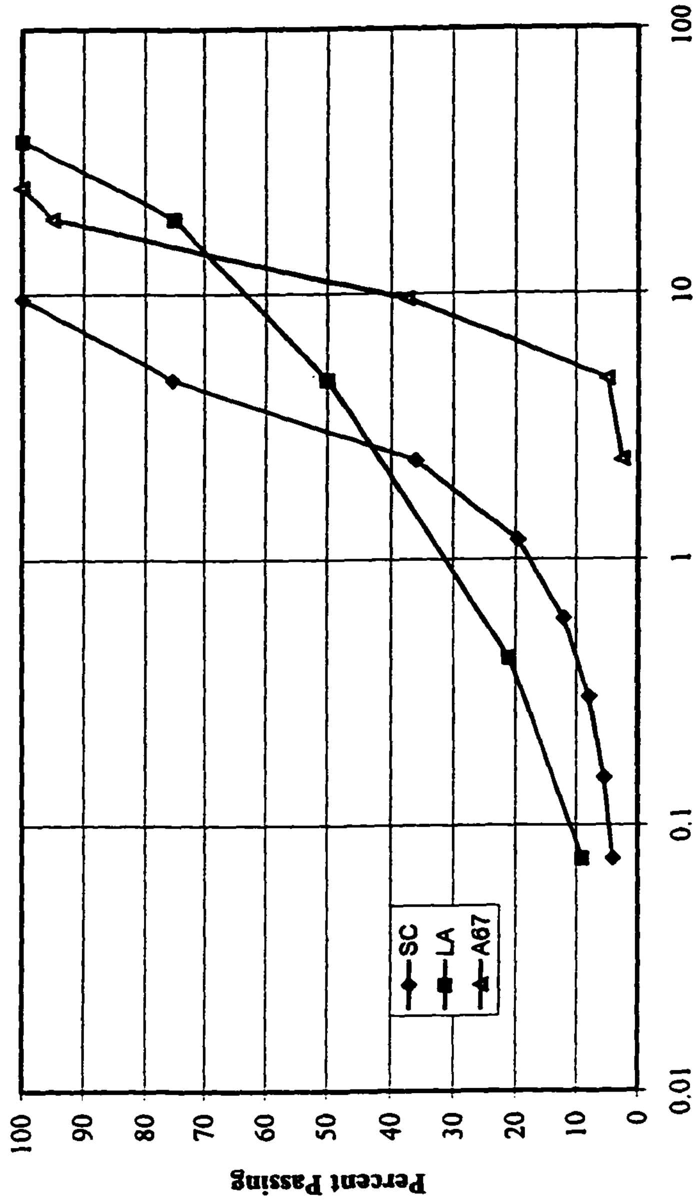

Figure 3.1 Gradation Curves for AASHTO #67, Louisiana Base and Screenings (mid-range specifications)

Table 3.1 Testing Program

	Number of Tests		
	Permeability (k)	Resilient Modulus (Mr)	Compressive Strength
Typical Base in LA Level #1	5	5	5
Level #2: Low 2,000 ft/day Gradation	5	5	5
Level #3: Medium 4,000 ft/day Gradation	5	5	5
Level #4: High 12,000 ft/day Gradation	5	5	5
Level #5 AASHTO 67	5	5	5

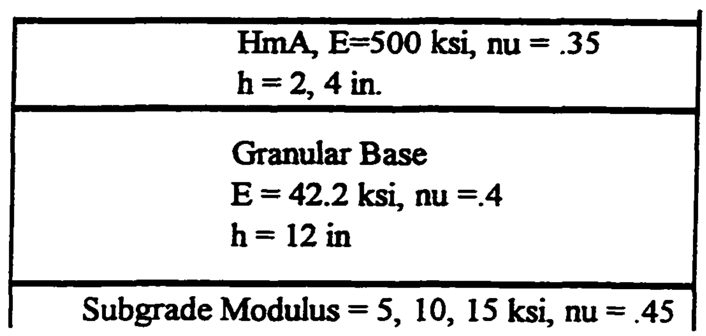

a) Thin Flexible Pavement

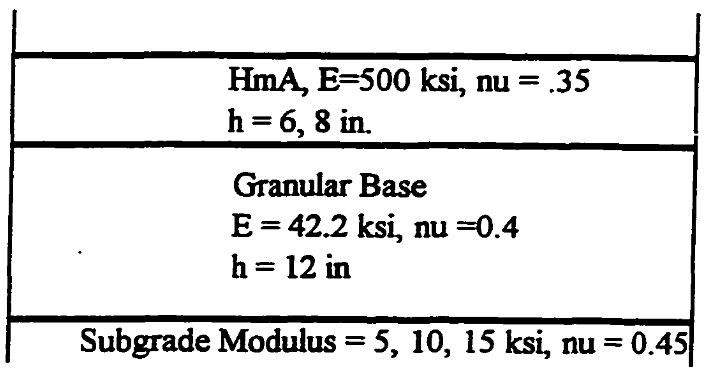

b) Thick Flexible Pavement

Figure 3.2 Cross-sections Used in Analysis

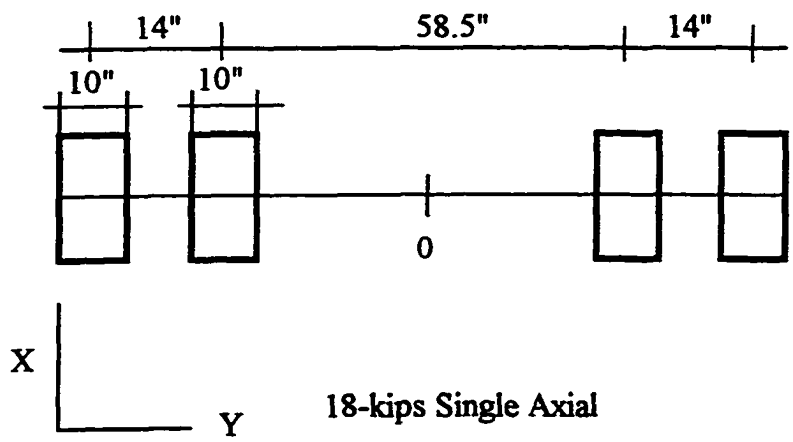

Figure 3.3 Load Configuration Used in Analysis

Table 3.2 Results of the Stress Analysis Using Elsym5

Surface Thickness, in.	Principal Stresses, psi	Subgrade Modulus, ksi		
		5	10	15
2	Sxx	11.21	4.24	-5.97
	Syy	17.99	9.74	5.41
	Szz	**-25.49 (10.2)**	**-29.13 (11.65)**	**-31.57 (12.8)**
4	Sxx	9.67	4.69	1.897
	Syy	14.29	8.19	4.87
	Szz	**-11.38 (4.55)**	**-13.79 (5.52)**	**-15.45 (6.18)**
6	Sxx	7.425	3.98	2.02
	Syy	10.72	6.44	4.04
	Szz	**-6.49 (2.60)**	**-8.17 (3.26)**	**-9.38 (3.75)**
8	Sxx	5.88	3.23	1.75
	Syy	8.16	5.08	3.31
	Szz	**-4.25 (1.7)**	**-5.43 (2.17)**	**-6.32 (2.52)**

Sxx, Syy and Szz represent respectively the principal stresses in x, y, and z directions. The boldface numbers between brackets represent the confining pressures. The boldface numbers, represent the vertical stresses, the range between the maximum and minimum was divided in five intervals representing the different stress levels used in collecting the resilient modulus testing data.

3.4 Tasks

The tasks of this research are below:

A. Conduct intensive laboratory testing on open and dense-graded materials with respect to their drainage (permeability) and stiffness and strength (resilient modulus and unconfined compressive strength) characteristics. The determination of permeability is necessary if an evaluation of drainage capability of an existing or new base layer is needed. The determination of the resilient modulus is necessary as it is an input data for pavement design using the AASHTO procedure.

B. Perform permeability and resilient modulus tests to study the effect of introducing fines (percent passing #4) added to an open-graded base layers on the base permeability and resilient modulus.

C. From the data collected from these tests on both drainage and strength characteristics, perform regression analysis to develop formulas that relate percent fines to permeability and to resilient modulus.

D. Combine the test results from permeability and resilient modulus, to provide a range of percent fines gradation band that will satisfy the two parameters as pavement design inputs.

E. Provide some tools and techniques used to prevent the base course from being contaminated by subgrade material and to check if the proposed base course is able to drain water as quickly as possible.

CHAPTER 4

TEST PROCEDURE

4.1 The Barber and Sawyer Permeameter

After reviewing the literature, the permeameter introduced by Barber and Sawyer in 1951 [47] was selected for use in the permeability test series since it was used successfully at the Pennsylvania Transportation Research Facility and for research in the College of Engineering at the University of Alabama-Tuscaloosa. This permeameter is a falling head permeameter, and the equations used to calculate the coefficient of permeability are explained by Yemington [29]. A low-head Barber and Sawyer permeameter was manufactured in the University of Alabama College of Engineering machine shop for use on this project. A description of the apparatus, test method and calculations for the coefficient of permeability were taken from Ashraf and Lindly [16] and are described next.

4.1.1 Apparatus Description

As shown on Figure 4.1 the Barber and Sawyer permeameter consists of an outer cylinder that is closed at the ends and equipped with a quick-opening valve near the bottom. The specimen is compacted in the inner cylinder. The specimen is supported on a base ring that has perforated walls. A No. 10 wire mesh (2.0mm opening size) is attached to the top of the base ring to support the specimen. A No. 200 wire mesh (0.075 mm opening size) is inserted between the specimen and the base to prevent the fines from exiting during the test. The permeameter has a 15.2 cm (6.0 in.) diameter inner cylinder and a 30.5 cm (12.0 in.) diameter outer cylinder.

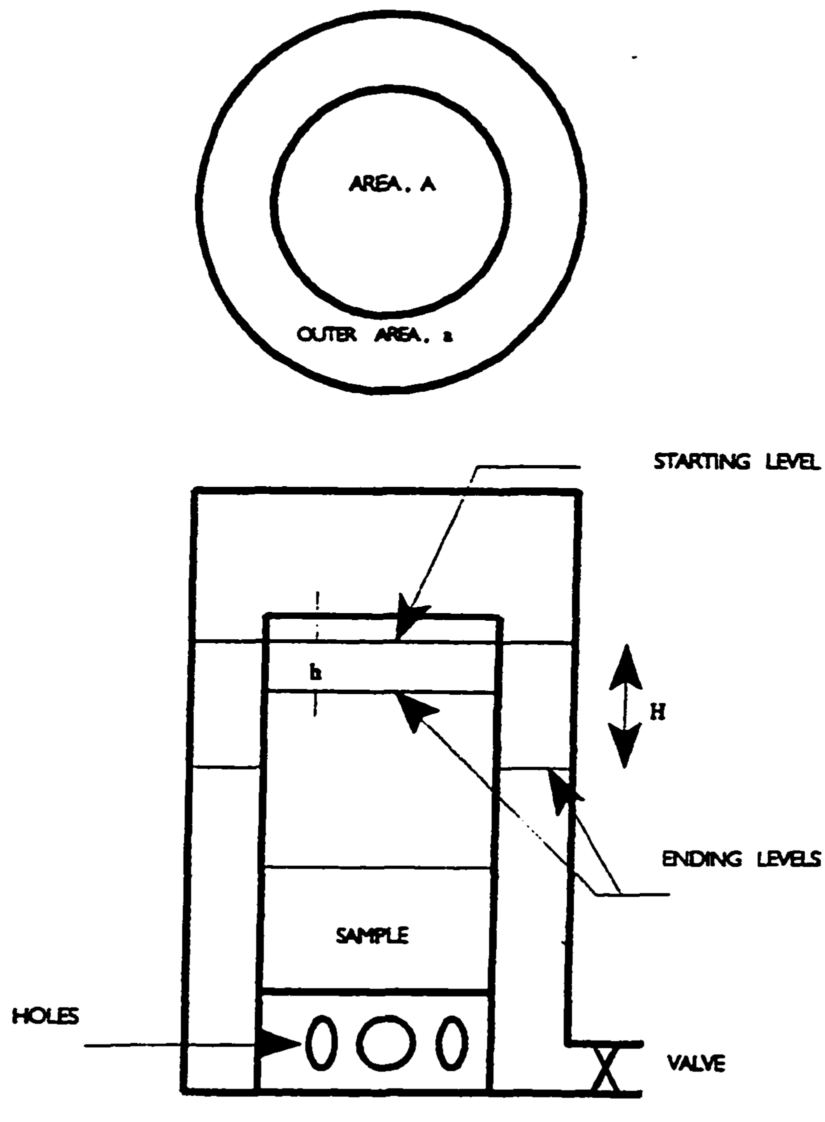

Figure 4.1 Sketch of a Barber and Sawyer Permeameter

4.2 Preliminary Tests

Before running the resilient and permeability tests, the specific gravity and maximum dry unit weight of the different gradations were needed. A sieve analysis was completed to determine how the compaction energy could change the gradation. All tests were conducted according to AASHTO specifications.

The optimum water content and the maximum dry unit weight was determined, using AASHTO specifications, for each of the five aggregate blends and are given in Chapter 5. During compaction the open-graded materials could not hold compaction water when the percent water exceeded 2% therefore the open-graded materials were compacted at 1.5-2% water content.

4.3 Permeability Tests

4.3.1 Using the Barber and Sawyer Permeameter

This permeameter was used to measure permeability of all specimens. Each gradation was mixed with a calculated weight of water to bring the water content close to the optimum for the Louisiana base. The open-graded gradations were mixed with only 1.5-2% water since, these gradations cannot hold a large amount of water. The inner cylinder was then placed on a solid plate, and the material to be tested was placed in the cylinder and compacted in three layers. The net mass and the average height of the specimen were measured. A cover was placed on the top of the specimen inside the cylinder and bolted to the body of the inner cylinder. The inner cylinder was then turned upside down again and the top was removed. Next, the inner cylinder was placed inside the outer cylinder. Water was added slowly to the outer cylinder until the sample was saturated and covered with at least 2.5 cm of water.

After reaching equilibrium, where the water level in both the inner and the outer cylinders was the same, the height of water in the inner cylinder was measured using two vertical scales fixed at right angles to a horizontal steel bar above the sample. The quick-opening valve at the bottom of the outer cylinder was opened, and the outflow was caught. A stop watch was used to determine the time required for the inner water level to reach a predetermined level, at which point the watch was stopped and the quick-opening valve were closed simultaneously. The drop in water level in the inner cylinder was recorded. Both the outflow volume and associated time in seconds were recorded. The cylinders were then refilled with water and the test repeated. Several runs were made until five consecutive consistent sets of data were recorded. The data from each of the five consistent runs were reported as the test result and that data used to calculate coefficients of permeability K which were averaged. The average was reported as the representative coefficient of permeability.

Calculation of the coefficient of permeability K, was accomplished using equation 4.1:

$$\mathbf{K} = \frac{\mathbf{F}}{1 - \frac{\mathbf{hs}}{\mathbf{Q}}} \frac{\mathbf{ad}}{\mathbf{St}} \qquad \mathbf{(4.1)}$$

where;

Q = the outflow volume caught in time t,

$S = A + a$,

A = cross-sectional area of the specimen,

a = outer area as referred in Figure 4.1,

h = the drop in water level inside the inner cylinder,

d = sample height,

F is a constant implicitly defined as follows

$$\frac{hS}{Q} = 1 - \frac{F}{\ln \frac{1}{1-F}} \tag{4.2}$$

F is difficult to calculate using equation 4.2. Since the value (hS/Q) could be calculated from the test data, a simple algorithm was written using a microcomputer spread sheet software to obtain the F value that corresponded to the (hS/Q) value from the test. The algorithm assumes a value for F and then calculates the corresponding (hS/Q) value. The calculated (hS/Q) value is compared to the measured test value. Then the algorithm changes the F value and goes through loops until the calculated hS/Q is equal (within some percent error) to the actual one. Yemington [29] provided a curve of F vs. hS/Q that can also be used (Figure 4.2).

4.4 Resilient Modulus Test Equipment

All specimens fabricated for the 5 levels of gradation were tested using a closed-loop, servo-controlled, electro-hydraulic system (MTS 810) installed in the Civil Engineering Material Research Lab. A 22-kip load cell calibrated to 20-kip was used to apply vertical loads to the 6 in. diameter by 12 in. high cylindrical specimens. Two

Keithley Series 500 data acquisition and control systems were used with two personal computers to control the loading and to acquire the test data (Figure 4.3). One system was used to generate the haversine load pulse form (Figure 4.4) through the MTS 810 and to apply the haversine load over 0.1 second followed by a 0.9-second rest period as required in the resilient modulus testing procedure (AASHTO T292-91).

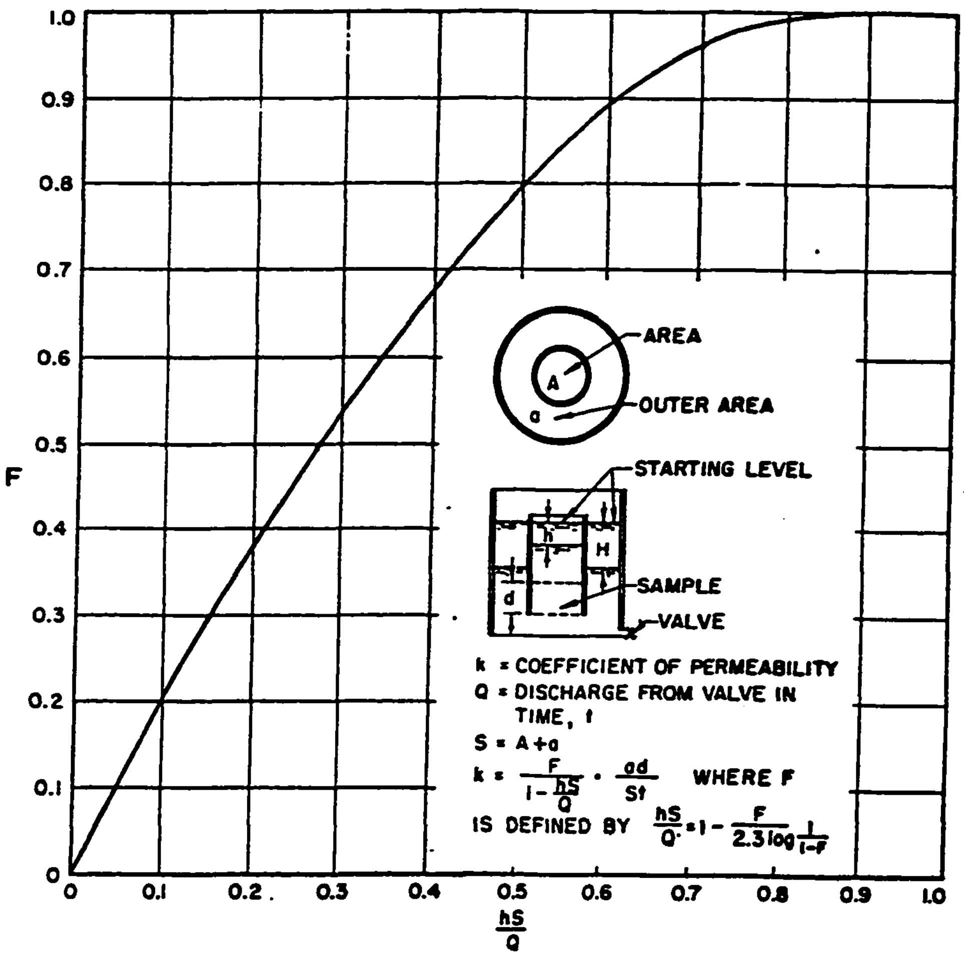

Figure 4.2 F vs. hS/Q [29]

The second system was used to acquire the voltage signals from the linear variable differential transducer (LVDT) and load cell mounted on the MTS actuator. All Keithley Series 500 data acquisition program configurations used during resilient modulus testing are included in Appendix B. Figure 4.5 shows a detailed sketch of the triaxial chamber with external LVDT and load cell. The single actuator-mounted LVDT was used for all sample deformation measurements instead of the dual external-mounted LVDTs shown on top of the triaxial cell in Figure 4.5. To transfer the load from the repeated load actuator to the sample cap via the chamber piston road, a steel ball was used at one end of the chamber piston rod. The lateral earth pressure was simulated by applying suitable air confining pressure through the cell pressure inlet, while two top caps outlets and two bottom cap outlets were opened to expose the sample to the atmosphere.

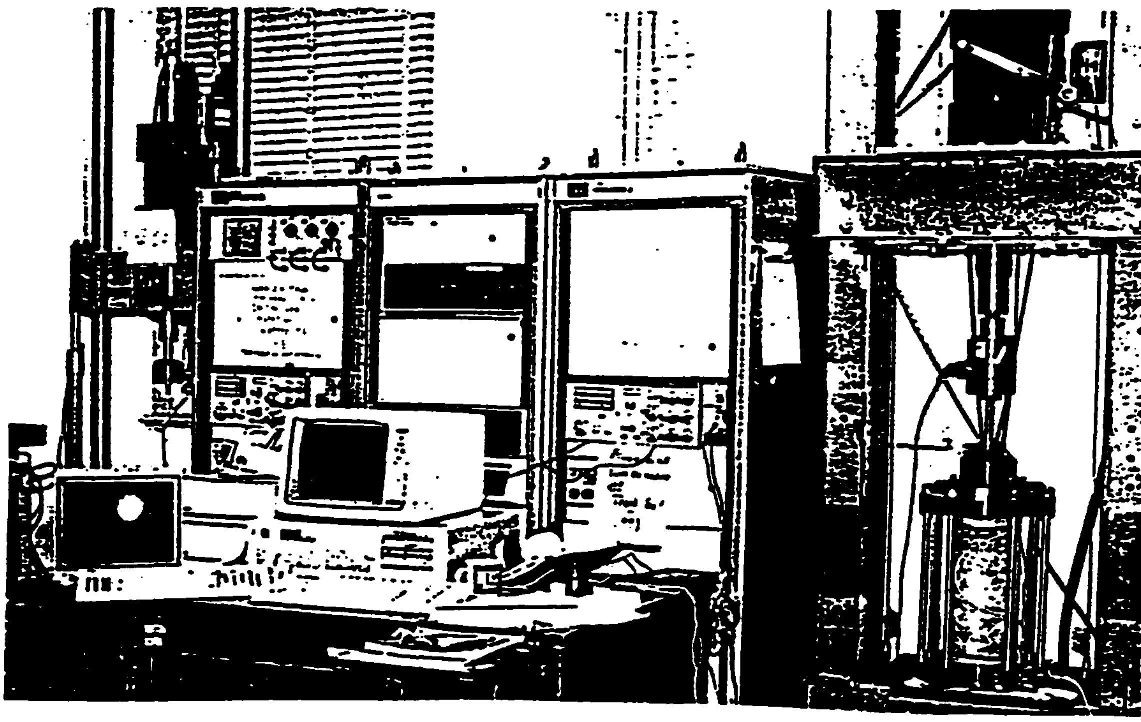

Figure 4.3 Testing System

4.4.1 Specimen Preparation for Resilient Modulus Tests

To reduce the variability in the test specimens, the Louisiana base, AASHTO 67 stone and screenings were oven-dried and sieved respectively into 3, 4, and 2 different sizes range and stored separately, respectively. The exact gradation for each specimen was obtained by weighing the appropriate amount from each size range according to its grain size distribution. Five-pound specimens were weighed, mixed and stored in plastic bugs until ready for compaction and testing. This procedure was instituted to minimize gradation variability.

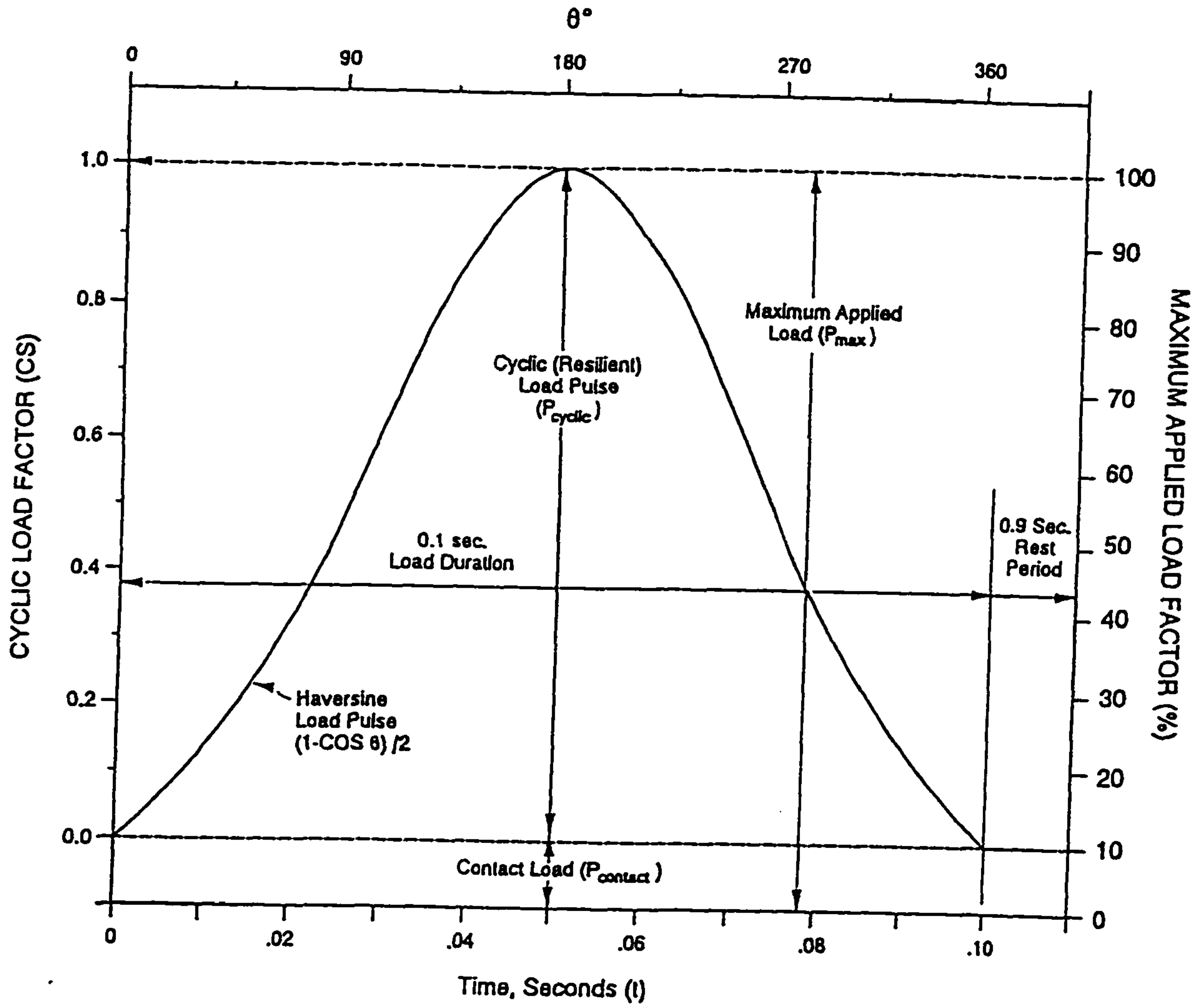

Figure 4.4 Haversine Load Pulse [39]

For each level, the appropriate moisture (obtained from the compaction test) was added to each five-pound bag, mixed and each specimen compacted in five equal lifts using a vibratory hammer. As shown in Figure 4.6, the specimen was prepared in a split

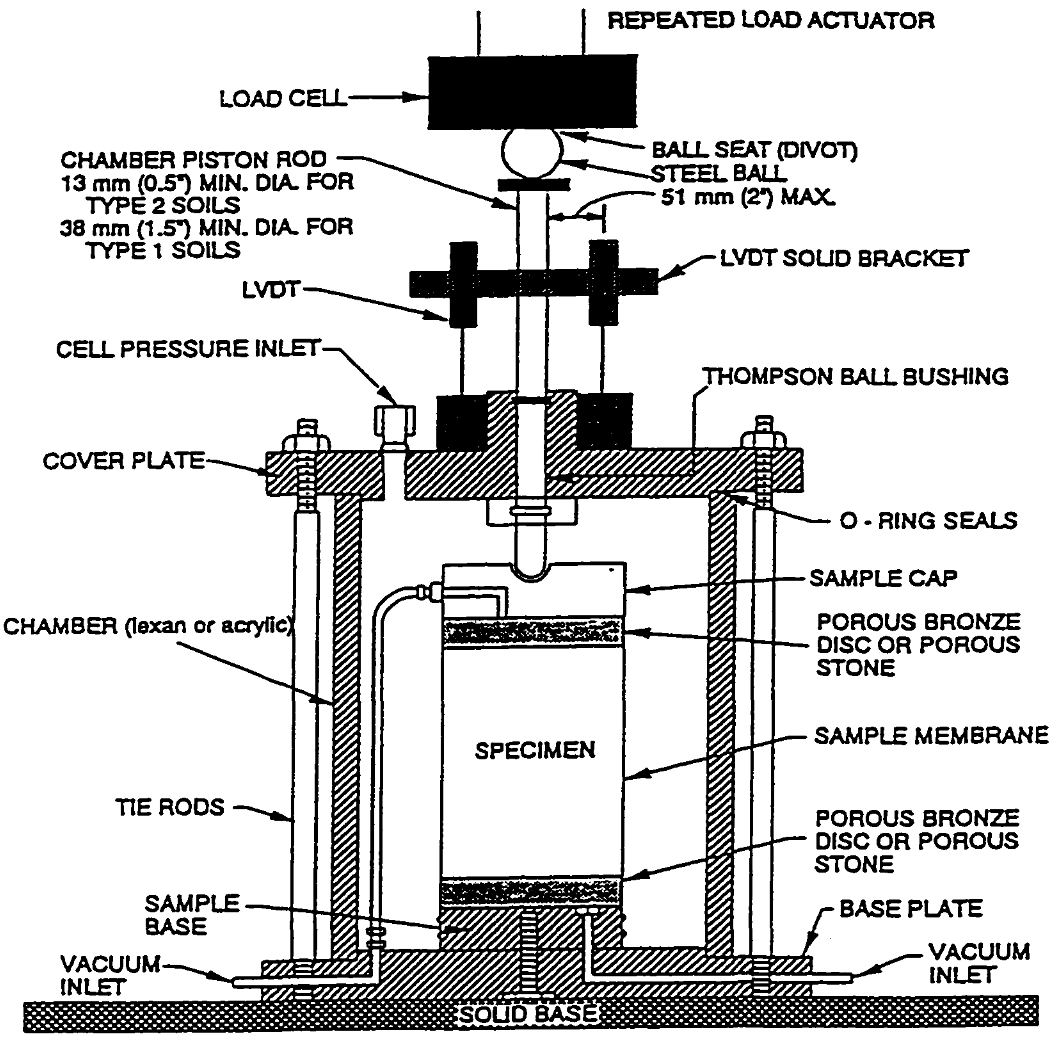

Figure 4.5 Triaxial Chamber with External Mounted LVDTs and Load Cell [39]

mold sitting on the bottom platen of the triaxial cell. To provide ample clearance for the specimen during compaction, a vacuum was applied to draw the membrane against the split mold.

After compacting the specimen, a ruler was used to measure the height of each lift, and the vibratory compaction was stopped when proper height was reached for each lift. Before removing the split compaction mold from the compacted specimen, a porous stone and the top cap were placed on the top of the specimen. O-rings were used to seal the membrane to both the top and the bottom caps. In the event that the membrane was punctured during compaction, a second membrane was placed around the specimen and sealed to both the top and the bottom caps by two additional O-rings. After being covered by the top platen and transparent plastic wall of the triaxial cell, the cell and the specimen were lifted into the MTS 810 loading frame and readied for testing.

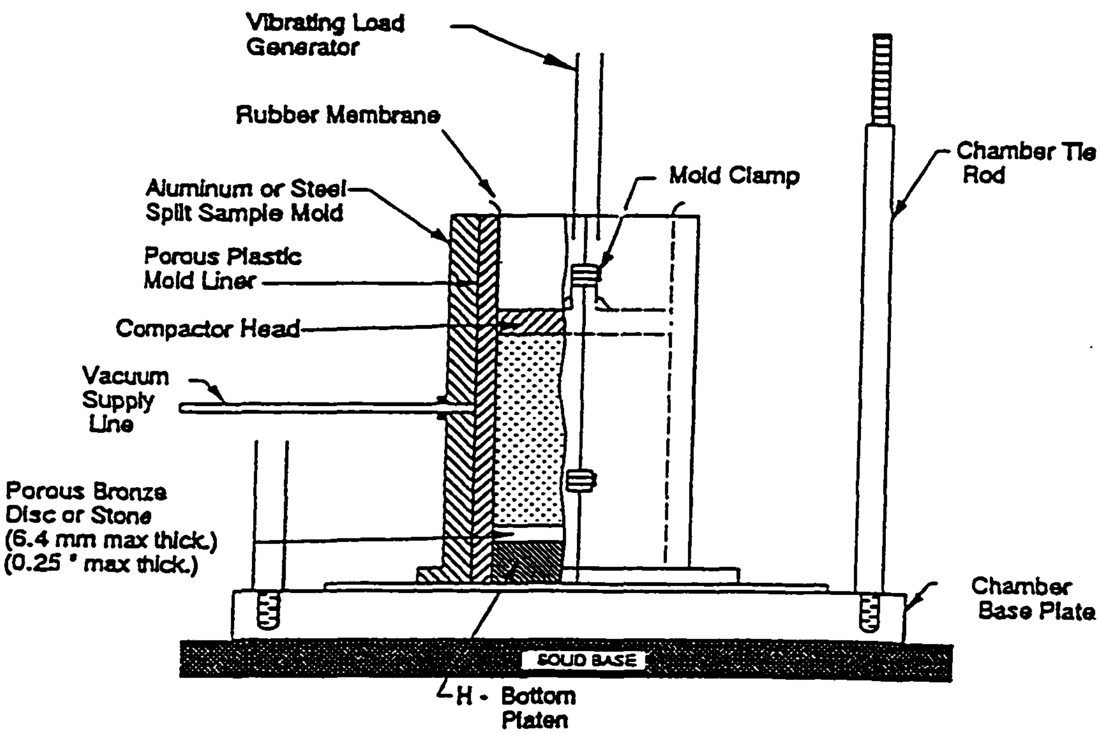

Figure 4.6 Apparatus for Vibratory Compaction of Unbound Materials [39]

4.4.2 Test Procedure

AASHTO T292-91 (Resilient Modulus of Unbound Base/Subbase Material and Sub-grade Soil) was generally followed. First, an air confining pressure equal to the highest level required in the AASHTO procedure was applied to the specimen. The specimen was conditioned using a cyclic deviator stress of 15 psi applied in a haversine type of pulse wave with 0.1-second load duration. The cyclic stress was then removed for a 0.9-second rest period at a constant deviator stress of 1.5 psi. This conditioning was repeated for 1000 cycles.

After conditioning each specimen, five different combinations of confining pressure and cyclic stress were applied. Each stress level was applied for 100 cycles, and the signals from the load cell and LVDT of the last five cycles were collected by the Keithley data acquisition and control system. The combination of stress states included in this study was selected to cover the expected in-service range and are presented in Table 4.1.

Table 4.1 Test Stress of States and Repetitions

Phase	Sequence No.	Maximum Deviator Stress	Confining Pressure	No. of Repetitions
Specimen Conditioning	0	15	13	1000
Testing	1	3	2.5	100
	2	5	5	100
	3	9	7	100
	4	13	9	100
	5	19.5	13	100

CHAPTER 5

TEST RESULTS

The test results from the permeability, resilient modulus, and unconfined compression tests are presented. Only those results used in the final analyses are contained in this chapter; a complete set of data is included in Appendix C.

5.1 Permeability Test Results

The Barber and Sawyer permeameter was used to test dense-graded (Louisiana) crushed limestone base and untreated open-graded material. Tables 5.1 through 5.5 show the permeability test results for the level gradations used in the study. The top section of each table contains the sieve analysis results performed on each specimen after the permeability test was run. The middle section of each table contains the coefficient of permeability, K. The reported values are the average of five measurements taken on each specimen as well as height of each specimen in centimeters. The bottom section contains the wet and dry unit weights and the water content of each specimen before testing.

A total of 25 tests were performed using the Barber and Sawyer permeameter. Figure 5.1 shows the relationship between percent fines passing #4 sieve contained in each gradation and the permeability coefficient, K. In this figure, permeability was chosen as the dependent variable and percent fines as independent variable. The SAS program was used to perform a simple regression analysis on the dependent variable (i.e., permeability).

Table 5.1 Permeability Test Results Using B/S Permeameter: AASHTO 67

Permeability Testing 100% AASHTO 67					
1- Sieve Analysis (AASHTO) after Permeability Testing					
Sieve	Specimen 1 % Passing	Specimen 2 % Passing	Specimen 3 % Passing	Specimen 4 % Passing	Specimen 5 % Passing
1	100.00	100.00	100.00	100.00	100.00
3/4	95.96	94.45	95.84	95.41	94.99
3/8	37.25	37.19	37.29	36.54	36.85
#4	6.46	6.48	6.21	6.21	6.17
#8	2.71	2.66	2.73	2.60	2.53
#30	1.83	1.80	1.89	1.70	1.70
#50	1.65	1.60	1.69	1.48	1.52
#100	0.79	0.68	0.64	0.44	0.98
#200	0.59	0.26	0.44	0.34	0.64
2- Coefficient of Permeability					
cm/sec	7.63	6.98	7.34	7.48	6.84
fpd	21633	19793	20810	21212	19392
Height, cm	15.05	14.93	14.73	14.93	14.83
3- Unit Weight, pcf					
Wet U. Wt.	103.20	104.06	105.47	104.06	104.76
Water C. %	1	1	1	1	1
Dry U. Wt.	102.18	103.03	104.43	103.03	103.72

Table 5.2 Permeability Test Results Using B/S Permeameter: A85_S15

Permeability Testing 85% AASHTO 67 mixed with 15% Screening					
1- Sieve Analysis (AASHTO) after Permeability Testing					
Sieve	Specimen 1 % Passing	Specimen 2 % Passing	Specimen 3 % Passing	Specimen 4 % Passing	Specimen 5 % Passing
1	100.00	100.00	100.00	100.00	100.00
3/4	94.87	95.65	96.31	96.28	95.72
3/8	46.26	46.98	46.59	47.32	47.53
#4	16.97	17.19	17.28	17.36	17.06
#8	7.61	7.23	7.74	8.11	7.69
#30	3.60	3.32	3.59	3.80	3.56
#50	2.84	2.60	2.75	2.90	2.78
#100	0.90	1.01	1.14	1.11	0.94
#200	0.46	0.53	0.50	0.52	0.40
2- Coefficient of Permeability					
cm/sec	3.66	3.37	3.80	3.86	3.88
fpd	10381	9554	10783	10941	10993
Height, cm	14.24	14.10	14.25	14.30	14.13
3- Unit Weight, pcf					
Wet U. Wt.	108.99	110.15	108.98	108.60	109.95
Water C. %	1.5	1.5	1.5	1.5	1.5
Dry U. Wt.	107.38	108.52	107.37	107.00	108.33

Table 5.3 Permeability Test Results Using B/S Permeameter: A75_S25

Permeability Testing 75% AASHTO 67 mixed with 25% Screening					
1- Sieve Analysis (AASHTO) after Permeability Testing					
Sieve	Specimen 1 % Passing	Specimen 2 % Passing	Specimen 3 % Passing	Specimen 4 % Passing	Specimen 5 % Passing
1	100.00	100.00	100.00	100.00	100.00
3/4	97.11	96.02	96.55	96.79	97.21
3/8	52.14	52.53	52.48	52.35	52.84
#4	24.40	24.47	24.89	24.71	25.11
#8	10.90	11.45	10.66	10.17	10.61
#30	4.65	4.92	4.58	4.21	4.43
#50	3.30	3.58	3.41	3.13	3.27
#100	1.05	1.84	1.45	1.46	1.56
#200	0.47	0.70	0.62	0.62	0.68
2- Coefficient of Permeability					
cm/sec	2.01	2.17	2.01	2.08	2.06
fpd	5691	6142	5698	5894	5839
Height, cm	13.63	13.81	13.68	13.80	13.85
3- Unit Weight, pcf					
Wet U. Wt.	114.00	112.44	113.57	112.54	112.13
Water C. %	1.5	1.5	1.5	1.5	1.5
Dry U. Wt.	112.32	110.78	111.89	110.88	110.47

Table 5.4 Permeability Test Results Using B/S Permeameter: A65_S35

Permeability Testing 65% AASHTO 67 mixed with 35% Screening					
1- Sieve Analysis (AASHTO) after Permeability Testing					
Sieve	Specimen 1 % Passing	Specimen 2 % Passing	Specimen 3 % Passing	Specimen 4 % Passing	Specimen 5 % Passing
1	100.00	100.00	100.00	100.00	100.00
3/4	96.32	96.73	97.23	95.40	96.48
3/8	57.97	58.70	58.45	58.75	59.22
#4	31.49	32.07	32.27	32.78	32.54
#8	13.90	13.16	12.81	13.68	13.93
#30	5.51	5.26	5.05	5.40	5.59
#50	4.01	3.87	3.66	3.91	4.00
#100	1.60	1.10	1.77	1.83	1.59
#200	0.69	0.39	0.66	0.46	0.48
2- Coefficient of Permeability					
cm/sec	1.90	1.88	1.66	1.46	1.48
fpd	5374	5327	4703	4152	4184
Height, cm	13.80	13.58	13.68	13.45	13.48
3- Unit Weight, pcf					
Wet U. Wt.	112.46	114.50	113.57	115.47	115.25
Water C. %	2	2	2	2	2
Dry U. Wt.	110.25	112.25	111.34	113.21	112.99

Table 5.5 Permeability Test Results Using B/S Permeameter: Louisiana Base

Permeability Testing Louisiana Typical Base Material					
1- Sieve Analysis after K (AASHTO) after Permeability Testing					
Sieve	Specimen 1 % Passing	Specimen 2 % Passing	Specimen 3 % Passing	Specimen 4 % Passing	Specimen 5 % Passing
1.5	100.00	100.00	100.00	100.00	100.00
3/4	86.64	85.60	86.64	86.17	86.02
3/8	60.16	60.32	60.32	60.62	60.51
#4	38.68	38.21	36.98	38.70	38.49
#8	26.11	25.85	25.93	26.14	26.80
#30	13.83	13.63	13.65	13.91	14.28
#40	10.82	11.47	10.61	11.46	11.25
#100	3.92	3.88	4.34	3.99	4.12
#200	1.09	0.35	1.55	0.67	0.90
2- Coefficient of Permeability					
cm/sec	0.17	0.16	0.20	0.11	0.20
fpd	482	453	580	321	566
Height, cm	13.63	13.81	13.68	13.80	13.85
3- Unit Weight, pcf					
Wet U. Wt.	133.98	133.60	133.36	135.79	135.05
Water C. %	4.5	4.5	4.5	4.5	4.5
Dry U. Wt.	128.21	127.85	127.62	129.94	129.23

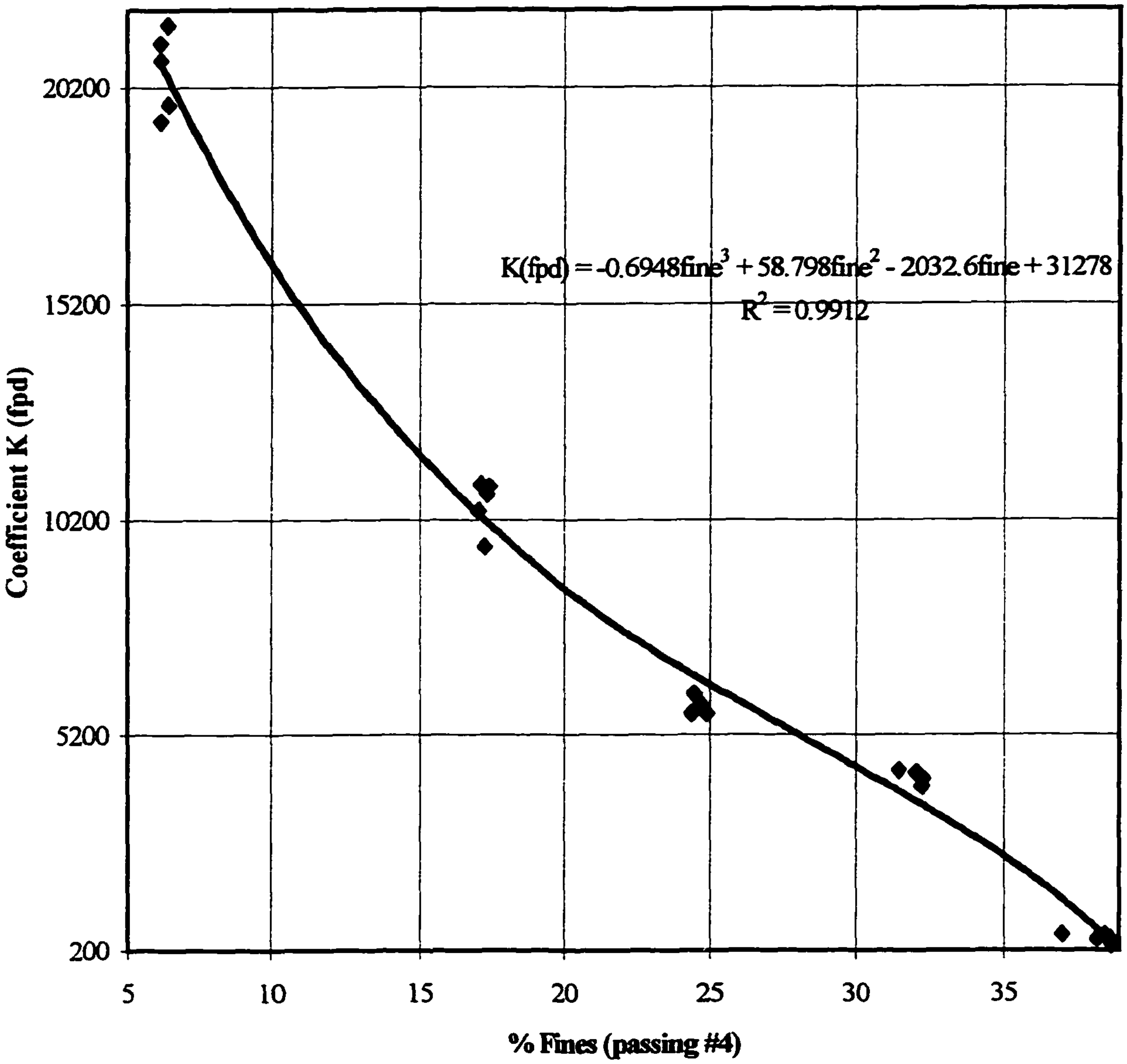

Figure 5.1 Coefficient of Permeability vs. % Passing #4

Nonlinear regression was performed, but the linear third degree polynomial regression provided the best fit and highest R-squared.

5.2 Resilient Modulus Test Results

All modulus tests were conducted over a range of confining pressures and vertical stresses as described in chapter 3. The order in which confining pressure and vertical stresses combinations were applied was the same for all gradations. For complete test results, see Appendix C.

The relationship between state of stress and resilient modulus has been characterized for this study using bulk stress (θ) which is defined as the sum of the three principal stresses:

$$\theta = \sigma_1 + \sigma_2 + \sigma_3 \tag{5.1}$$

where

σ_1 = major principal stress or total vertical stress,

σ_2 = intermediate principal stress, and

σ_3 = minor principal stress.

For the triaxial testing procedure used in this study, $\sigma_2 = \sigma_3$ and both of these stresses are equal to the confining pressure. The test data from Appendix C were fitted to the following equation using regression techniques:

$$M_r = k_1 \theta^{k_2} \tag{5.2}$$

where

M_r = resilient modulus of the aggregate base,

k_1 and k_2 = constants determined in the regression analysis

θ = bulk stress.

The relationship between M_r and θ was developed using the data corresponding to bulk stress of 10.5, 20, 30, 40, and 58.5 psi for each gradation. Tables 5.6 summarizes the values for k_1, k_2, θ and M_r for each base gradation levels. Figures 5.2 through 5.6 show the relationship between θ and M_r for each gradation. The relationship between resilient modulus of the four open-graded gradations and the percentage of fines is show in Figures 5.7 and 5.8. The resilient modulus for all gradations have been plotted in Figure 5.7 as a function of the bulk stress (θ). Figure 5.8 show resilient modulus as a function of the percentage of fines for the five levels of bulk stress, θ, of 10.5, 20, 30, 40, and 58.5 psi. Note that the percent fines is defined as the percent materials passing the #4 sieve in the original aggregate base plus the percentage passing #4 in the stone screenings. Figure 5.9 contains a plot of both the resilient modulus and permeability coefficient as a function of the percent fines.

Figure 5.10 shows an example of load-time and displacement-time histories as recorded by the acquisition system from the load cell and the LVDTs during resilient modulus testing. The computed maximum cyclic stress and maximum resilient strain were used to compute the resilient modulus contained in Appendix C. In all cases the minimum values of resilient modulus occurred during Sequence 1 and the maximum values were obtained during Sequence 5.

Table 5.6 Summaries of Values of k_1, k_2 and R^2 as Function of Fines

	k_1	k_2	R-squared
AASHTO 67	3924	0.42	0.99
A85_S15	7275	0.345	0.98
A75_S25	17486	0.181	0.98
A65_S35	16890	0.188	0.97
LA Base	26186	0.143	0.98

5.3 Unconfined Compression Tests Results

The unconfined compression tests were performed on each specimen after the resilient modulus testing was completed. The test results for each of the four gradations used in the study is shown in Table 5.7. Figure 5.11 shows the observed and predicted values of the unconfined compression test. The fitted curve was obtained using regression techniques.

Table 5.7 Unconfined Compression Test Results

AAHTO 67		A85_S15		A75_S25		A65_S35	
% Fines	U. C., pounds	% Fines	U. C., pounds	% Fines	U. C., pounds	% Fines	U. C., pounds
6.46	742	16.97	928	24.4	1242	31.49	1183
6.48	735	17.19	970	24.47	1247	32.07	1146
6.21	703	17.28	885	24.89	1194	32.27	1125
6.21	738	17.36	908	24.71	1244	32.28	1205
6.21	748	17.06	910	24.71	1210	32.28	1232

U. C.: Unconfined Compression.

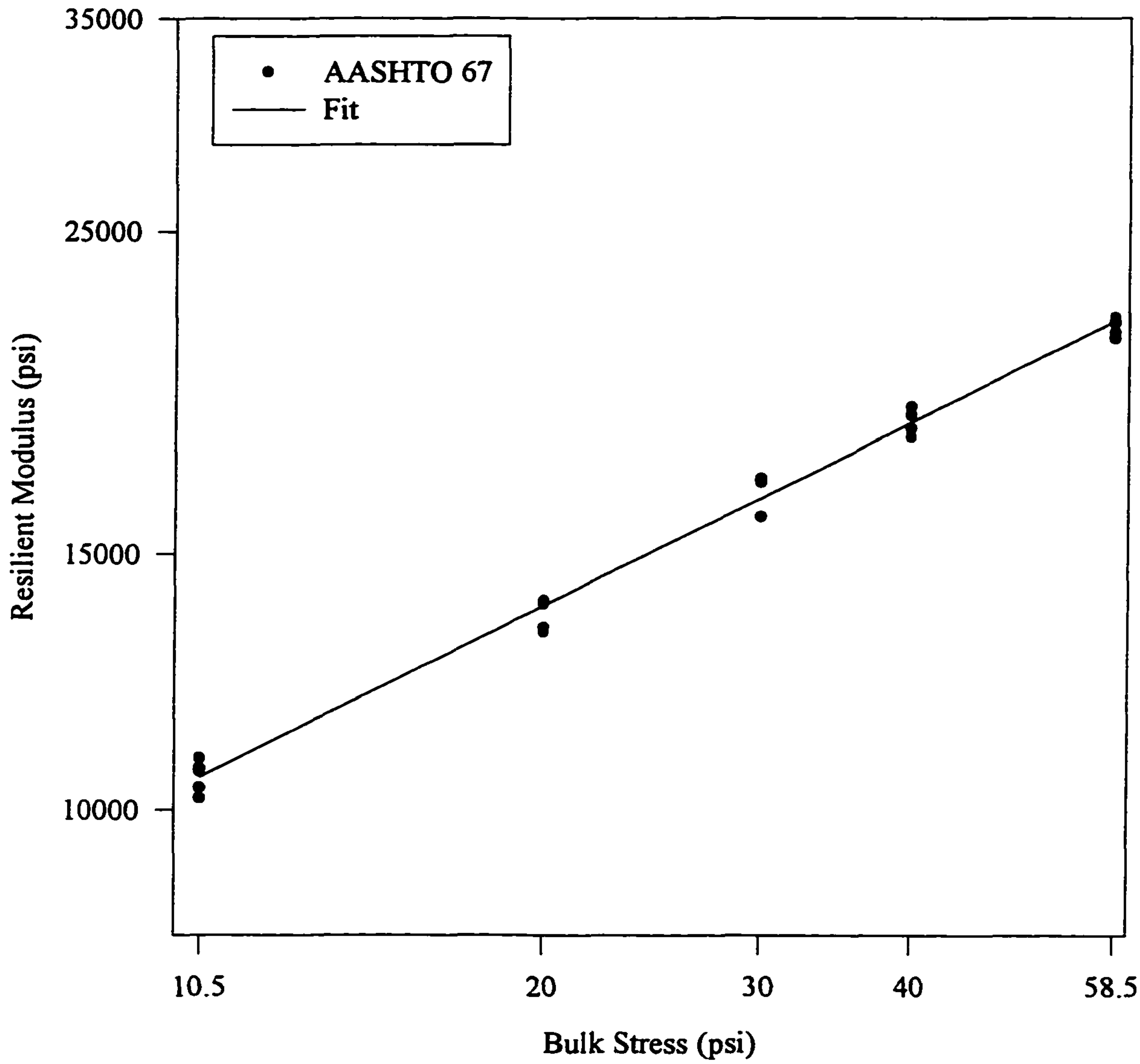

Figure 5.2 Resilient Modulus vs. Bulk Stress: AASHTO 67

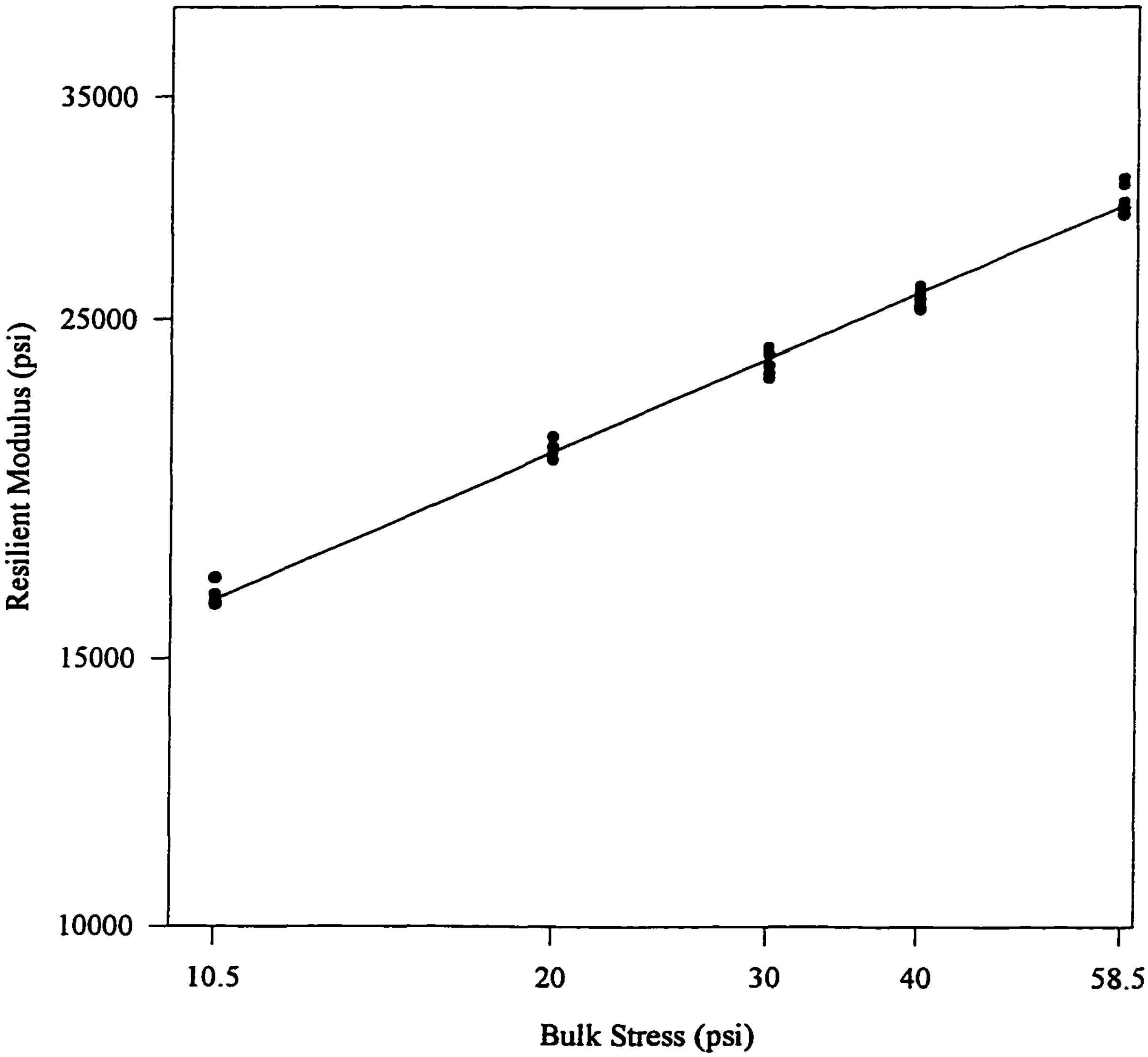

Figure 5.3 Resilient Modulus vs. Bulk Stress: A85_S15

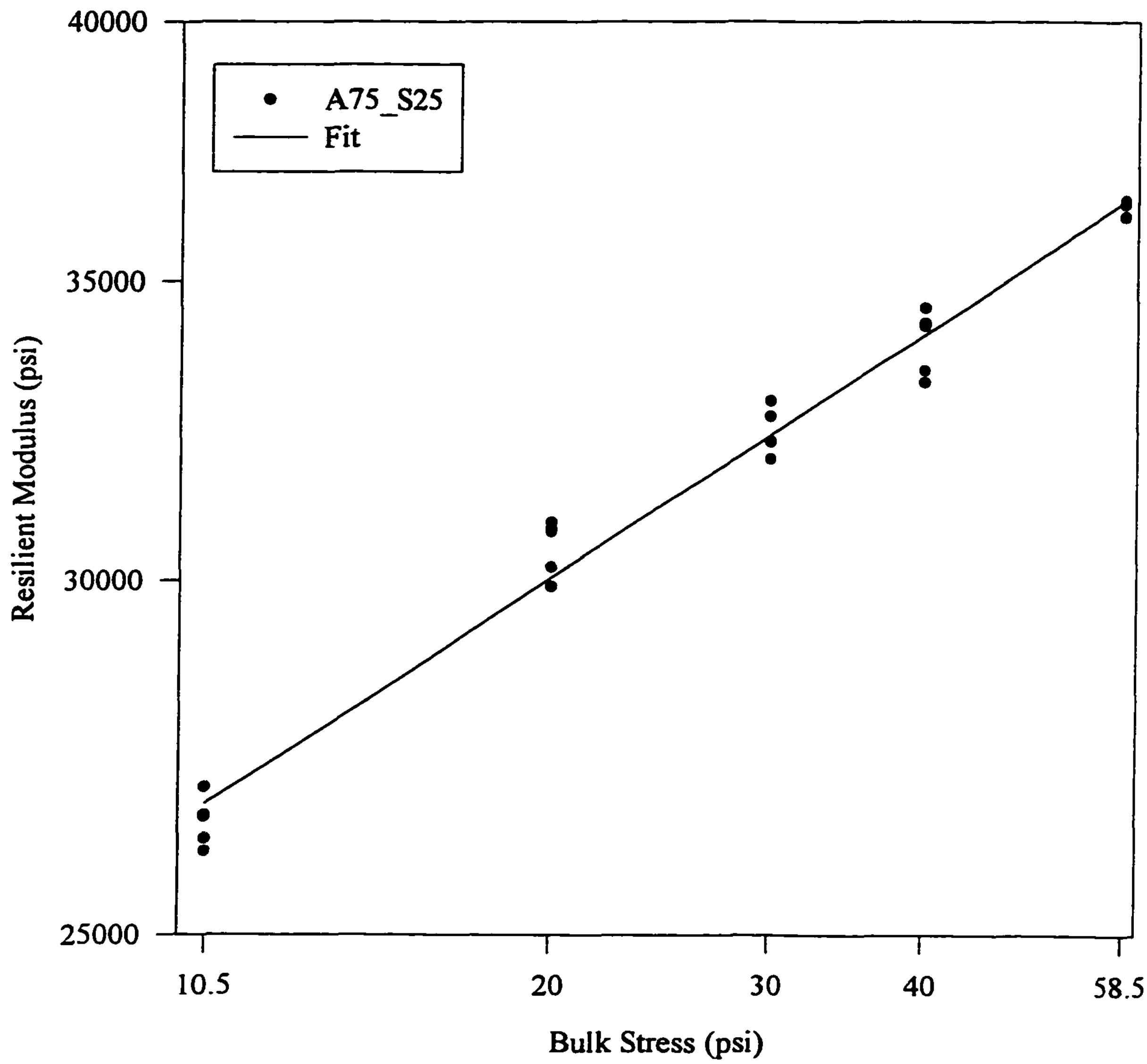

Figure 5.4 Resilient Modulus vs. Bulk Stress: A75_S25

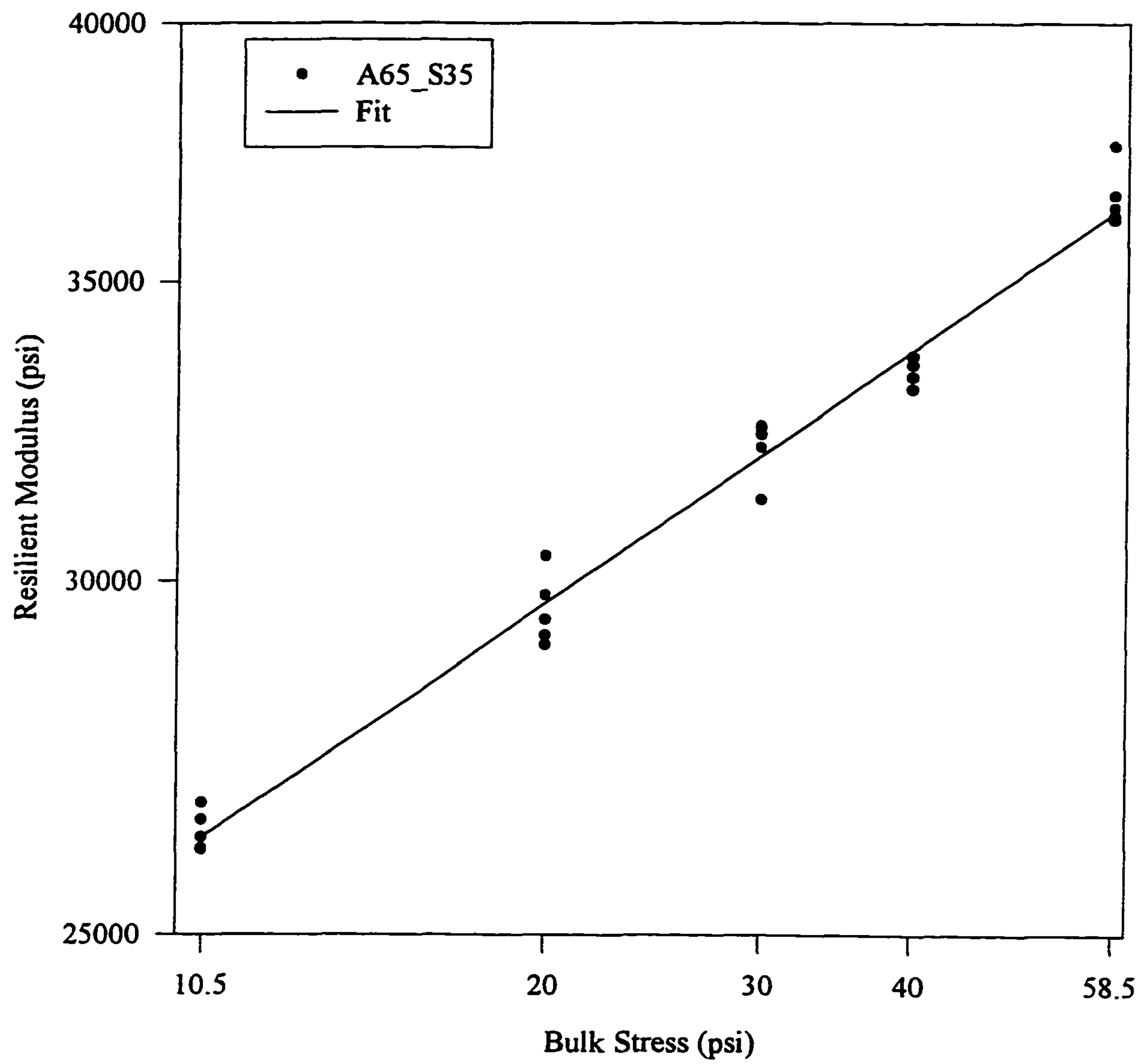

Figure 5.5 Resilient Modulus vs. Bulk Stress: A65_S35

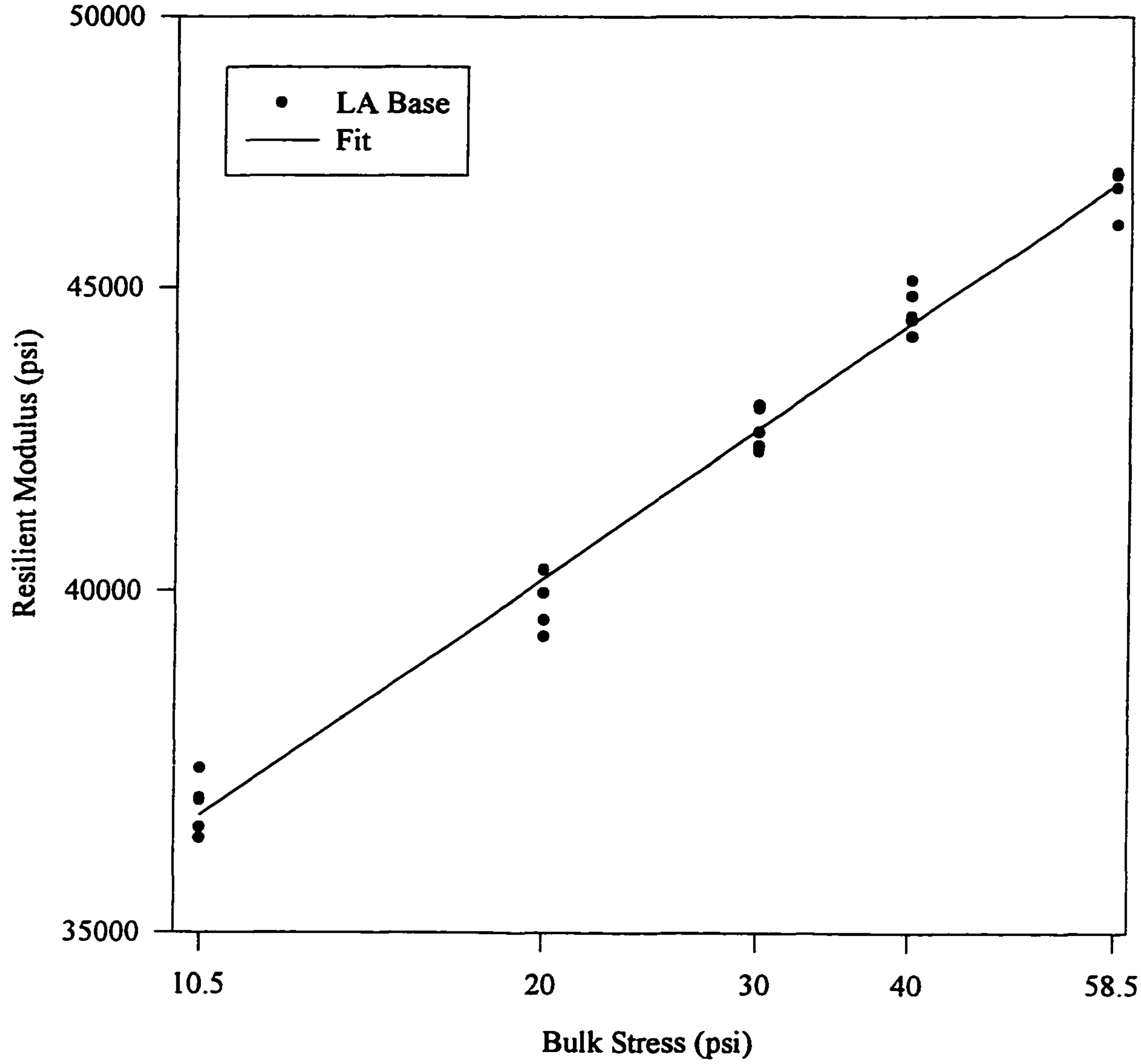

Figure 5.6 Resilient Modulus vs. Bulk Stress: LA Typical Base

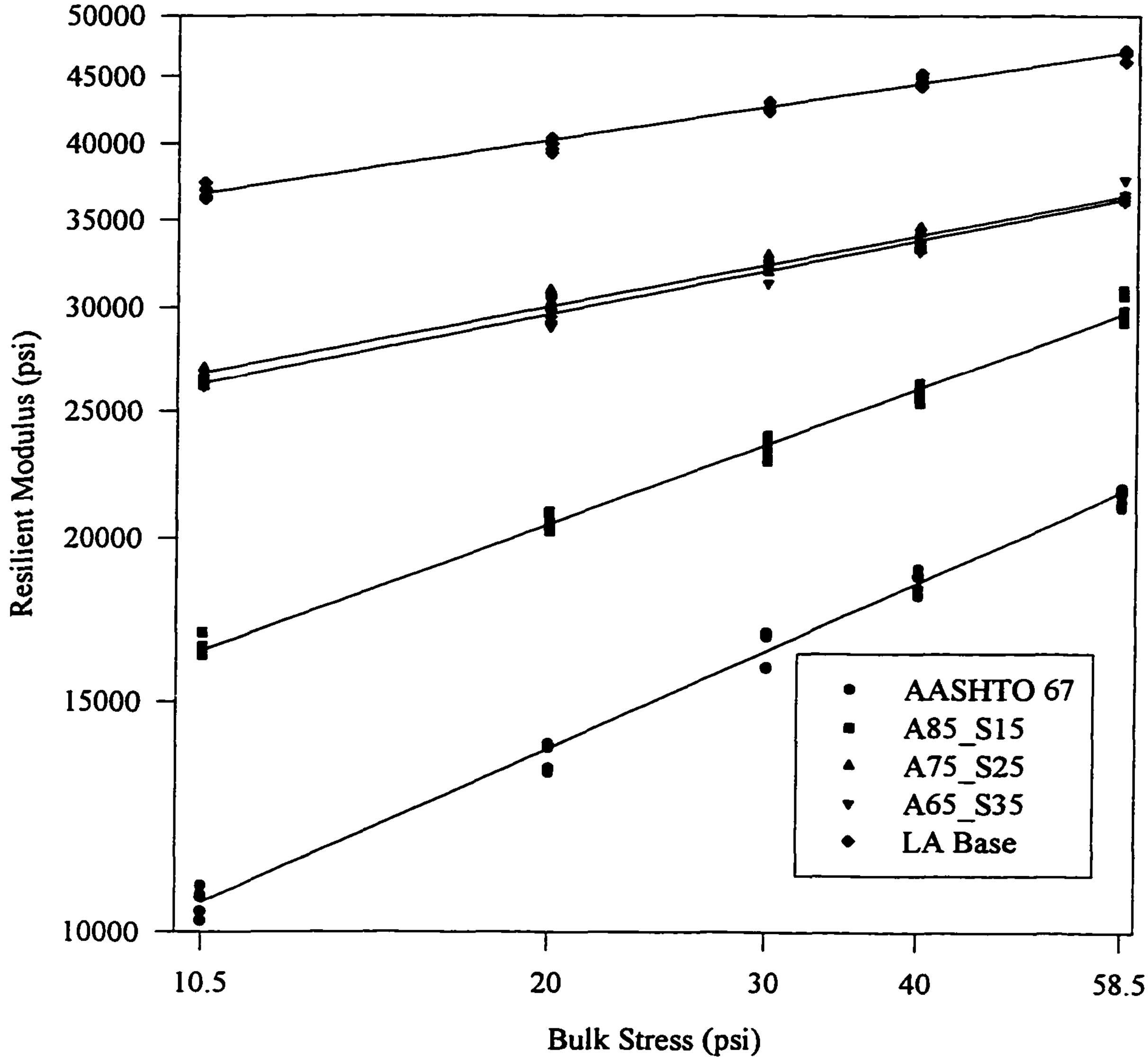

Figure 5.7 Resilient Modulus vs. Bulk Stress: All Gradations

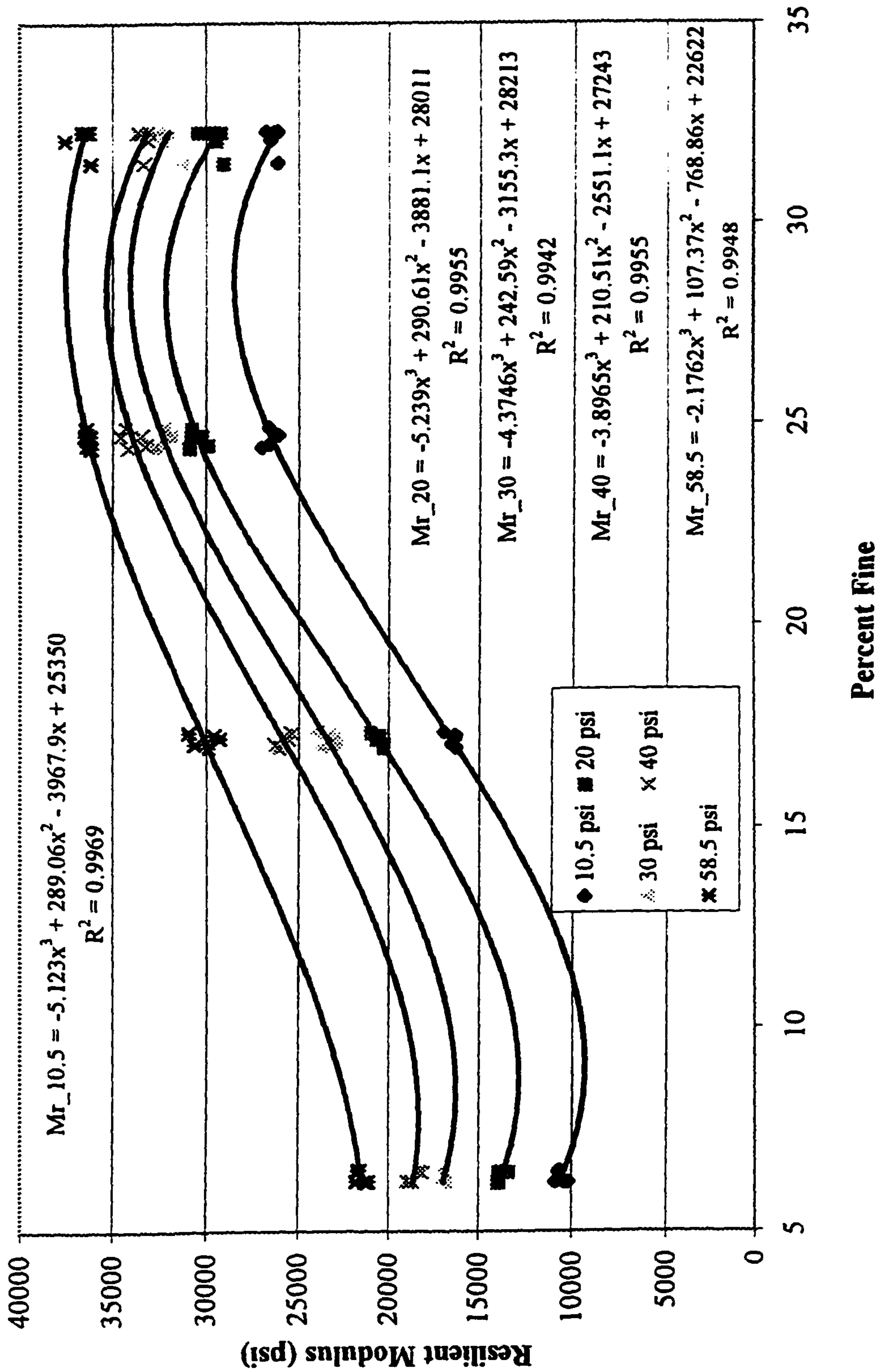

Figure 5.8 Resilient Modulus vs. % Fines: θ = 10.5, 20, 30, 40, 58.5 psi

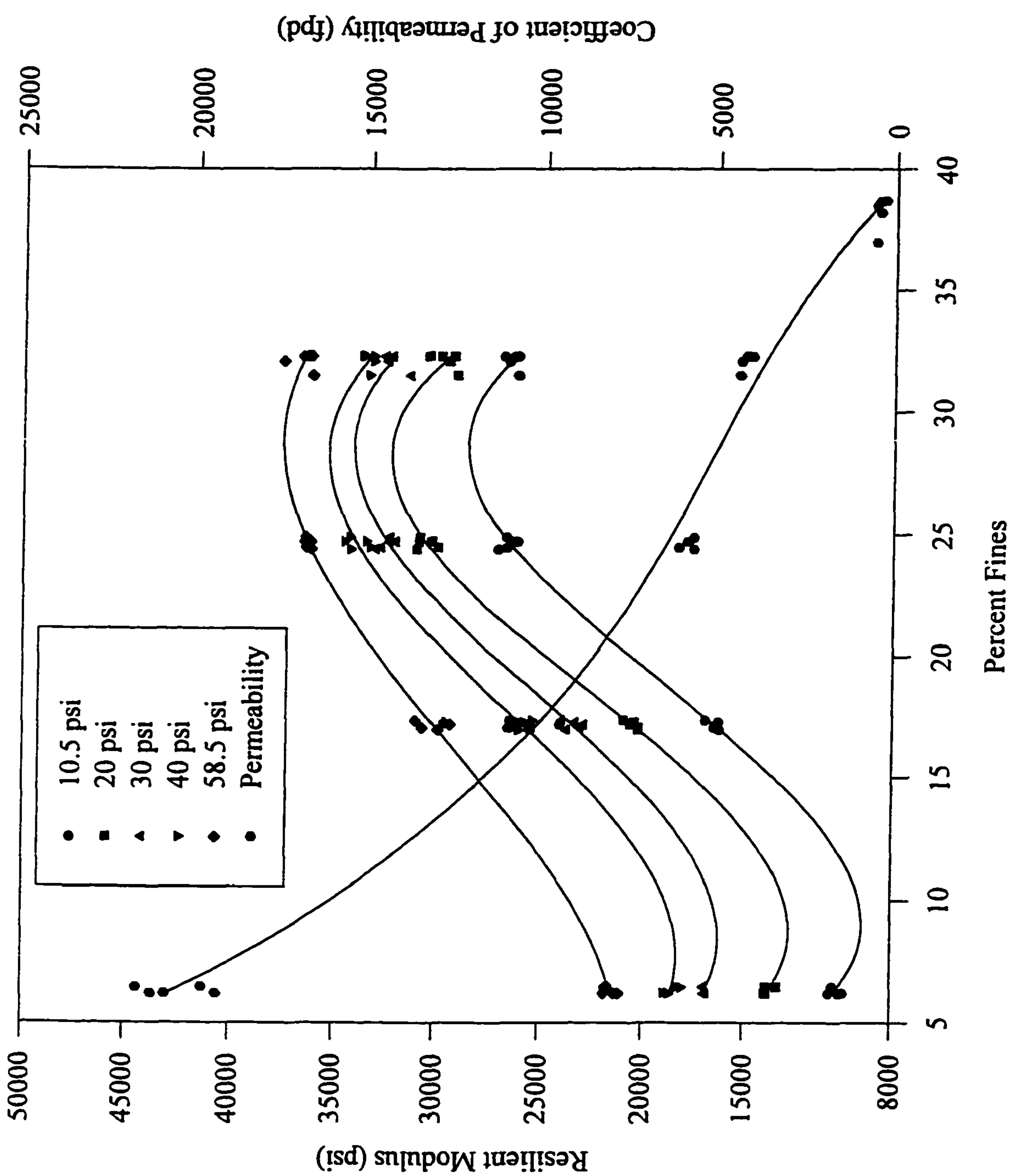

Figure 5.9 Resilient Modulus and Permeability vs. Percent Fines

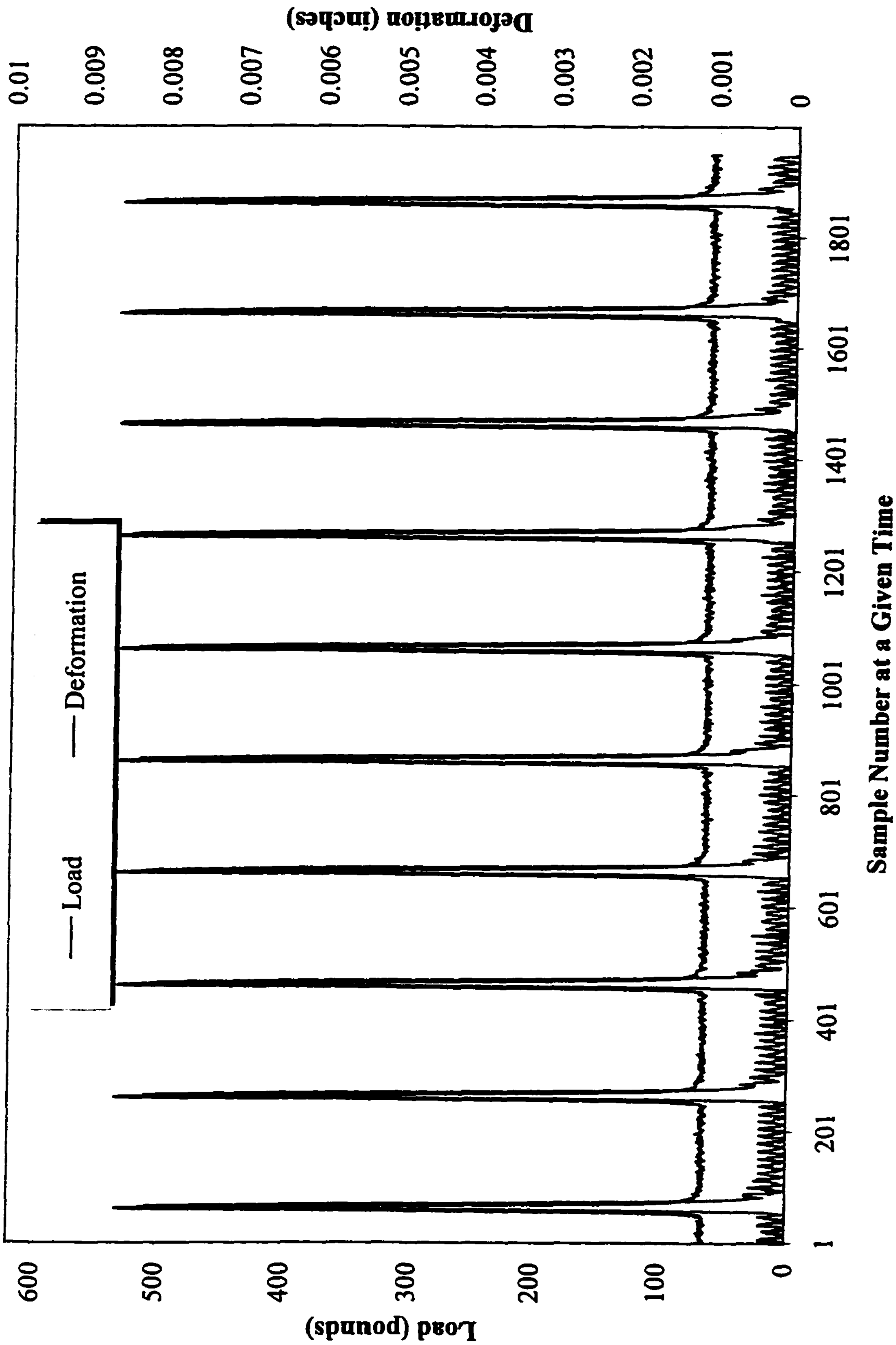

Figure 5.10 Load and Deformation Time History: A65_S35_1 Sequence #5

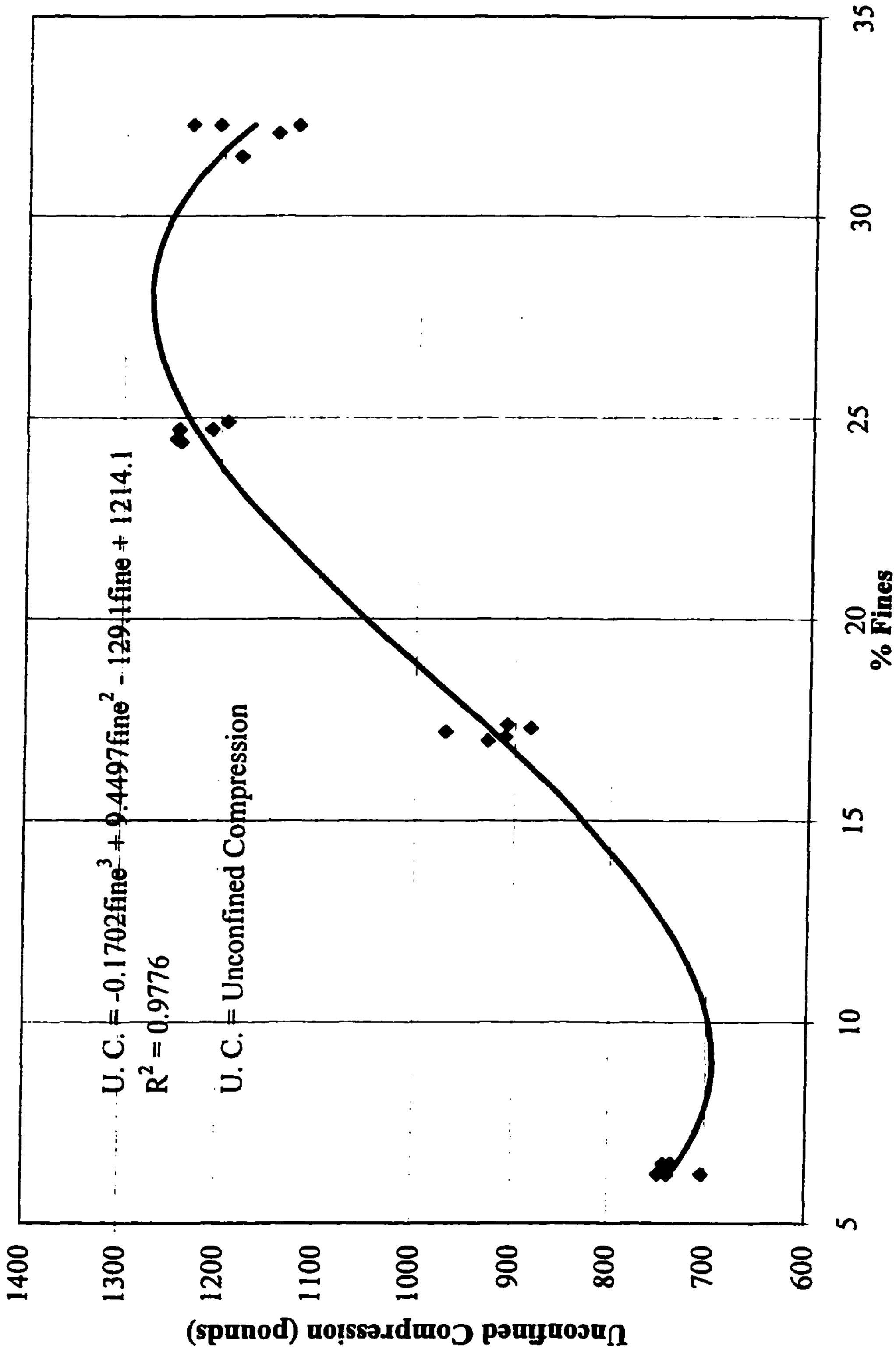

Figure 5.11 Unconfined Compression vs % Fines

CHAPTER 6

ANALYSIS OF RESULTS

In this chapter, the effect of fines on permeability coefficient and resilient modulus will be evaluated. Further an "optimum" gradation that allow both effective drainage and provides adequate strength will be identified. The development of statistical models that predict the coefficient of permeability and resilient modulus will be discussed. Finally, some general discussions on geotextiles and pavement filtration will be introduced.

6.1 Permeability

One dense-graded limestone and four open-graded materials were tested for permeability using the Barber and Sawyer permeameter. The results are shown in chapter 5. Comparing the tests results for the dense-graded (Louisiana base) material shows that the coefficients of permeability are considerably lower than the measured coefficients for the four more open-graded materials (Tables 5.1 through 5.5). In the open-graded soils, even the small hydraulic gradient applied moved some of the fine particles in the direction of the flow and flow out of the specimen. That result made the specimen more open-graded during the test to produce the relatively high measured coefficients of permeability. The color of the outflow water for these gradations verified that some fine material flowed out of the specimens.

Figure 5.1 shows coefficient of permeability versus percent passing sieve #4 (percent fines). This figure shows that permeability decreased as the percent fines increases because the voids and the seepage channels in the aggregate are reduced as the finer percent increased. A regression analysis resulted in a R-squared value of 99%, meaning that 99% of the variability in measuring the coefficient of permeability data can be accounted for by using the percent fine as predictor variable. Based on the observation and results above, one could conclude that changing the percent fines in an aggregate gradation have a significant effect on the coefficient of untreated base material. Therefore, for the type of aggregate used in this study, this analysis provides the highway engineer with a relationship to estimate the laboratory coefficient of permeability of untreated open-graded base layers under specified gradation, density, and water content.

Although the R-squared is high in this relationship (Figure 5.1), the author believes that percent fine is not sufficient to accurately represent the permeability of a material. Therefore, it is advisable to investigate the use of multiple regression analysis that will include more than one variable in the prediction equation so that the prediction equation will have better representation of the materials' porosity and gradation characteristics. However, for a preliminary study, the simple regression equation from Figure 5.1 will do a good job of predicting permeability coefficient. This equation can be used to estimate the permeability of an existing layer or for the design of new drainage layer. In the latter situation, the engineer can perform laboratory tests to verify the layer properties he selects.

To determine if any significant migration of fines from the top to the bottom of the specimens was occurring during the tests, gradation tests were performed after completion of tests on all specimens. Grain-size distribution (Table 5.1 through 5.5) after permeability testing showed no indication migration of fines in the dense graded material (Tables A5 with 5.5). However for the open-graded material the change in gradation is noticeable compared with the original gradation (Tables A1 through A4 with 5.1 through 5.4).

As previously mentioned, the ability to estimate the coefficient of permeability is important in selecting a layer requirement for the pavement engineer. One design requirement used to evaluate for whether the drainage system is adequate in handling the maximum seepage flow is to provide drainage of the base course so that a 50% degree of drainage occurs in less than 10 days from a rainfall event. Degree of drainage is defined as the ratio, expressed in percent, of the amount of water drained to the total amount of water that can be drained by gravity from the material. Factors, that affect gravity drainage, are the effective porosity, physical characteristics of the drainage system, the geometry of the pavement and the coefficient of permeability of the drainage layer. The equation often used to determine the time required for a saturated base course to reach a degree of drainage of 50 percent is

$$t = 24T\,m \tag{6.1}$$

where

t = time to drain, hours;

T = time factor;

m = "m" factor = $N_e L_R^2 / (K H)$

N_e = effective porosity;

L_R = resultant length of drainage, ft;

K = coefficient of permeability, fpd;

H = Thickness of the drainage layer, ft.

The assumptions made in applying the above equation are:

1. The drainage layer is initially 100 percent saturated;
2. No recharge occurs once drainage begins;
3. The sub-grade is impervious and drainage occurs mainly in the transverse direction of the drainage material; and
4. The coefficient of the permeability, and effective porosity of the drainage material are constant and the same in all direction for the existing conditions.

The test results from this study show that the drainage characteristics of open-graded materials can be determined with sufficient reproducibility by following the test procedure describe in Chapter 4. This information provides a means of evaluating the effect of gradation, or specially the effect of fines on permeability when selecting materials for design. It is recognized that to obtain reliable laboratory test results that will reflect the actual field conditions, the permeability test specimens should be prepared and compacted to simulate the field conditions as closely as possible. Laminar flow condition cannot be anticipated in permeability tests on very open-graded base material; thus, expected field conditions for hydraulic gradient of permeating water should be approximated in the laboratory.

Consideration of permeability alone is not sufficient in characterizing a pavement base course, which doubles as a drainage layer; strength characteristics are a requirement for pavement design.

6.2 Resilient Modulus and Unconfined Compression Tests

As stated earlier, the K-θ model was used to characterize the resilient modulus test results for all gradations. Figures 5.2 through 5.6 (Chapter 5) show a stress stiffening response for specimens of all gradations; that is, as the stresses increased, the resilient modulus increases because the deformation characteristics of granular material are significantly affected by stress magnitude and path.

Table 5.6 (Chapter 5) summarizes the of k_1 and k_2 values for all gradations. Each gradation appears to have its own unique $k_1$and k_2 values. The overall mean values for k_1 and k_2 for all gradation--excluding the Louisiana typical base course values--are 11394 and 0.284 respectively. These values are generally in excellent agreement with typical values assumed in design and as reported in the literature.

In general, one can observe from Table 5.6 that k_1 increases and k_2 decreases as the gradations move from open to dense graded. This trend indicates that the overall degree of linearity increases from the AASHTO 67 to the Louisiana dense graded base. The order also corresponds generally to what one would associate with increasing shear strength behavior by the aggregate as shown by an increase in the resilient modulus as the percent fines increases, as shown in Figure 5.7.

The only exception is for A65_S35, where the resulting moduli are not significantly different from the A75_S25 (Figure 5.7). The reason is that with the addition of more fines from the A75_S25, the coarse aggregate particles are pushed apart. In this state, the coarse aggregate floats in a matrix of fine material. This type of aggregate structure has lower shear strength because of the loss of large particles interlock as the percent fines increases. This phenomenon results in a decrease in both shear strength and resilient modulus. Based on the results, the most significant parameters that affect the behavior of the unbound granular base are the bulk stress and the percent fines passing sieve #4.

Figure 5.8 shows resilient modulus as a function of percentage of fines for five level of bulk stress, 10.5, 20, 30, 40, and 58.5 psi. As can be noted on this figure, at a given level of stress, the resilient modulus increases as the percent fines increases until reaching a maximum between 24 and 32% fines. The resilient modulus values at 32% (A65_S35) are generally less than those for 24% fines (A75_S25). That trend results because of the floating aggregate phenomenon mentioned previously. In other words, at every level of bulk stress, the test data show an increase in resilient modulus of the aggregate base, as the percent of fine increases up to about 25% to 27%. An apparent peak in M_r is reached when the percent fines is between 24% and 32%. Above this maximum, a drop in M_r occurs. The shape of the fit in Figure 5.8 between approximately 5% and 15% fines has no physical interpretation; for lower bulk stresses, the modulus appears to decrease for no readily recognizable reason. This anomaly is probably related to the type of regression model (polynomial of third degrees) used to fit the observed data.

In summary, it appears that fine content between 24% to 32% can be tolerated in terms of stiffness criteria for the gradation and types of aggregate used and at all stress levels tested. Beyond this range, the base will probably acts as a sub-grade material with lower M_r and permeability, resulting in reduced the pavement life. When the effect of percent fines on resilient modulus is being evaluated, maintaining adequate permeability within the aggregate base also needs to be considered.

Unconfined compression strength (Figure 5.11) plotted versus versus percent fines shows similar trend as found in figure 5.8. As the percent fine increases, the unconfined compression strength increases with an apparent peak between 24% and 32%. This maximum occurred over the same range of percent fines as that found in the resilient modulus analysis. The load is dynamic for the M_r test, whereas the load is applied statically in the unconfined compression tests.

For the pavement to remove the amount of water entering the base course and at the same time be stiff enough to withstand heavy load traffic, the effect of percent fines on these two characteristics-permeability and resilient modulus-should be evaluated in a single analysis procedure.

6.3 Permeability and Resilient Modulus

Figure 5.9 represents an attempt to incorporate stiffness with drainability characteristics in the evaluation of the open-graded base materials as function of percent fines. It is evident from this figure that the two characteristics works in opposition to each other as the fines content increases, i.e. permeability decreases while resilient modulus increases with increasing fines content. The maximum shear strength and the maximum resilient modulus are developed through aggregate interlock and particle-to-particle friction which occurs as fines are added up to about 28%.

According to the literature [12], a base is free draining if the coefficient of permeability is in the range of 1000 to 5000 fpd, with most state using 3000 fpd as design permeability. The compromise between permeability and resilient modulus should take into account the problem of frost (which is not critical in Louisiana) and moisture susceptibility. Use of an open-graded base minimizes water susceptibility but these bases are considerably harder to construct than dense graded bases. On the other hand, increasing of the percent fines increases frost and moisture susceptibility while increasing the resilient modulus values.

Using an available mathematics software and the data gathered in this project, the precise optimum of fines versus resilient modulus is 28.5%, which correspond, to a coefficient of permeability of 4994 fpd from the regression equation in Figure 5.1. Because of the variability involved in the gradation and field conditions it is advisable to propose a range of fines that would satisfy both resilient modulus and permeability requirement of unbound open-graded base materials instead of providing the single value found above. From figure 5.9, the range of fines corresponding to the 3500 to 6500 fpd permeability range is between 24.72% and 32.23 %. The range of gradation corresponding to this permeability range and to the percent fines that gave the maximum resilient modulus for all stress levels is included in Table 6.1 along with the corresponding permeability coefficient ranges. These gradations should provide reasonable resilient modulus and, at the same time, be permeable enough to drain water entering the base course. Figure 6.1 shows the compromise gradation. In order to ensure that pavement maintains the design permeability, a filter layer to prevent the base should protect the base course from becoming clogged with fines from the underlying subgrade material. Geotextiles are commonly used for these filter layers.

Table 6.1 Compromise Gradation

US Sieve Number	Gradation Band		
	% Passing - Lower	Mid-range	% Passing - Upper
1"	100	100	100
3/4"	96.74	96.585	96.43
3/8"	52.47	55.54	58.62
#4	24.72	28.46	32.23
#8	10.76	12.13	13.5
#30	4.56	4.96	5.36
#50	3.34	3.62	3.89
#100	1.47	1.52	1.58
#200	0.62	0.58	0.54
Permeability (fpd)	6467	5038	3583
Mr in psi at 10.5 psi	25510	28460	26220
Mr in psi at 20 psi	30520	32170	29400
Mr in psi at 30 psi	32370	34060	32050
Mr in psi at 40 psi	33960	35320	33240
Mr in psi at 58.5 psi	36350	37540	36520

6.4 Geotextiles

Contamination of the base layer occurs primarily through intrusion of subgrade materials into the aggregate base. This intrusion changes the gradation of the base and results in reduced strength or stiffness as well as lower permeability.

Because the subgrade soils in Louisiana have a high percentage of fines, in this study (Appendix D) a geotextile is be a preferred filter material rather than an aggregate separator layer. The principal advantage of a geotextile is its filtration capacity. A geotextile will allow any rising water, due to capillary action or rising water table, to enter the permeable base and rapidly drain to the edgedrain system. Its main disadvantage is that if the geotextile clogs or binds, rising water will be trapped under the

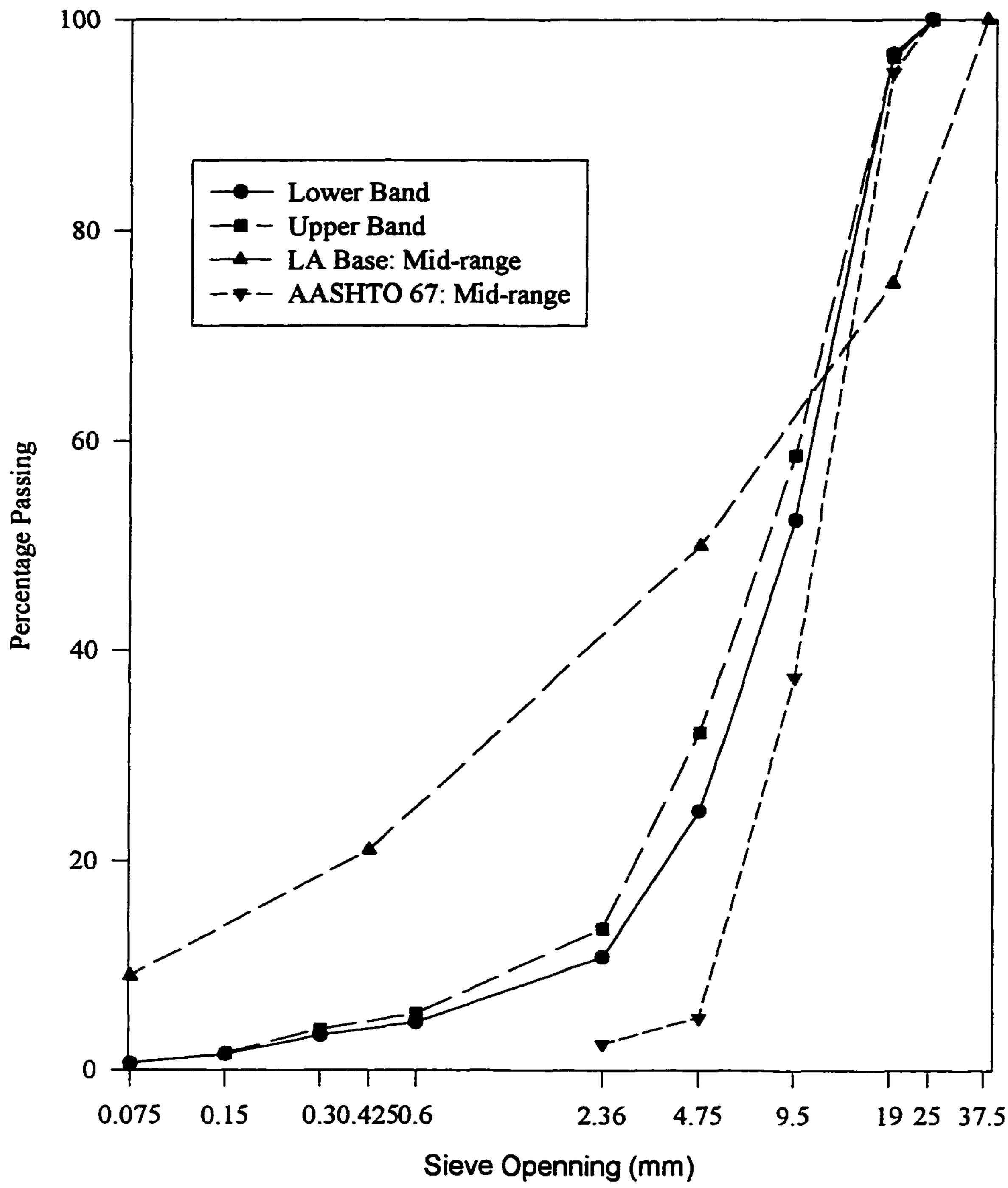

Figure 6.1 Compromise Gradation

geotextile, saturating the subgrade and reducing its support. In most cases, a small amount of fines will pass through the geotextile into the permeable base. This phenomenon starts the formation of a soil filter zone adjacent to the geotextile. The larger soil particles are retained by the geotextile, and a bridging action occurs creating a zone called the "soil bridge network" as shown in Figure 6.2. Immediately behind this zone is another zone where the finer soil particles are trapped, called a "filter cake" and has a lower permeability. In the last zone, the subgrade soil particles will be undisturbed.

The physical properties of geotextiles have not been considered in this study to achieve the performance objectives of a separation layer. Properties required in the 1986 AASHTO-AGC-ARTBA Taskforce 25 are given in Table 6.2. Research by others to date suggests that the amount of contamination depends on percentage of open area, porosity, effective size, and thickness of the geotextile. Performance criteria that need to be established for separation geotextiles are those that limit the amount of subgrade fines to an acceptable level for permeability and stiffness of the permeable base. A summary of the design criteria for selecting geotextiles is given in Table 6.3.

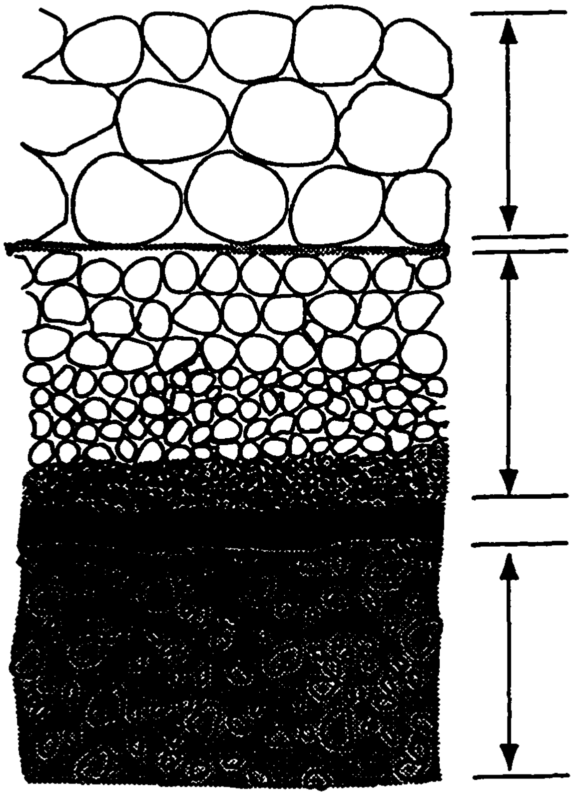

Figure 6.2 Filter formation [11]

6.5 Pavement Infiltration

After introducing geotextiles as a separator layer, the hydraulic aspect of the permeable base can be considered. It is important to classify the drainage quality in terms of how this drainage affects the performance of the pavement. The most recommended hydraulic design of permeable base is the time to drain approach, based on flow entering the pavement until the permeable base is saturated. Excessive runoff will not enter the pavement section after it is saturated; this flow will simply run off on the pavement surface. So it is imperative that the permeable base drains in a relatively short

Table 6.2 Physical Requirements[1,2] for Drainage Textiles (AASHTO-AGC-ARTBA TASK FORCE 25, July 86)

Test Method	Drainage[3]		Test Method
	Class A[4]	Class B[5]	
Grab Strength	180 lbs.	80 lbs	ASTM D 4632
Elongation	Not Specified		
Seam Strength[6]	80 lbs.	25 lbs.	ASTM D 4632
Puncture Strength	80 lbs.	25 lbs.	ASTM D 4833
Burst Strength	290 psi.	130 psi	ASTM D 3787
Trapezoidal Tear	50 lbs.	25 lbs.	ASTM D 4533

1. Acceptance of geotextile material shall be based on ASTM D 4759.
2. Contracting agency may require a letter from the supplier certifying that its geotextile meets specification requirements.
3. Minimum: Use value in weaker principal direction. All numerical values represent minimum average roll values (i.e., test results from any sampled roll in a lot shall meet or exceed the minimum values in the Table). Stated values are for non-critical, non-severe applications. Lot samples according to ASTM D 4354.
4. Class A drainage applications for geotextiles are where installation stresses are more severe than Class B applications, i.e., very coarse, sharp, angular aggregate is used, a heavy degree of compaction (> 95% AASHTO T 99) is specified or depth of trench is greater than 10 feet.
5. Class B drainage applications are those where geotextile is used for smooth graded surfaces having no sharp angular projections, no sharp angular aggregate is used; compaction requirements are light, (< 95% AASHTO T 99), and trenches are less than 10 feet in depth.
6. Values apply to both field and manufactured seams.

Table 6.3 Summary of Design Criteria for Selecting Geotextiles [11]

I. SOIL RETENTION CRITERIA

Less than 50% Passing No. 200 Sieve		
Steady-State Flow	**Dynamic Flow**	
AOS $O_{95} \leq B\,D_{85}$	**Can Move**	**Cannot Move**
$Cu \leq 2$ or ≥ 8 $B = 1$ $2 \leq Cu \leq 4$ $B = 0.5\,Cu$ $4 \leq Cu \leq 8$ $B = \frac{8}{Cu}$	$O_{95} \leq D_{15}$	$O_{50} \leq 0.5\,D_{85}$

Greater Than 50% Passing No. 200 Sieve		
Steady-State Flow		**Dynamic Flow**
Woven	**Nonwoven**	
$O_{95} \leq D_{85}$	$O_{95} \leq 1.8\,D_{85}$	$O_{50} \leq 0.5\,D_{85}$
AOS No.(fabric) $\geq$ No.50 Sieve		

II. PERMEABILITY CRITERIA

A. Critical / Severe Applications	*B. Less Critical / Less Severe Applications (with Clean Medium to Coarse Sands and Gravels)*
k (fabric) $\geq$ 10 k (soil)	k (fabric) $\geq$ k (soil)

III. CLOGGING CRITERIA

A. Critical / Severe Applications	*B. Less Critical / Less Severe Applications*
Select fabrics meeting Criteria I, II, IIIB, and perform soil/fabric filtration tests before specifying. Suggested performance test method: Gradient Ratio $\leq$ 3.	1. Select fabric with maximum opening size possible (lowest AOS No.). 2. Effective Open Area Qualifiers: Woven fabrics: Percent Open Area $\geq$ 4% Nonwoven fabrics: Porosity $\geq$ 30% 3. Additional Qualifier (Optional): $O_{95} \geq 3\,D_{15}$ 4. Additional Qualifier (Optional): $O_{15} \geq 3\,D_{15}$

AOS = Apparent Opening Size
Cu = Coefficient of Uniformity
0_x = Geotextile opening corresponding to x% cumulative passing

time to keep moisture damage to a minimum. Table 6.4 contains the AASHTO Guide for the Design of Pavement Structures [48] guidance based on draining 50 percent of the free water:

Table 6.4 AASHTO Drainage Recommendation for Time to Drain Based on 50% Saturation [48]

Quality of Drainage	Time to Drain
Excellent	2 Hours
Good	1 Day
Fair	2 Days
Poor	1 Month
Very Poor	Does not Drain

It does not consider the water retained by the effective porosity quality of the material.

Some engineers argues that the 85 percent saturation level is a better threshold for pavement damage due to moisture. Table 6.5 [14] provides guidance based on 85 percent saturation. This method considers both water that can drain and water retained by

Table 6.5 Pavement Rehabilitation Manual Guidance for Time to Drain Based on 85% Saturation[14]

Quality of Drainage	Time to Drain
Excellent	Less than 2 Hours
Good	2 to 5 Hours
Fair	5 to 10 Hours
Poor	Greater Than 10 Hours
Very Poor	Much Greater Than 10 Hours

the effective porosity quality of the material. According to the FHWA Drainage Manual [11], the two methods will produce identical results when the water loss of the material is 100 percent or, stated another way, when the effective porosity of a material is equal to its porosity. For permeable bases, this distinction is somewhat meaningless since the base material is so open-graded and contains a small number of fines. For permeable bases the water loss-defined as the percent of water that drains under gravity from the soil compare to the total volume of the sample-will be quite high, in the range of 80 to 90 percent. For practical purpose, the results produced by both methods will be quite close. The FHWA Drainage Manual, recommends a time to drain 50 percent of the drainable water in 1 hour as a criterion for the highest class roads with the greatest amount of traffic. For most other Interstate highways and freeways, a time to drain 50 percent of the drainable water in two hours is recommended.

The time to drain equation was given in section 6.1 (Equation 6.1) and is repeated here:

$$\mathbf{t = 24Tm} \qquad \textbf{(6.1)}$$

where

t = time to drain, hours;

T = time factor;

m = "m" factor = $N_e L_R^2 / (K H)$

N_e = effective porosity;

L_R = resultant length of drainage, ft;

K = coefficient of permeability, fpd;

H = Thickness of base, ft.

A design chart for determining the time factor (T) is provided by Figure 6.3. The time factor (T) is based on the geometry of the base course; that is, the resultant slope

(S_R) and length (L_R), the thickness of the base (H), and the percent drained (U). To used the chart, first calculate the slope factor (S_1):

$$S_1 = \frac{L_R S_R}{H} \tag{6.2}$$

where

S_1 = slope factor;

H and L_R are defined above;

S_R = Resultant slope of the base (Figure 6.3), ft.

Figure 6.3 is then entered with the slope factor (S_1) and the desired percent drained (U). The resulting time factor is then read off the chart. In this study, only one degree of drainage 50% will be used . By selecting time factors for 50% degree of drainage over a wide range of slope factors, a simplified chart can be developed as shown in Figure 6.4. These application of these design considerations is demonstrated in the following example problem:

Consider that the roadway geometry has the following characteristics:

Resultant slope (S_R) = 0.02 ft

Resultant length (L_R) = 24 ft

Base thickness (H) = 0.5 ft

The permeable base material is assumed to have the following permeability for a mid-range gradation of 3583 fpd. From previous laboratory test results on similar permeable bases, the unit weights range between 115 and 100 pounds per cubic foot. These densities produce a range of porosity of 0.28 to 0.4, respectively, based on a bulk specific gravity between 2.68.

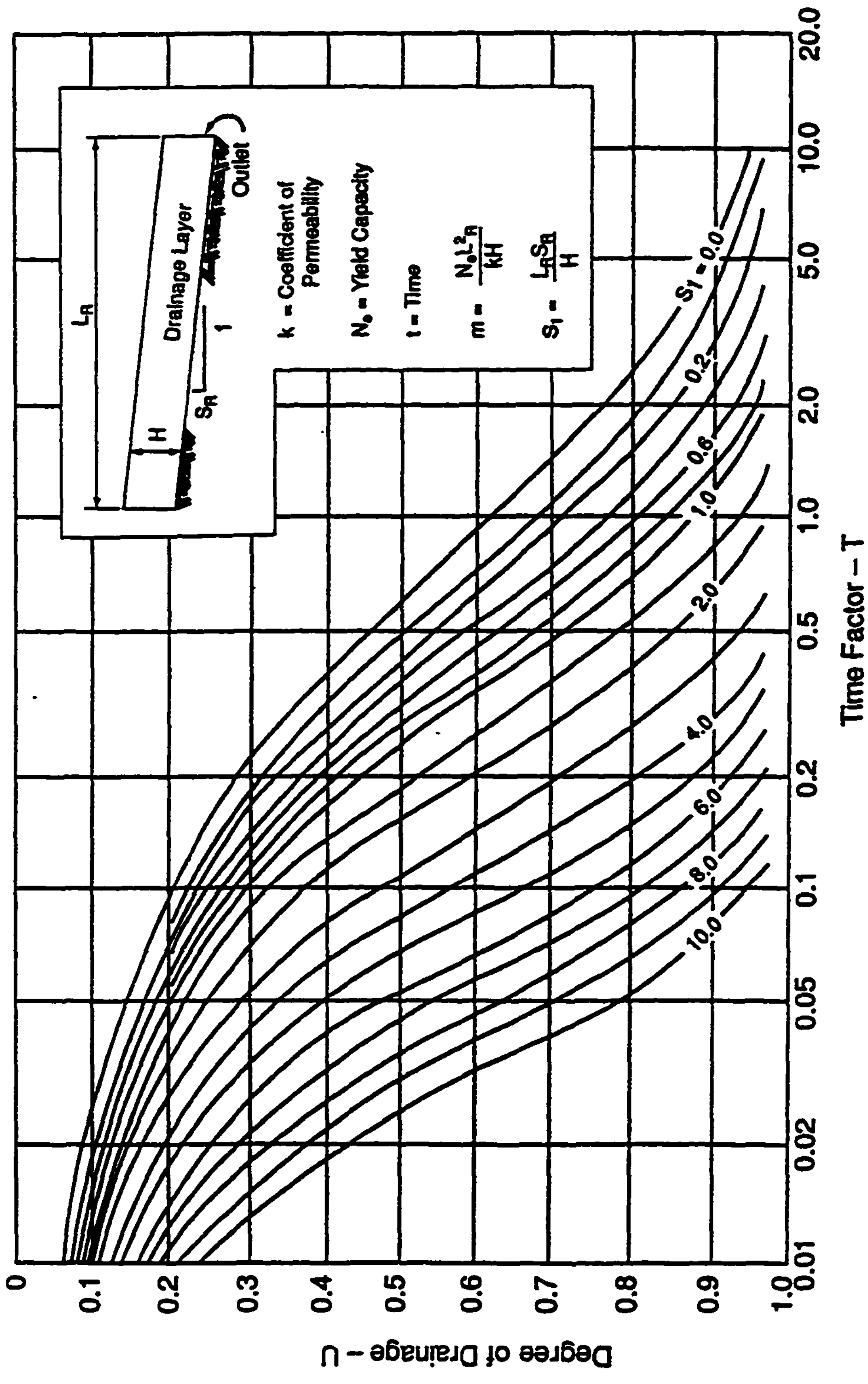

Figure 6.3 Time Factor T [11]

The effective porosity of the material can be obtained by multiplying the porosity of the permeable base by the water loss under gravity forces, which is usually taken to be 80%. In these conditions, the effective porosity (N_e) of the permeable base will be 0.23 and the porosity will be 0.29.

For the above conditions, the slope factor can be calculated.

$S_1 = (L_R/S_R)/H = 24 \times 0.02 / 0.5 = 0.96$

Entering figure 6.5 with the slope factor, produces a time factor (T50) of 0.245

Calculate the "m" factor:

$m = N_e L_R^2 / K H = 0.23 \times (24)^2 / (3583 \times 0.5) = 0.074$

Now calculate the time to drain (t)

$t = T_{50}\, m\, 24 = 0.245 \times 0.074 \times 24 = 0.43$ hours

In table 6.4 with $t = 0.43$ hours, the open-graded base has a quality of drainage level as excellent.

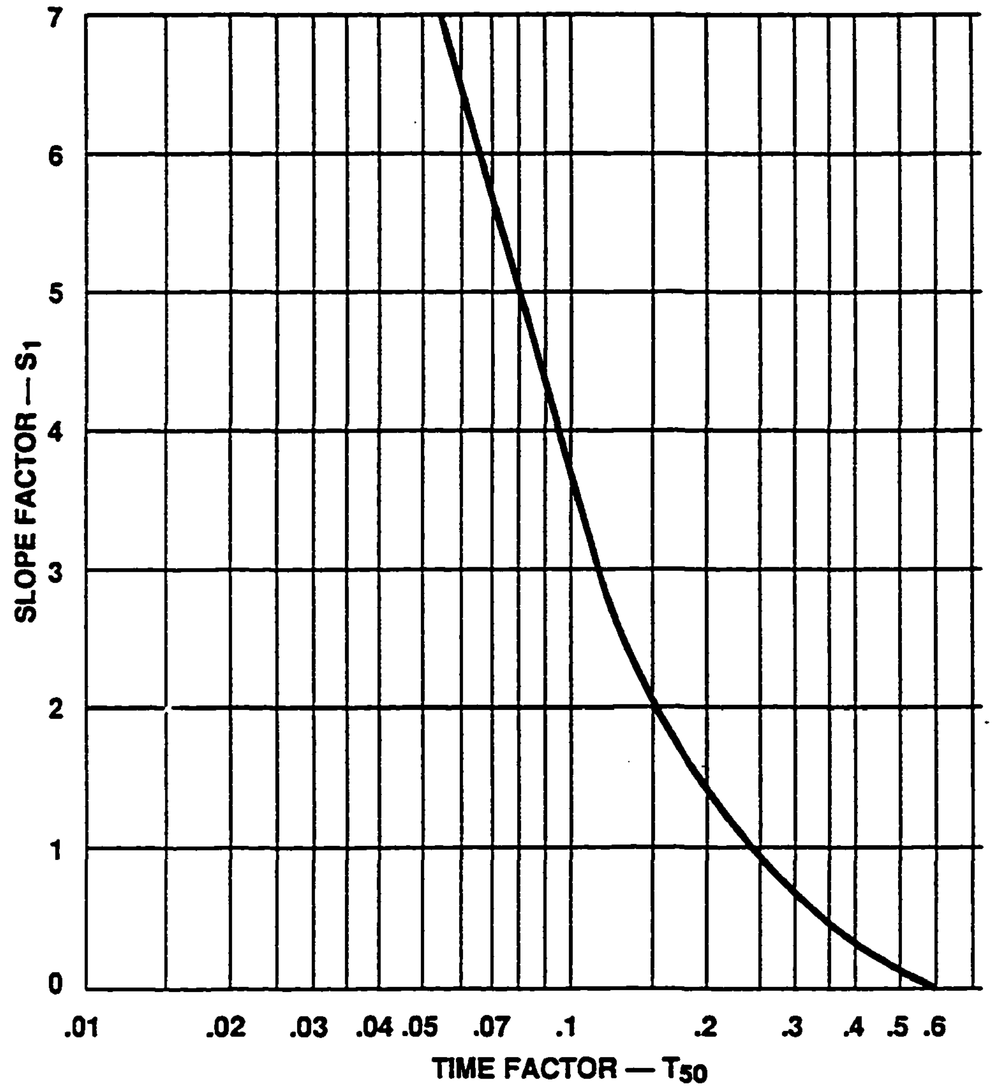

Figure 6.4 Time Factor for 50 Percent Drainage [11]

6.6 Summary of Analysis

The untreated material test results on permeability were statistically analyzed to produce a regression equation (shown in Figure 5.1, Chapter 5) to estimate the coefficient of permeability of both dense-graded and open-graded untreated materials with percent fines passing # 4 sieve as dependent variable. This equation has an R-squared value of 0.99.

Over the range of confining pressure and vertical stresses considered, the resilient modulus characterization using the K-θ showed a good fit as illustrated by the higher coefficient of determination (R-squared) for all gradations considered in this study. Resilient modulus as a function of percent fines showed that as the percent fines increased, the resilient modulus increased for all stress level until reaching a maximum values beyond which the values of the resilient modulus began to decrease. The percent fines at which the resilient modulus reached a maximum was 28.5%.

Consideration of both permeability and resilient modulus resulted in the identification of a compromise gradation optimum, which provided data suitable for input in pavement design.

6.7 Summary of the Results

The results of this research can be summarized as follows:

A. Percent added fines have an effect on resilient modulus and permeability. Resilient modulus increased until an optimum percent fines was reached, beyond which resilient modulus decreased. Increased in percent fines resulted in a decreased in permeability.

B. A regression equation that estimates the coefficient of permeability of both dense-graded and open-graded untreated aggregate bases with percent fines as independent variable was produced. This equation is as follows:

$$\mathbf{K(ftd) = -0.6948fine^3 + 58.798fine^2 - 2032.6fine + 31278} \quad \mathbf{(6.3)}$$

C. Non-linear regression equations (K-θ) to estimate resilient modulus for all gradations considered in this study were produced. These equations were as follows:

$$\mathbf{M_{r(AASHTO\ 67)} = 3924\theta^{0.42}} \quad \mathbf{(6.4)}$$

$$\mathbf{M_{r(A85\_S15)} = 7275\theta^{0.345}} \quad \mathbf{(6.5)}$$

$$\mathbf{M_{r(A75\_S25)} = 17486\theta^{0.181}} \quad \mathbf{(6.6)}$$

$$\mathbf{M_{r(A65\_S35)} = 16890\theta^{0.188}} \quad \mathbf{(6.7)}$$

$$\mathbf{M_{r(LA\ Base)} = 26186\theta^{0.143}} \quad \mathbf{(6.8)}$$

D. Regression equations that estimate the resilient modulus (M_r) as function of percent fines for all stress levels studied were also produced. These equation were as follows:

$$\mathbf{M_{r\_10.5\ psi} = -5.123x^3 + 289.06x^2 - 3967.9x + 25350} \quad \mathbf{(6.9)}$$

$$\mathbf{M_{r\_20\ psi} = -5.239x^3 + 290.61x^2 - 3881.1x + 28011} \quad \mathbf{(6.10)}$$

$$\mathbf{M_{r\_30\ psi} = -4.374x^3 + 242.59x^2 - 3155.3x + 28213} \quad \mathbf{(6.11)}$$

$$M_{r\_40\,psi} = -3.896x^3 + 210.51x^2 - 2551.1x + 27243 \quad (6.12)$$

$$M_{r\_58.5\,psi} = -2.176x^3 + 107.37x^2 - 768.86x + 22622 \quad (6.13)$$

where, x represents the percentage fines passing #4 sieve.

E. The optimum percent fine that produced the maximum values of resilient modulus for the range of stress considered was found to be 28.5%

F. The compromise gradation recommended to withstand stresses induced by traffic and at the same time be permeable enough to drain water is as follows:

Table 6.6 Compromise Gradation

US Sieve Number	Gradation Band		
	% Passing - Lower	Mid-range	% Passing - Upper
1"	100	100	100
3/4"	96.74	96.585	96.43
3/8"	52.47	55.54	58.62
#4	24.72	28.46	32.23
#8	10.76	12.13	13.5
#30	4.56	4.96	5.36
#50	3.34	3.62	3.89
#100	1.47	1.52	1.58
#200	0.62	0.58	0.54

CHAPTER 7

CONCLUSIONS AND RECOMMENDATIONS

7.1 Conclusions

The current investigation provided some relationships between aggregate resilient modulus, permeability and % fines. These relationships can be used to predict K and Mr for the open-graded material tested.

The study also provides an optimum gradation that provides reasonable stiffness while maintaining acceptable drainage characteristics. This gradation has considerably lower K and higher Mr than that of a conventional AASHTO 67 open-graded material and higher K and lower Mr than Louisiana Base.

A chart was developed to assist engineers in estimating Mr values, based on the permeability requirements. These values can be compared to the specified values or used as input for pavement design.

The findings of this research should be helpful to highway personnel. When it is required to test highway bases for permeability, the Barber and Sawyer permeameter is recommended as testing device because it was successfully used in this study. Highway personnel can also use Equation 7.1 to estimate the coefficient of permeability (K) of untreated base materials. Once the K value is estimated, it can then be used to either analyze the drainage capability of an existing highway layer, or to design a new one.

Equations 7.2 through 7.11 can be used to estimate the resilient modulus as it is input for the AASHTO pavement design procedures.

7.2 Recommendations

A. The proposed compromise gradation should be validated through a pilot project by monitoring data over its entire duration. This data must be analyzed to appreciate the effectiveness of the proposed gradation.

B. Instead of considering one type of aggregate, expand the study to consider other aggregate sources.

C. Study the effect of aggregate shape on K and Mr.

D. Include permanent deformation behavior of the aggregate.

E. Study the effect of other variables (porosity, voids ratio) on permeability and the influence of maximum aggregate size on K and Mr.

F. Develop a structural number for the proposed gradation for use in the 86 AASHTO Design Guide.

G. Because of the gradation variability involved in the handling and placing of aggregate in the field versus the laboratory, it is recommended to study the band of the proposed gradation. The investigation should consider increasing the amount of finer material passing sieves with opening sizes 2.36 mm, 4.75 mm, and 9.5 mm while maintaining good permeability and resilient modulus characteristics.

APPENDIX A

GRAIN SIZE DISTRIBUTION BEFORE AND AFTER PERMEABILITY TESTING AND PERMEABILITY

Table A.1 Grain Size Distribution: AASHTO 67

Sieve Analysis (AASHTO) before Permeability Testing					
Sieve	Specimen 1 % Passing	Specimen 2 % Passing	Specimen 3 % Passing	Specimen 4 % Passing	Specimen 5 % Passing
1	100.00	100.00	100.00	100.00	100.00
3/4	96.92	95.25	96.58	96.05	95.94
3/8	37.62	37.51	37.58	36.78	37.22
#4	6.52	6.54	6.26	6.25	6.23
#8	2.74	2.68	2.75	2.62	2.55
#30	1.85	1.82	1.90	1.71	1.72
#50	1.67	1.61	1.70	1.49	1.54
#100	0.80	0.69	0.64	0.44	0.99
#200	0.60	0.26	0.44	0.34	0.65

Table A.2 Grain Size Distribution: A85_S15

85% AASHTO 67 mixed with 15% Screening					
Sieve Analysis (AASHTO) before Permeability Testing					
Sieve	Specimen 1 % Passing	Specimen 2 % Passing	Specimen 3 % Passing	Specimen 4 % Passing	Specimen 5 % Passing
1	100	100	100	100	100
3/4	95.80	96.61	97.16	97.02	96.68
3/8	46.71	47.45	47.00	47.68	48.00
#4	17.14	17.36	17.43	17.49	17.23
#8	7.68	7.30	7.81	8.17	7.77
#30	3.64	3.35	3.62	3.83	3.60
#50	2.87	2.63	2.77	2.92	2.81
#100	0.91	1.02	1.15	1.12	0.95
#200	0.46	0.54	0.50	0.52	0.40

Table A.3 Grain Size Distribution: A75_S25

75% AASHTO 67 mixed with 25% Screening					
Sieve Analysis (AASHTO) before Permeability Testing					
Sieve	Specimen1 % Passing	Specimen2 % Passing	Specimen 3 % Passing	Specimen 4 % Passing	Specimen 5 % Passing
1	100	100	100	100	100
3/4	98.08	96.98	97.61	97.62	98.13
3/8	52.66	53.05	53.06	52.80	53.34
#4	24.64	24.71	25.16	24.92	25.35
#8	11.01	11.56	10.78	10.26	10.71
#30	4.70	4.97	4.63	4.25	4.47
#50	3.33	3.62	3.45	3.16	3.30
#100	1.06	1.86	1.47	1.47	1.57
#200	0.47	0.71	0.63	0.63	0.69

Table A.4 Grain Size Distribution: A65_S35

65% AASHTO 67 mixed with 35% Screening					
Sieve Analysis (AASHTO) before Permeability Testing					
Sieve	Specimen 1 % Passing	Specimen 2 % Passing	Specimen 3 % Passing	Specimen 4 % Passing	Specimen 5 % Passing
1	100	100	100	100	100
3/4	97.17	97.70	98.07	96.35	97.25
3/8	58.48	59.29	58.95	59.34	59.69
#4	31.77	32.39	32.55	33.11	32.80
#8	14.02	13.29	12.92	13.82	14.04
#30	5.56	5.31	5.09	5.45	5.63
#50	4.05	3.91	3.69	3.95	4.03
#100	1.61	1.11	1.79	1.85	1.60
#200	0.70	0.39	0.67	0.46	0.48

Table A.5 Grain Size Distribution: Louisiana Base

Louisiana Typical Base Material					
Sieve Analysis (AASHTO) before Permeability Testing					
Sieve	Specimen 1 % Passing	Specimen 2 % Passing	Specimen 3 % Passing	Specimen4 % Passing	Specimen 5 % Passing
1.5	100	100	100	100	100
3/4	86.81	85.86	86.86	86.48	86.28
3/8	60.28	60.50	60.48	60.84	60.69
#4	38.76	38.32	37.08	38.84	38.61
#8	26.16	25.93	26.00	26.23	26.88
#30	13.86	13.67	13.69	13.96	14.32
#40	10.84	11.50	10.64	11.50	11.28
#100	3.93	3.89	4.35	4.00	4.13
#200	1.09	0.35	1.55	0.67	0.90

Table A.6 Permeability Test Results Using B/S Permeameter: AASHTO 67

Permeability Testing 100% AASHTO 67					
1- Sieve Analysis (AASHTO) after Permeability Testing					
Sieve	Specimen 1 % Passing	Specimen 2 % Passing	Specimen 3 % Passing	Specimen 4 % Passing	Specimen 5 % Passing
1	100.00	100.00	100.00	100.00	100.00
3/4	95.96	94.45	95.84	95.41	94.99
3/8	37.25	37.19	37.29	36.54	36.85
#4	6.46	6.48	6.21	6.21	6.17
#8	2.71	2.66	2.73	2.60	2.53
#30	1.83	1.80	1.89	1.70	1.70
#50	1.65	1.60	1.69	1.48	1.52
#100	0.79	0.68	0.64	0.44	0.98
#200	0.59	0.26	0.44	0.34	0.64
2- Coefficient of Permeability					
cm/sec	7.63	6.98	7.34	7.48	6.84
fpd	21633	19793	20810	21212	19392
Height, cm	15.05	14.93	14.73	14.93	14.83
3- Unit Weight, pcf					
Wet U. Wt.	103.20	104.06	105.47	104.06	104.76
Water C. %	1	1	1	1	1
Dry U. Wt.	102.18	103.03	104.43	103.03	103.72

Table A.7 Permeability Test Results Using B/S Permeameter: A85_S15

Permeability Testing 85% AASHTO 67 mixed with 15% Screening					
1- Sieve Analysis (AASHTO) after Permeability Testing					
Sieve	Specimen 1 % Passing	Specimen 2 % Passing	Specimen 3 % Passing	Specimen 4 % Passing	Specimen 5 % Passing
1	100.00	100.00	100.00	100.00	100.00
3/4	94.87	95.65	96.31	96.28	95.72
3/8	46.26	46.98	46.59	47.32	47.53
#4	16.97	17.19	17.28	17.36	17.06
#8	7.61	7.23	7.74	8.11	7.69
#30	3.60	3.32	3.59	3.80	3.56
#50	2.84	2.60	2.75	2.90	2.78
#100	0.90	1.01	1.14	1.11	0.94
#200	0.46	0.53	0.50	0.52	0.40
2- Coefficient of Permeability					
cm/sec	3.66	3.37	3.80	3.86	3.88
fpd	10381	9554	10783	10941	10993
Height, cm	14.24	14.10	14.25	14.30	14.13
3- Unit Weight, pcf					
Wet U. Wt.	108.99	110.15	108.98	108.60	109.95
Water C. %	1.5	1.5	1.5	1.5	1.5
Dry U. Wt.	107.38	108.52	107.37	107.00	108.33

Table A.8 Permeability Test Results Using B/S Permeameter: A75_S25

Permeability Testing 75% AASHTO 67 mixed with 25% Screening					
1- Sieve Analysis (AASHTO) after Permeability Testing					
Sieve	Specimen 1 % Passing	Specimen 2 % Passing	Specimen 3 % Passing	Specimen 4 % Passing	Specimen 5 % Passing
1	100.00	100.00	100.00	100.00	100.00
3/4	97.11	96.02	96.55	96.79	97.21
3/8	52.14	52.53	52.48	52.35	52.84
#4	24.40	24.47	24.89	24.71	25.11
#8	10.90	11.45	10.66	10.17	10.61
#30	4.65	4.92	4.58	4.21	4.43
#50	3.30	3.58	3.41	3.13	3.27
#100	1.05	1.84	1.45	1.46	1.56
#200	0.47	0.70	0.62	0.62	0.68
2- Coefficient of Permeability					
cm/sec	2.01	2.17	2.01	2.08	2.06
fpd	5691	6142	5698	5894	5839
Height, cm	13.63	13.81	13.68	13.80	13.85
3- Unit Weight, pcf					
Wet U. Wt.	114.00	112.44	113.57	112.54	112.13
Water C. %	1.5	1.5	1.5	1.5	1.5
Dry U. Wt.	112.32	110.78	111.89	110.88	110.47

Table A.9 Permeability Test Results Using B/S Permeameter: A65_S35

Permeability Testing 65% AASHTO 67 mixed with 35% Screening					
1- Sieve Analysis (AASHTO) after Permeability Testing					
Sieve	Specimen 1 % Passing	Specimen 2 % Passing	Specimen 3 % Passing	Specimen 4 % Passing	Specimen 5 % Passing
1	100.00	100.00	100.00	100.00	100.00
3/4	96.32	96.73	97.23	95.40	96.48
3/8	57.97	58.70	58.45	58.75	59.22
#4	31.49	32.07	32.27	32.78	32.54
#8	13.90	13.16	12.81	13.68	13.93
#30	5.51	5.26	5.05	5.40	5.59
#50	4.01	3.87	3.66	3.91	4.00
#100	1.60	1.10	1.77	1.83	1.59
#200	0.69	0.39	0.66	0.46	0.48
2- Coefficient of Permeability					
cm/sec	1.90	1.88	1.66	1.46	1.48
fpd	5374	5327	4703	4152	4184
Height, cm	13.80	13.58	13.68	13.45	13.48
3- Unit Weight, pcf					
Wet U. Wt.	112.46	114.50	113.57	115.47	115.25
Water C. %	2	2	2	2	2
Dry U. Wt.	110.25	112.25	111.34	113.21	112.99

Table A.10 Permeability Test Results Using B/S Permeameter: Louisiana Base

Permeability Testing Louisiana Typical Base Material					
1- Sieve Analysis after K (AASHTO) after Permeability Testing					
Sieve	Specimen 1 % Passing	Specimen 2 % Passing	Specimen 3 % Passing	Specimen 4 % Passing	Specimen 5 % Passing
1.5	100.00	100.00	100.00	100.00	100.00
3/4	86.64	85.60	86.64	86.17	86.02
3/8	60.16	60.32	60.32	60.62	60.51
#4	38.68	38.21	36.98	38.70	38.49
#8	26.11	25.85	25.93	26.14	26.80
#30	13.83	13.63	13.65	13.91	14.28
#40	10.82	11.47	10.61	11.46	11.25
#100	3.92	3.88	4.34	3.99	4.12
#200	1.09	0.35	1.55	0.67	0.90
2- Coefficient of Permeability					
cm/sec	0.17	0.16	0.20	0.11	0.20
fpd	482	453	580	321	566
Height, cm	13.63	13.81	13.68	13.80	13.85
3- Unit Weight, pcf					
Wet U. Wt.	133.98	133.60	133.36	135.79	135.05
Water C. %	4.5	4.5	4.5	4.5	4.5
Dry U. Wt.	128.21	127.85	127.62	129.94	129.23

APPENDIX B

PROGRAMS USED FOR DATA ACQUISITION

Here is a sample program which can generate the haversine wave form used in the resilient modulus testing:

```
100 STAT%=10
130 CLS
140 CALL KDINIT
160 DIM SINEPOINTS!(1000)
180 LOCATE 1, 1:PRINT"Making output array. Please wait..."
190 FOR T%=0 TO 99
192 C=T%*2*3.14159/99
200     SINEPOINTS!(T%)=10-20*(1-COS(C))/2
210 NEXT T%
212 FOR T%=100 TO 999
214 SINEPOINTS!(T%)=10
216 NEXT T%
250 PRINT:PRINT "Transferring array contents to KDAC500 array
'OUTARRAY%'..."
260 CALL ARMAKE'("outarray%", 1000., "outchan")
270 CALL ARPUT'("outarray%", 1., 1000., "outchan", 1, sinepoints!(), "c.volts")
300 BEEP:BEEP
310 CALL BGWRITE'("outarray%", "outchan", 1, 100, "NT", "task")
370 CALL INTON'(1, "MIL")
400 CALL BGSTATUS'("task",STAT%)
410 IF STAT%<>0 GOTO 400
420 CALL INTOFF
430 BEEP:BEEP
440 END
```

Here is another sample program which can record the voltage signals from LVDT and load cell used in the resilient modulus testing.

```
5 CLS:CALL KDINIT
10 DIM LVDT(3000),LDSS(3000)
15 DIM CC(1),DD(1)
20 CALL INTOFF
30 LOCATE 1,5:PRINT"ATTENTION!"
35 BEEP:BEEP:BEEP:BEEP:BEEP
36 PRINT "Please input the test sequence number !"
37 INPUT E$:CLS
40 LOCATE 2,5:PRINT"FIRST DO FOREGROUND READING TO CHECK THE
SYSTEM."
80 CALL FGREAD'("S1C0","NONE",CC(),"C.VOLTS","NT")
```

```
85 CALL FGREAD'("S1C2","NONE",DD(),"C.VOLTS","NT")
110 LOCATE 6,5:PRINT "THE VOLTAGE FROM S1C0";:PRINT USING "###.#####";CC(0):LOCATE 6,60:PRINT "VOLTS"
115 LOCATE 7,5:PRINT "THE VOLTAGE FROM S1C2";:PRINT USING "###.#####";DD(0):LOCATE 7,60:PRINT "VOLTS"
120 LOCATE 20,5: PRINT "IF THE SYSTEM IS 'OK', THEN PRESS 'S' TO START THE EXPERIMENT!"
130 U$=INKEY$:IF U$="S" OR U$="s" THEN 140 ELSE 80
140 CLS
150 CALL BGCLEAR
160 LOCATE 10,10 :PRINT "THE SYSTEM IS COLLECTING DATA.............."
170 STAT%=10
175 CALL INTON'(5,"mil")
190 CALL BGREAD'("array3", 2000., "s1c0", 1, "none", 1, "nt", "st")
195 CALL BGREAD'("array4", 2000., "s1c2", 1, "none", 1, "nt", "st")
200 CALL BGSTATUS'("st",stat%)
210 IF STAT%<>0 GOTO 200
220 CALL INTOFF
230 BEEP:BEEP:BEEP
240 LOCATE 10,10:PRINT"FINISH COLLECTING DATA!                    "
250 LOCATE 12,10:PRINT"NOW COMPUTER IS CREATING DATA FILES......."
252 OPEN"C:\KEITHLEY\LVDT-"+E$+".DAT" FOR OUTPUT AS #2
260 OPEN"C:\KEITHLEY\LOAD-"+E$+".DAT" FOR OUTPUT AS #3
590 CALL ARGET'("array3",1.,2000.,"s1c0",1,LVDT(),"c.volts")
600 CALL ARGET'("array4",1.,2000.,"s1c2",1,LDSS(),"c.volts")
620 FOR I=1 TO 2000
650 WRITE #2, I, LVDT(I)
655 WRITE #3, I, LDSS(I)
660 NEXT I
3000 CLOSE #2:CLOSE #3:BEEP:BEEP
3100 END
```

APPENDIX C

RESULTS FOR RESILIENT MODULUS TESTS AND UNCONFINED COMPRESSION TESTS

Table C.1 Test Data of Specimen A67_1

Sequence	Confining Stress	Bulk Stress	Max. Axial Stress	Contact Stress	Cyclic Stress	Resilient Strain	Resilient Mod. (psi)
1	2.5	10.5	4.8857	0.151	4.73	0.0004429	10679
2	5	20	5.08441	0.531	4.55	0.000341	13345
3	7	30	9.03272	0.84236	9.19036	0.0005441	16891
4	9	40	10.85557	1.42122	9.43446	0.0005221	18071
5	13	58.5	18.1043	2.16422	15.9401	0.0007339	21721

Table C.2 Test Data of Specimen A67_2

Sequence	Confining Stress	Bulk Stress	Max. Axial Stress	Contact Stress	Cyclic Stress	Resilient Strain	Resilient Mod. (psi)
1	2.5	10.5	4.50556	0.125	4.38	0.0004119	10633
2	5	20	4.70427	0.514	4.19	0.0003025	13850
3	7	30	8.73897	0.86828	7.87069	0.0004654	16912
4	9	40	10.7002	1.42986	9.27031	0.0005063	18309
5	13	58.5	17.7501	2.19878	15.5513	0.0007197	21609

Table C.3 Test Data of Specimen A67_3

Sequence	Confining Stress	Bulk Stress	Max. Axial Stress	Contact Stress	Cyclic Stress	Resilient Strain	Resilient Mod. (psi)
1	2.5	10.5	4.79931	0.15	4.64931	0.0004489	10356
2	5	20	5.04122	0.687	4.35	0.0003123	13930
3	7	30	9.19687	0.86828	8.32859	0.0004955	16809
4	9	40	11.1581	1.36938	9.78868	0.0005232	18708
5	13	58.5	18.9424	2.15558	16.7868	0.0007883	21296

Table C.4 Test Data of Specimen A67_4

Sequence	Confining Stress	Bulk Stress	Max. Axial Stress	Contact Stress	Cyclic Stress	Resilient Strain	Resilient Mod. (psi)
1	2.5	10.5	4.69563	0.138	4.55763	0.0004473	10190
2	5	20	4.89434	0.5225	4.37184	0.0003148	13886
3	7	30	8.885845	0.85532	8.03053	0.0004749	16909
4	9	40	10.777885	1.42554	9.35235	0.0005005	18687
5	13	58.5	17.9272	2.1815	15.7457	0.000722	21807

Table C.5 Test Data of Specimen A67_5

Sequence	Confining Stress	Bulk Stress	Max. Axial Stress	Contact Stress	Cyclic Stress	Resilient Strain	Resilient Mod. (psi)
1	2.5	10.5	4.790665	0.1445	4.64617	0.000428	10855
2	5	20	4.989375	0.52675	4.46263	0.0003214	13886
3	7	30	8.9592825	0.84884	8.11044	0.0004819	16830
4	9	40	10.816728	1.42338	9.39335	0.0004958	18944
5	13	58.5	18.01575	2.17286	15.8429	0.0007512	21090

Table C.6 Test Data of Specimen A85_S15_1

Sequence	Confining Stress	Bulk Stress	Max. Axial Stress	Contact Stress	Cyclic Stress	Resilient Strain	Resilient Mod. (psi)
1	2.5	10.5	4.66971	0.125	4.54	0.0002791	16264
2	5	20	4.80795	0.479	4.33	0.000214	20236
3	7	30	9.3103	0.85964	8.50138	0.0003585	23714
4	9	40	11.2963	1.44714	9.4916	0.0003651	25994
5	13	58.5	18.5104	2.16422	16.3462	0.0005475	29854

Table C.7 Test Data of Specimen A85_S15_2

Sequence	Confining Stress	Bulk Stress	Max. Axial Stress	Contact Stress	Cyclic Stress	Resilient Strain	Resilient Mod. (psi)
1	2.5	10.5	4.49692	0.151	4.35	0.0002661	16345
2	5	20	4.80795	0.583	4.22	0.0002045	20640
3	7	30	9.25735	0.8942	8.36315	0.0003658	22863
4	9	40	11.1926	1.42986	9.76277	0.0003831	25485
5	13	58.5	18.519	2.13831	16.3807	0.00056	29252

Table C.8 Test Data of Specimen A85_S15_3

Sequence	Confining Stress	Bulk Stress	Max. Axial Stress	Contact Stress	Cyclic Stress	Resilient Strain	Resilient Mod. (psi)
1	2.5	10.5	4.41052	0.307	4.1	0.0002515	16305
2	5	20	4.66107	0.575	4.01	0.0001962	20438
3	7	30	9.67205	0.86828	8.80377	0.000378	23289
4	9	40	11.5123	1.40394	10.1083	0.0003927	25740
5	13	58.5	18.7436	2.15558	16.588	0.0005613	29553

Table C.9 Test Data of Specimen A85_S15_4

Sequence	Confining Stress	Bulk Stress	Max. Axial Stress	Contact Stress	Cyclic Stress	Resilient Strain	Resilient Mod. (psi)
1	2.5	10.5	4.540115	0.216	4.32412	0.0002554	16930
2	5	20	4.73451	0.527	4.20751	0.0002009	20943
3	7	30	9.491175	0.86396	8.62722	0.0003603	23942
4	9	40	11.4043	1.42554	9.97876	0.0003933	25370
5	13	58.5	18.627	2.1599	16.4671	0.0005323	30937

Table C.10 Test Data of Specimen A85_S15_5

Sequence	Confining Stress	Bulk Stress	Max. Axial Stress	Contact Stress	Cyclic Stress	Resilient Strain	Resilient Mod. (psi)
1	2.5	10.5	4.5185175	0.1835	4.33502	0.0002625	16514
2	5	20	4.77123	0.555	4.21623	0.0002083	20246
3	7	30	9.3742625	0.87908	8.49518	0.000369	23020
4	9	40	11.29845	1.4277	9.87075	0.000376	26254
5	13	58.5	18.573	2.14911	16.4239	0.0005363	30622

Table C.11 Test Data of Specimen A75_S25_1

Sequence	Confining Stress	Bulk Stress	Max. Axial Stress	Contact Stress	Cyclic Stress	Resilient Strain	Resilient Mod. (psi)
1	2.5	10.5	5.43864	0.212	5.22696	0.0001938	26966
2	5	20	5.68055	0.53998	5.14057	0.0001663	30907
3	7	30	10.0436	0.88556	9.15799	0.0002783	32906
4	9	40	11.8752	1.47305	10.4021	0.000304	34213
5	13	58.5	18.5795	2.19878	16.3807	0.0004529	36172

Table C.12 Test Data of Specimen A75_S25_2

Sequence	Confining Stress	Bulk Stress	Max. Axial Stress	Contact Stress	Cyclic Stress	Resilient Strain	Resilient Mod. (psi)
1	2.5	10.5	4.85114	0.151	4.7	0.000177	26558
2	5	20	5.04122	0.53998	4.50124	0.0001505	29907
3	7	30	9.47334	0.82508	8.64826	0.0002649	32652
4	9	40	11.5555	1.4385	10.117	0.0003045	33226
5	13	58.5	19.072	2.17286	16.8991	0.0004642	36406

Table C.13 Test Data of Specimen A75_S25_3

Sequence	Confining Stress	Bulk Stress	Max. Axial Stress	Contact Stress	Cyclic Stress	Resilient Strain	Resilient Mod. (psi)
1	2.5	10.5	4.67835	0.134	4.54	0.0001708	26584
2	5	20	5.00666	0.514	4.49	0.000146	30759
3	7	30	9.24871	0.81644	8.43227	0.0002617	32224
4	9	40	11.2445	1.4385	9.80596	0.0002862	34268
5	13	58.5	18.5363	2.13831	16.398	0.0004501	36431

Table C.14 Test Data of Specimen A75_S25_4

Sequence	Confining Stress	Bulk Stress	Max. Axial Stress	Contact Stress	Cyclic Stress	Resilient Strain	Reslient Mod. (psi)
1	2.5	10.5	4.82523	0.16	4.67	0.0001778	26265
2	5	20	4.96346	0.566	4.4	0.0001457	30206
3	7	30	9.19687	0.86828	8.32859	0.0002583	32238
4	9	40	11.0889	1.46441	9.62453	0.0002879	33430
5	13	58.5	18.0438	2.14694	15.8969	0.0004393	36188

Table C.15 Test Data of Specimen A75_S25_5

Sequence	Confining Stress	Bulk Stress	Max. Axial Stress	Contact Stress	Cyclic Stress	Resilient Strain	Resilient Mod. (psi)
1	2.5	10.5	5.14489	0.151	4.89	0.0001874	26100
2	5	20	5.3436	0.53998	4.80363	0.000156	30801
3	7	30	9.35238	0.85964	8.49274	0.0002659	31939
4	9	40	11.0889	1.4385	9.65045	0.0002794	34536
5	13	58.5	18.6486	2.16422	16.4844	0.0004518	36488

Table C.16 Test Data of Specimen A65_S35_1

Sequence	Confining Stress	Bulk Stress	Max. Axial Stress	Contact Stress	Cyclic Stress	Resilient Strain	Resilient Mod. (psi)
1	2.5	10.5	4.9721	0.168	4.8041	0.000184	26114
2	5	20	5.16217	0.497	4.66517	0.0001607	29024
3	7	30	9.32647	0.84236	8.48411	0.0002711	31300
4	9	40	11.3049	1.31754	9.98736	0.0002996	33331
5	13	58.5	18.9251	2.15558	16.7695	0.0004638	36153

Table C.17 Test Data of Specimen A65_S35_2

Sequence	Confining Stress	Bulk Stress	Max. Axial Stress	Contact Stress	Cyclic Stress	Resilient Strain	Resilient Mod. (psi)
1	2.5	10.5	4.73883	0.186	4.55283	0.0001717	26520
2	5	20	5.03258	0.53998	4.4926	0.0001528	29404
3	7	30	9.26599	1.03243	8.23356	0.0002544	32365
4	9	40	10.9939	1.47305	9.52085	0.0002874	33127
5	13	58.5	18.5277	2.19878	16.3289	0.0004348	37551

Table C.18 Test Data of Specimen A65_S35_3

Sequence	Confining Stress	Bulk Stress	Max. Axial Stress	Contact Stress	Cyclic Stress	Resilient Strain	Resilient Mod. (psi)
1	2.5	10.5	6.66107	0.151	4.51007	0.0001716	26275
2	5	20	4.9721	0.566	4.4061	0.000148	29781
3	7	30	9.08456	0.85964	8.22492	0.0002531	32500
4	9	40	11.0025	1.41258	9.58992	0.0002895	33128
5	13	58.5	18.6318	2.14694	16.4849	0.0004503	36610

Table C.19 Test Data of Specimen A65_S35_4

Sequence	Confining Stress	Bulk Stress	Max. Axial Stress	Contact Stress	Cyclic Stress	Resilient Strain	Resilient Mod. (psi)
1	2.5	10.5	4.72155	0.177	4.54455	0.0001699	26749
2	5	20	5.02394	0.53998	4.48396	0.0001537	29167
3	7	30	9.26599	0.81644	8.44955	0.0002628	32149
4	9	40	11.2272	1.44714	9.78006	0.0002903	33691
5	13	58.5	18.3289	1.57673	16.7522	0.0004606	36371

Table C.20 Test Data of Specimen A65_S35_5

Sequence	Confining Stress	Bulk Stress	Max. Axial Stress	Contact Stress	Cyclic Stress	Resilient Strain	Resilient Mod. (psi)
1	2.5	10.5	5.04122	0.13	4.91122	0.000188	26128
2	5	20	5.22265	0.50542	4.71723	0.0001552	30395
3	7	30	9.32647	0.83372	8.49275	0.0002615	32479
4	9	40	11.0976	1.41258	9.68502	0.0002888	33541
5	13	58.5	18.1734	2.12967	16.0437	0.0004429	36221

Table C.21 Test Data of Specimen Louisiana Base_1

Sequence	Confining Stress	Bulk Stress	Max. Axial Stress	Contact Stress	Cyclic Stress	Resilient Strain	Resilient Mod. (psi)
1	2.5	10.5	4.8425	0.16	4.6825	0.0001284	36477
2	5	20	5.00666	0.531	4.47566	0.0001139	39300
3	7	30	9.26599	0.83372	8.43227	0.0001982	42536
4	9	40	11.2877	1.42986	9.85784	0.0002218	44439
5	13	58.5	18.6572	2.17286	16.4843	0.0003503	47052

Table C.22 Test Data of Specimen Louisiana Base_2

Sequence	Confining Stress	Bulk Stress	Max. Axial Stress	Contact Stress	Cyclic Stress	Resilient Strain	Resilient Mod. (psi)
1	2.5	10.5	4.89002	0.1685	4.72152	0.0001281	36867
2	5	20	5.054175	0.527	4.52718	0.0001123	40325
3	7	30	9.300545	0.85964	8.44091	0.0001964	42984
4	9	40	11.27905	1.45146	9.8276	0.0002191	44860
5	13	58.5	18.7782	2.19446	16.5837	0.0003527	47013

Table C.23 Test Data of Specimen Louisiana Base_3

Sequence	Confining Stress	Bulk Stress	Max. Axial Stress	Contact Stress	Cyclic Stress	Resilient Strain	Resilient Mod. (psi)
1	2.5	10.5	4.93754	0.177	4.76054	7841.7574	37331
2	5	20	5.10169	0.523	4.57869	0.0001135	40334
3	7	30	9.3351	0.88556	8.44954	0.0001968	42928
4	9	40	11.2704	1.47305	9.79735	0.0002201	44507
5	13	58.5	18.8992	2.21606	16.6831	0.0003617	46118

Table C.24 Test Data of Specimen Louisiana Base_4

Sequence	Confining Stress	Bulk Stress	Max. Axial Stress	Contact Stress	Cyclic Stress	Resilient Strain	Resilient Mod. (psi)
1	2.5	10.5	4.72155	0.11663	4.60492	0.0001248	36901
2	5	20	4.96346	0.488	4.47546	0.0001132	39553
3	7	30	9.36103	0.85964	8.50139	0.0002014	42219
4	9	40	11.2963	1.44714	9.84916	0.0002231	44154
5	13	58.5	18.6313	2.1815	16.4498	0.0003517	46776

Table C.25 Test Data of Specimen Louisiana Base_5

Sequence	Confining Stress	Bulk Stress	Max. Axial Stress	Contact Stress	Cyclic Stress	Resilient Strain	Resilient Mod. (psi)
1	2.5	10.5	5.13626	0.11663	5.01962	0.0001382	36325
2	5	20	5.26585	0.53998	4.72587	0.0001183	39964
3	7	30	9.24871	0.8942	8.35451	0.0001974	42313
4	9	40	11.0112	1.42122	9.58997	0.0002125	45137
5	13	58.5	18.6227	2.11239	16.5103	0.0003513	46999

Mod. = Modulus

Table C.26 Unconfined Compression Test Results

AAHTO 67		A85_S15		A75_S25		A65_S35	
% Fines	U. C., pounds	% Fines	U. C., pounds	% Fines	U. C., pounds	% Fines	U. C., pounds
6.46	742	16.97	928	24.4	1242	31.49	1183
6.48	735	17.19	970	24.47	1247	32.07	1146
6.21	703	17.28	885	24.89	1194	32.27	1125
6.21	738	17.36	908	24.71	1244	32.28	1205
6.21	748	17.06	910	24.71	1210	32.28	1232

U. C.: Unconfined Compression.

APPENDIX D

SUBGRADE SOIL MATERIAL

NOV-25-98 03:36 PM
[MATT MENU SELECTION - 14]

P.02
2/94

Louisiana Department of Transportation and Development

SOILS/SOIL AGGREGATE

Project No. 038-01-0001
Date Sampled 08-10-98
Purpose Code 1
Date Tested 08-13-98
From Station 14009
Location L S
Hole No.
Depth 0.20 0.70
Item No.

Material Code 401
Submitted By 0304
Pit No.
Ident. S-3
To Station
Log Mile
Sampled by: CKH, DC, TS

Lab. No. 05-214016
Quantity
Spec Code 1
Parish No. 37

Purp. Codes
1. Quality Control
2. Verification
3. Acceptance
4. Check
5. Resample
6. Source Approval
7. Design
8. Indep. Assurance
9. Pre Source Appr.

Remarks 1

Hydrometer Analysis (DOTD TR 407)			Graduate No.	Dry Wt of Sample, g (1-50.0, 2-100.0) 1			
Time	Elapsed time	Temp°C (0.5° increments)	Hydro Reading (0.5 increments)	Correction (0.5 increments)	Corrected Reading	% Finer	Effective Grain Size
	60 Minutes	21.5	24.0	8.5			
	120 Minutes	21.3	22.5	8.3			

RETAINED ON 40

Wt. Cup + Soil, g 1.1
Cup No. 216
Wt. Cup, g
Wt. Soil

RETAINED ON 200

Wt. Cup + Soil, g 17.1
Cup No. 223
Wt. Cup, g
Wt. Soil

Size	Weight	%
Total, lb		
3/4, lb		
# 4, lb		
# 10, lb		
# 40, g		
#200, g		
% Silt		
% Clay & Colloids		
Pass #4		
Pass #10		

(DOTD TR 407)

% Retained 3/4	
% Retained # 4	
% Retained #10	
% Retained #40	2
% Retained #200	34
% Silt (Tot Matl)	35
% Clay & Colloids	29
% Pass #10	100
% Pass #40	98
% Pass #200	64
% Sand (Tot Matl)	36
% Unadjusted Silt	35
% Unadjusted Sand	36

LIQUID LIMIT

No. Blows 21
Wt. Cup + Wet Soil, g 57.4
Wt. Cup + Dry Soil, g 46.7
Wt. Water
Factor
Cup No. WW
Wt. Cup, g 10.4
Wt. Dry Soil
% Moisture

PLASTIC LIMIT

Wt. Cup + Wet Soil, g 37.6
Wt. Cup + Dry Soil, g 34.8
Wt. Water
Cup No. 19
Wt. Cup, g 14.9
Wt. Dry Soil
% Moisture

% Organic Matter (TR 413)
Liquid Limit (TR 428) 29
Plasticity Index (TR 428) 15

Natural Moisture Content, % (TR 403)
Optimum Moisture Content, % (TR 418)
Maximum Density, lb/cf (TR 418)
Laboratory Compaction Method (TR 418)

% Cement (TR 432)
% Lime (TR 416)
% Fly Ash
% Other (Additive) Material Code Percent

Soil Group (TR 423) A-6 (07)
Classification (TR 423) CL LM

pH (TR 430)
Resistivity, ohm cm (TR 429)
Classification Prefix (TR 423) (0=Recy 8=Shell)
(Required only if No. 10 material outside or exceeds 5%)

Remarks 2

Tested By: DB & DC
Date: 08/13/98

Checked By: CKH
Date: 8/14/98

APPROVED BY.
DATE:

NOV-25-98 03:37 PM

P.03
DOTD 03 22 0723
2/84

Louisiana Department of Transportation and Development
SOILS/SOIL-AGGREGATE

Proj. No.	451-06-0072	Material Code	401	Lab. No.	05-213801
Date Sampled	07-30-98	Submitted By	0504	Quantity	
Purpose Code	7	Pit No.		Spec Code	1
Date Tested	08-03-98	Ident.	S-4	Parish No.	37
From Station	Westbound	To Station			
Location	3 m Lt.				
Hole No.					
Depth, ft.	00.30 - 00.90	Log Mile			
Item No.		Sampled by:	CKH, DJ, JDB		

Purp. Codes
1. Quality Control
2. Verification
3. Acceptance
4. Check
5. Resample
6. Source Approval
7. Design
8. Indep. Assurance
9. Pre-Source Appr.

Remarks 1 Shoulder borings I-20
Carter Rd. Milhaven

Hydrometer Analysis (DOTD TR 407) Graduate No. ___ Dry Wt of Sample, g (1=50.0, 2=100.0) 1

Time	Elapsed Time	Temp °C (0.5° increments)	Hydro Reading (0.5 increments)	Correction (0.5 increments)	Corrected Reading	% Fines	Effective Grain Size
	60 Minutes	23.0	25.0	1.5			
	120 Minutes	22.5	24.0	2.0			

RETAINED ON 40

Wt. Cup + Soil, g .3
Cup No. 131
Wt. Cup, g
Wt. Soil

RETAINED ON 200

Wt. Cup + Soil, g 14.2
Cup No. 203
Wt. Cup, g
Wt. Soil

Size	Weight	%
Total, lb		
3/4, lb		
# 4, lb		
# 10, lb		
# 40, g		
#200, g		
% Silt		
% Clay & Colloids		
Pass #4		
Pass #10		

(DOTD TR 407)

% Retained 3/4	
% Retained # 4	
% Retained #10	
% Retained #40	1
% Retained #200	28
% Silt (Tot Matl)	38
% Clay & Colloids	33
% Pass #10	100
% Pass #40	99
% Pass #200	71
% Sand (Tot Matl)	29
% Unadjusted Silt	38
% Unadjusted Sand	29

LIQUID LIMIT

No. Blows 27
Wt. Cup + Wet Soil, g 62.3
Wt. Cup + Dry Soil, g 50.6
Wt. Water
Factor
Cup No.
Wt. Cup, g 10.4
Wt. Dry Soil
% Moisture

PLASTIC LIMIT

Wt. Cup + Wet Soil, g 33.1
Wt. Cup + Dry Soil, g 30.2
Wt. Water
Cup No.
Wt. Cup, g 13.9
Wt. Dry Soil
% Moisture

% Organic Matter (TR 413)	
Liquid Limit (TR 428)	29
Plasticity Index (TR 428)	11
Natural Moisture Content, % (TR 403)	
Optimum Moisture Content, % (TR 418)	
Maximum Density, lb/cf (TR 418)	
Laboratory Compaction Method (TR 418)	
% Cement (TR 432)	
% Lime (TR 416)	
% Fly Ash	
% Other (Additive) Material Code ___ Percent	
Soil Group (TR 423)	A-6 (0-6)
Classification (TR 423)	LT STY CL
pH (TR 430)	
Resistivity, ohm-cm (TR 429)	
Classification Prefix (TR 423) (G=Grav S=Shell) (Required only if + No 10 material equals or exceeds 8%)	

Remarks 2

Tested By: DC Checked By: CKH APPROVED BY:
Date: 08-03-98 Date: 8/04/98 DATE:

REFERENCES

1. Cedergren, H. R., "Why All Important Pavements Should Be Well Drained," presented at the 67th annual meeting of the Transportation Research Board, Washington, D. C., 1988.

2. Mathis, D. M., "Permeable Bases Prolong Pavements, Studies Show," Roads and Bridges, Vol. 28, No. 5, 1990, pp. 33-35.

3. Cook, M. and Dykins, S., "Treated Permeable Base Offers Drainage, Stability," Roads and Bridges, May 1991, pp. 46-49.

4. Ridgeway, H. H., National Pavement Cooperative Highway Research Program #96, Transportation Research Board, November 1982.

5. Baldwin, J. S. and Donal, C. L., "Design, Construction, and Evaluation of West Virginia's First Free-Draining Pavement System," Transportation Research Record #1159, 1988.

6. Marks, P., Hajeck, J., Sturn, H. and Kazmierowski, T., "Ontario's Experience with Pavement Drainage Layers," Presented at TAC Conference 1992, Quebec, Canada, September 1992.

7. Bathrust, R. J., and Raymond, G.P., "Stability of Open Graded Drainage Layers, (Phase I)," Final Report, Royal Military College of Canada; Queen University, September 1989.

8. Balwin, J. S., "Use of Open, Free Draining Layers in Pavement Systems," A National Synthesis Report. TRR 1121, TRB, National Research Council, Washington, D.C., 1987.

9. Batrust, R. J., and Raymond, G. P., "Stability of Open-Graded Highway Aggregates," Canadian Geotechnical Conference (45th: 1992, Toronto, Ontario, Canada).

10. John, S. B., and Donald, C L, "Design, Construction, and Evaluation of West

Virginia's First Free-Draining Pavement System, TRR 1159, 1988, Washington, D.C.

11. Drainable Pavement Systems, Federal Highway Administration, Publication No. FHWA-SA-92-008, Washington D.C, 1992.

12. Baumgardner, Robert H., "Overview of Permeable Bases," Proceedings of the Materials Engineering Congress, 1992 Atlanta, GA, 1992, pp. 275-287.

13. Christine, M. R., "Design and Construction of Open-graded Base Courses," Final Report Number 114, Illinois Department of Transportation, November 1993 .

14. ERS Consultants, Inc., "Techniques for Pavement Rehabilitation," Participant's Notebook, October 1987, P.O. Box 1003, Champaign, IL 61820.

15. "Guidelines for the Design of Subsurface Drainage Systems for Highway Structural Sections," FHWA-RD-72-30, Federal Highway Administration, Washington, DC, 1972.

16. Ashraf, S. E. and Lindly, J. K., "Estimating Permeability of Untreated Roadway Bases," TRR No. 1519, 1986.

17. Permeable Base Design and Construction, Demonstration Project No. 975, Federal Highway Administration, Washington, D.C., 1988.

18. Zhou, H., Moore, L., Huddleston, J., and Gower, J., "Determination of Free-Draining Base Material Properties," Presented at 72nd Annual Meeting of TRB, Washington, D. C., January 1993.

19. Grogan, W. P. ed., "Performance of Free Draining Base Course at Fort Campbell," Material: Performance and Prevention of Deficiencies and Failure, New York, NY, pp. 434-448, 1992.

20. Randolph, B. W.; Jiangeng, C.; Heydinger, A. G. and Gupta, J. D., "A Laboratory Study of Hydraulic Conductivity of Coarse Aggregate Bases," Presented at 75th Annual Meeting of Transportation Research Board, Paper No. 960408, Washington, D. C., January 1996.

21. Jones, H. A. and Jones, R. H., "Horizontal Permeability of Compacted Aggregates," Unbound Aggregates in Roads, Proceedings UNBAR3, 1989, pp. 70-77.

22. Tandon, V. and Picornell, M., "Proposed Evaluation of Base Materials for

Drainability," Presented at 76th Annual Meeting of TRB, Paper No. 971314, Washington, D. C. January, 1997.

23. Hall, M., "Cement Stabilized Permeable Bases Drain Water and Increase Life to Pavements," Roads and Bridges, September, pp. 32-33, 1994.

24. Richard, D. B. ed., "The Aggregate Handbook," National Stone Association Washington, D.C., 1993.

25. Milligan, V., "Field Measurement of Permeability in Soil and Rock," Vol. II Proceedings ASCE Conference on In Situ Measurement of Soil Properties, N. C. State University, pp. 3-36, 1975.

26. Moulton, L. K. and Seals, R. K., "In Situ Determination of Permeability of Base and Subbase Courses," Report No. FHWA-RD-79-88, Final Report, Federal Highway Administration, Washington, D. C., May, 1979.

27. Moulton, L. K., "In Situ Permeability Measurements, State of the Art of Pavement Monitoring Systems," Special Report No. 89-23 U. S. Army Corps of Engineers Cold Regions Research and Engineering Laboratory, Hanover, NH, September, pp. 63-73, 1989.

28. Cedergren, H. R., "Seepage Drainage and Flow Nets," 2nd Edition, John Wiley and Sons, New York, 1977.

29. Yemington, E. G., "A Low-Head Permeameter for Testing Granular Soils," Permeability of Soils, ASTM Special Technical Publication No. 163, American Society for Testing Materials, Philadelphia, PA, pp. 37-42, 1955.

30. Loudon, A. G., "The Computation of Permeability From Simple Soil Tests," Geotechnical, Vol. 3, pp. 165-183, 1953.

31. Amer, A. M., and Awad, A. A., "Permeability of Cohesionless Soils," Journal of the Geotechnical Engineering Division, ASCE, Vol. 100, No. GT12, pp. 1309-1316, December 1974.

32. Moulton, L. K., "Highway Subdrainage Design," Report No. FHWA-TS-80-224, FHWA, Washington, D. C., August, 1980.

33. Cedergren, H. R., "Drainage of Highway and Airfield Pavement," John Wiley and Sons, 1977.

34. Vinson, T. S., "Fundamentals of Resilient Modulus Testing," Workshop on Resilient Modulus Testing," Oregon State University, Corvallis, OR, March 1989, pp.28-30,

35. Louay, N. M., Anand J. P., and Prasad A., "Investigation of the Use of Resilient Modulus for Louisiana Soils in the Design of Pavements," Report No. FHWA/LA-94/283, Final Report June 1994.

36. Hicks, R. G., and Monismith, G. L., "Factors Influencing the Resilient Response of Granular Materials," Highway Research Record, No. 345, pp. 15-31, 1971.

37. Rada, G, and Witczak, M. W., "Comprehensive Evaluation of Laboratory Resilient Moduli Results for Granular Materials," Transportation Research Record No. 810, National Research Council, Washington, D. C., pp. 23-33, 1981.

38. Allan, R. F. and Jon A. C., "Ground Water," Prentice-Hall, Inc. 1979.

39. "Resilient Modulus of Unbound Base/Subbase Materials and Subgrade Soils," Specifications for Transportation Materials and Methods of Sampling and Testing, American Association of State Highway and Transportation Officials, 1997.

40. Allen, J. J., and Marshall, T. R., "Resilient Response of Granular Materials Subjected to Time Dependent Lateral Stresses," Transportation Research Record No. 510, Transportation Research Board, Washington, D. C., 1994.

41. Thompson, M. R., "Factors Affecting the Resilient Modulus of Soils and Granular Materials," Workshop on Resilient Modulus Testing, Oregon State University Corvallis, Oregon, March, 1989.

42. Thompson, M. R. and Robnett, Q. L., "Resilient Properties of Subgrade Soils," Transportation Engineering Journal, ASCE Vol. 105, No. 10, 1976, pp. 71-89.

43. Elliot, R. P., and Thornton S. I., "Resilient Modulus and AASHTO Pavement Design," Transportation Research Record No. 1196, 1988 pp. 116-124.

44. Sein, D. K., "A Comprehensive Study on Resilient Modulus of Subgrade Soils," Workshop on Resilient Modulus Testing, Oregon State University, Corvallis, OR, 1989.

45. William, M. Webb., "Graded Aggregate Base Permeability Study and Effect of Trapped Water on Flexible Pavements," Georgia Department of Transportation, Special Research Study No. 9008, Final Report, December 1990.

46. Keith, L. Highlands, Gary, L. Hoffman, "Subbase Permeability and Pavement

Performance," Pennsylvania Department of Transportation, Research Project No. 79-3, Final Report, 1987.

47. Barber, E. S. And Sawyer, C. L., "Highway Subdrainage," Publics Roads, Vol. 26 #12, 1952, pp. 251-268.

48. American Association of State Highway and Transportation Officials AASHTO Guide for the Design of Pavement Structures, Washington, D.C., 1986.

VITA

The author was born in Say, Niger Republic in 1962. He completed his high school studies in 1982. In the same year, he passed the College Entrance Examination and enrolled in the University of Tunis (Tunisia) in the Department of Civil Engineering. In 1991, he received his bachelor degree in Civil Engineering majoring in Structures.

In 1992 he was awarded a Fullbright Scholarship from the Canadian Agency for International Development (C.A.I.D) to pursue his Master in Civil Engineering at the University of Moncton , New-brunswick (Canada).

The author went to United States and pursued his Doctorate of Engineering at Louisiana Tech University in 1995. He was awarded a Letter of Commendation in 1998 and received an Outstanding Civil Engineering Graduate Student Award in 1999.

IMAGE EVALUATION TEST TARGET (QA-3)

150mm

6"

APPLIED IMAGE . Inc
1653 East Main Street
Rochester, NY 14609 USA
Phone: 716/482-0300
Fax: 716/288-5989